



# Treatment of oily wastewater using photocatalytic membrane reactors: A critical review

Ojo Samuel<sup>a,b</sup>, Mohd Hafiz Dzarfan Othman<sup>a,\*</sup>, Roziana Kamaludin<sup>a</sup>,  
Tonni Agustiono Kurniawan<sup>c</sup>, Tao Li<sup>d</sup>, Hazlini Dzinun<sup>e</sup>, Aniqah Imtiaz<sup>a</sup>

<sup>a</sup> Advanced Membrane Technology Research Centre (AMTEC), School of Chemical and Energy Engineering, Universiti Teknologi Malaysia, 81310, UTM JB, Skudai, Johor, Malaysia

<sup>b</sup> Department of Chemical Engineering, Federal Polytechnic, Mubi, P.M.B 35, Mubi, Adamawa State, Nigeria

<sup>c</sup> College of the Environment and Ecology, Xiamen University, Xiamen 361102, Fujian, China

<sup>d</sup> School of Energy & Environment, Southeast University, Nanjing 210096, China

<sup>e</sup> Universiti Tun Hussein Onn Malaysia, Batu Pahat, Johor, Malaysia

## ARTICLE INFO

### Keywords:

Anti-Fouling and self-cleaning, Oily wastewater  
Physico-chemical treatment  
Photocatalytic membrane  
Advanced oxidation process

## ABSTRACT

Oily wastewater is generated from various sources such as oil/gas exploration (produced water), oil refining, pharmaceutical, food industries, and household waste. Toxins in oily wastewater often percolate into drinking water, seawater, and groundwater. This becomes a source of environmental and public health concern. Due to its hazardous nature, the discharge of oily wastewater into the environment is strictly regulated. This work critically reviews progress in photocatalytic membrane reactor (PMR) for oily wastewater treatment, regulations on allowable oil discharge, various factors that affect PMR performance, and its self-cleaning and anti-fouling properties in oily wastewater treatment. Their removal performance for stabilized oil emulsion and trace oil contaminants is highlighted. This work also evaluates trends of integrated techniques, utilization of functional materials, PMR scale-up and the outlook of PMR. It was evident from 226 published articles (1976–2022) that oily waste water contamination has been a source of concern and PMR which integrates both membrane filtration and photodegradation processes, has emerged as a promising technology for oily wastewater treatment, simultaneously degrading oil emulsion and undertaking separation. The PMRs attained over 96% oil rejection. Both the UV and visible light aided the degradation of oil using the PMR. High membrane surface area, provides additional sites for the photocatalyst to occupy, contributing to an efficient degradation. Concludingly, PMRs can exhibit a high flux of recovery ratio after several filtration cycles under UV/Vis irradiation, and with proper design and fabrication methods, the membranes can do self-cleaning and be re-used for several cycles of filtration with high efficiency.

## 1. Introduction

Oily wastewater which contains oil with varying concentrations, is produced from various sources such as metal finishing, mining, transportation, oil refining, etc [1–3]. Oily substances such as phenols,

petroleum hydrocarbons, and polyaromatic hydrocarbons are toxic and inhibit the growth of plants and animals. They bring mutagenic and carcinogenic risks that threaten public health. Therefore, direct disposal of oily wastewater is banned by government regulations [2,4].

To protect the environment, oils in oily wastewater must be treated

**Abbreviations:** UV, ultraviolet light; Vis, visible light; API, American petroleum institute separators; PMRs, photocatalytic membrane reactors; PCRs, photocatalytic reactors; PAHs, polycyclic aromatic hydrocarbons; VOCs, volatile organic compounds; DNA, deoxyribonucleic acid; COD, chemical oxygen demand; BOD, biological oxygen demand; PTFE, polytetrafluoroethylene; PAN, polyacrylonitrile; OPW, oilfield-produced water; GCN, carbon nitride; FRR, flux recovery ratio; POME, palm oil mill effluent; MWCNT, multi-walled carbon nanotube; 2D, two dimensions; WCAs, water contact angles; OCA, oil contact angle; PVDF-HFP, polyvinylidene fluoride-co-hexafluoro propylene; CA-PEI, catechol-polyethyleneimine; TNM, tubular nanofiber membrane; TRL, technological readiness level; SEC, specific energy consumption; HRT, hydraulic residence times; TBL, triple bottom line; DPSIR, driver- pressure-state-impact-response; BAT, best available technology; LCA, life cycle assessment; EIA, environmental impact assessment; MOF, metal-organic frame work; AFM, Atomic Force Microscopy; CNT, carbon nanotubes.

\* Corresponding author.

E-mail address: [hafiz@petroleum.utm.my](mailto:hafiz@petroleum.utm.my) (M.H.D. Othman).

<https://doi.org/10.1016/j.jece.2022.108539>

Received 25 June 2022; Received in revised form 12 August 2022; Accepted 2 September 2022

Available online 6 September 2022

2213-3437/© 2022 Elsevier Ltd. All rights reserved.

to comply with the required discharge standard. For example, the effluent limit of oil/grease concentration in the wastewater ranges from 5 to 42 mg/L depending on the country's legislation [4]. Around 250 million gallons of produced water and 80 million and 88.4 million barrels of oil have been produced daily in 2003 and 2020 respectively worldwide [5–7]. Without any stabilizer, such as a polymer surfactant and alkali in crude oil, the micrometer-sized oil droplets of oily wastewater result in a stable oil/water emulsion in the presence of natural surfactants [5].

In the upstream operation such as crude oil production, storage, and transportation, oil spills, crude oil tank bottom sediments, and drilling mud leftovers are the main sources of oily wastewater, while the principal sources of oily wastewater in downstream operations include (a) secondary pollutants from separators (such as interceptors, corrugated parallel plate, American petroleum institute (API) separators), (b) sediments from trail or trucks, storage tanks, and (c) solids from slop oil emulsion (such as petrochemical synthesis, oil refining) [8].

A variety of treatment methods have been tested to remove oil impurities and minimize the adverse effects of oily wastewater on the environment. They include physico-chemical techniques such as electrochemical treatment, membrane filtration, adsorption, flotation, chemical coagulation, as well as biological processes and their combined technologies [4]. Each has technological strengths and drawbacks in its applications.

Despite their strengths, it is difficult and complicated to treat oily wastewater using a single treatment only [4]. Most physico-chemical treatments have drawbacks, which limit their capability of effectively treating emulsified oil in wastewater with droplet sizes less than 10  $\mu\text{m}$  [2,9]. Therefore, there is a growing need to develop an effective and efficient method to remove emulsified oils in wastewater before its discharge.

Integrating two or more physico-chemical treatments has been tested to attain the desired level of effluent discharge standard. One of the most promising options is to synergize photocatalysis technology with membrane treatment. With minimum operational cost, membrane filtration is considered an alternative to separate oil-water without undertaking phase change or chemical consumption [10]. Membrane filtration has the advantage of easy scalability, simplicity in operation, and high efficiency compared to other conventional methods for oil-water separation [11].

To improve the efficiency of membrane filtration, their surface is modified to minimize fouling. This involves increasing hydrophilicity or hydrophobicity of membrane surface [12], chemical modification [13], surface coating [14], and the use of UV irradiation [15]. Trace oil sticks to the surface of the membrane when the membrane allows water molecules to pass through during treatment. Membranes with smooth surfaces and hydrophobicity are prone to fouling due to the thick oil layer that covers the membrane surface during oil-water separation. The fouling layer decreases permeate flux, resulting in low rejection efficiency. This constitutes a major challenge for the long-term operation of membrane filtration [16]. Overcoming the fouling problem due to the sticking oil layer onto the membrane surface requires the membrane to have self-cleaning and anti-fouling characteristics such as a photocatalytic membrane.

Photocatalytic membrane reactors (PMRs) consist of a system that integrates photocatalysts with the membrane filtration process. This process has gained popularity for the treatment of wastewater. Titanium dioxide ( $\text{TiO}_2$ ) is widely used in PMR systems due to its excellent properties such as high chemical stability, high surface-to-volume ratio, less toxicity, and quantum confinement effects [17]. PMRs have distinguishing features such as simultaneous separation of photocatalysts from treated water while retaining the photocatalyst in the system. This feature contributes to the higher efficiency, stability, and controllability of the system. PMRs have the advantage to save energy and minimize installation size while avoiding additional costs arising due to sedimentation, coagulation, and flocculation, unlike in conventional

photocatalytic reactors (PCRs) [18]. The photocatalyst in the PMR system can absorb energy from sunlight, visible and UV lights depending on the light source to be used for the photodegradation of trace oil pollutant that sticks onto the surface of the membrane. Various polymeric and inorganic membranes have demonstrated superior self-cleaning and anti-fouling ability using photodegradation under UV and visible light irradiation.

The technological strengths of a membrane are attributed to its ability to prevent and self-clean up foulants that would be stuck to the surface of the membrane during the filtration process. This makes it to be efficient and effective in removing target substances in the wastewater. To enable a photocatalytic membrane to possess the self-cleaning and anti-fouling ability, the membrane needs to harness the absorbed energy from the solar spectrum for the degradation of pollutants onto its surface. This facilitates the filtration to proceed for a longer period with less reduction in filtration efficiency.

In spite of its outstanding features, most of the few published review articles on photocatalytic membranes for oily wastewater mainly focused on its use for oil-water degradation and treatment [19–21] without considering its anti-fouling and self-cleaning properties. To the best knowledge of the authors, so far none has reviewed and discussed the potential of the PMR reactors with self-cleaning anti-fouling properties for the treatment of oily wastewater. To reflect its novelty, this work critically reviews various studies on the use of PMRs for oily wastewater treatment and highlighted its potential for anti-fouling and self-cleaning properties. This article also discussed various factors that affect PMR performance, PMR scale-up as well as its self-cleaning and anti-fouling properties for oily wastewater treatment. Their removal performance for stabilized oil emulsion and trace oil contaminants was discussed. This article also evaluates trends of integrated techniques, utilization of functional materials, and the outlook of PMR.

It is expected that the scientific contribution of this work would pave the way for the PMR's widespread applications for industrial wastewater treatment to mitigate the long-term impacts of climate change on the environment while promoting resource recovery and the circular economy (CE) paradigm of critical raw materials from treated effluents.

## 2. State of the scientific focus on PMR

To present an overview of the PMR for oily wastewater treatment, the authors analyzed pertinent articles in the field of study using relevant keywords such as 'photocatalytic membrane', 'oily wastewater', 'photodegradation', and 'resource recovery'. About 226 articles related to "PMR" and oily waste water were retrieved from the literature search on the Web of Science (WoS) from the period between 1976 and 2022. Selected journal articles were chosen based on their application of photocatalytic membrane and filtration technologies and according to their title and abstract to address the thematic topic of this review.

Fig. 1 indicates that over the past years, the number of journal articles on PMR has exponentially increased in the body of literature. By 2022, over 4694 PMR-related articles have been cumulatively recorded in the WoS database. This implies the novelty of PMR in removing target pollutants in oily wastewater.

### 2.1. Characteristics of oily waste water

Oil such as crude oil is made up of a variety of hydrocarbons, which contains hydrogen and carbon atoms. Its color varies from black to brown, and it is less dense than water [22]. It also has a distinctive smell. Generally, oils may contain a range of compounds, depending on their source, including oils and grease, aromatic and aliphatic hydrocarbons, radioactive material, metals, and organic salts [23]. The growth and reproduction of marine species can be affected by polycyclic aromatic hydrocarbons (PAHs), volatile organic compounds (VOCs), and other harmful and poisonous compounds present in oil products [24].

Oily wastes from various sources will contain a wide range of

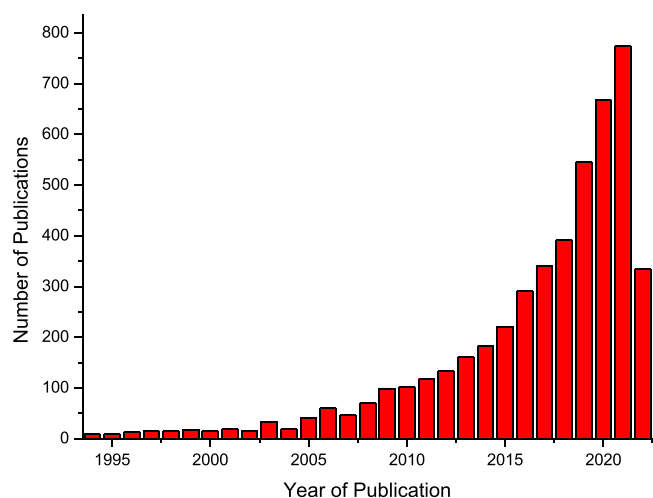


Fig. 1. Depicts an increase in PMR-related publications from 1980 to 2022 (Source: Web of Science, Accessed on June 2022).

pollutants, both in terms of concentration and type. The type of pollutant may be one or a combination of the following: oily sludge, seawater; emulsifying agents; gasoline; heavy metals; solvents, and particulate debris (settleable and floatable) such as paint skins, dirt, sand, and gravel. A general description of the chemical and physical characteristics of untreated oily waste based on available data from composite influents to oily waste treatment systems and discharges from shipboards is shown in Table 1 [25].

### 3. Implications of oily wastewater on sustainability and regulatory framework

Food and beverage businesses produce a significant amount of oily wastewater, while the majority of oil in water comes from metal and petrochemical processing industries in the form of petroleum fractions such as diesel oil, gasoline, kerosene, hydrocarbons, and fats. These oil components are found as oil-in-water emulsions [26]. According to the National Research Council of the United States, 1.3 million tonnes of oil were spilled into the sea annually in 2002 [27]. Oily wastewater has a variety of negative implications on environmental sustainability [28, 29].

Saturated straight and branched-chain hydrocarbons, cyclic hydrocarbons, olefins, aromatic hydrocarbons, and other components such as sulfur compounds, nitrogen-oxygen compounds, and heavy metals are found in oily wastewater. The toxicity of oil-contaminated water is determined by the type, volume, and quality of the polluting oil, as well as the location of the discharge. Oily wastewater can affect organisms through sublethal and stress effects, impacting the diversity of fauna and flora [30].

Table 1  
Characteristics and constituents of untreated oily wastewater [23,25].

Parameters	Concentration (mg/L)	
	Average	Peak
Oil and grease	200–2000	10,000 – 100,000
Suspended solids	50 – 500	5000
pH	6 – 8 units	8.5
Phenolics	0.01 – 0.5	2
Lead	0.03 – 0.1	0.5
Sulfides	0 – 80	NA
Copper	0.02 – 2	5 – 10
Nickel	0.01 – 0.2	0.5
Mercury	Negligible	NA
Zinc	0.1 – 1	2

NA-not available

Oil contamination also has impacts on soil and lowers microbial activity by altering root elongation and germination [31]. Accumulation of oily contaminants in the food chain could damage the deoxyribonucleic acid (DNA) and cause genotoxic, carcinogenic, and mutagenic consequences in living organisms [32,33].

Without proper treatment, oily wastewater discharge raises the chemical oxygen demand (COD) and biological oxygen demand (BOD) of a water body. This restricts the penetration of sunlight into the water environment by generating layers on the surface of the water and disrupting the aquatic environment [34]. As a result, oily wastewater treatment is critical to reducing its impact on the environment [35–38].

Due to its long-term implications, several countries established regulatory frameworks for maximum effluent discharge limits in oily wastewater discharge. The limits range from 5 to 100 mg/L. Table 2 lists country-specific regulations for oily wastewater. China and Malaysia have the most stringent discharge limit (10 mg/L) of oil in wastewater, while the United Arab Emirates has a less stringent limit (100 mg/L) of oil in water. Since the presence of oil in wastewater has environmental implications, the development of cost-effective technology for oily wastewater treatment is a priority to protect the environment [39].

### 4. Membrane filtration in the treatment of oily wastewater

While the widely used methods for the treatment of oily wastewater are electro-coagulation and electroflotation [47], membrane filtration involves the physical separation of liquid content from suspension via a membrane by applying certain pressures. The commonly used membranes are ultrafiltration (UF) and microfiltration (MF) membranes, made of ceramic and polymeric materials. In addition, membrane filtration, biological processes are used for the treatment of oily wastewater [48,49]. Biological treatment involves microorganisms producing lipase enzymes, which degrade biodegradable organic substances in oily wastewater [50].

In adsorption treatment, the oil is removed using adsorbents such as polypropylene, activated carbon, and chitosan-based polyacrylamide [5, 51]. In the flotation method, with a lower density than water, the oil is

Table 2  
Effluent discharge limits of oily wastewater.

Regulatory body/ Country	Legal Basis	Maximum Limits of oil discharge	References
UAE Environmental Regulation	Kuwait convention	Oil and grease content in industrial effluent: 100 mg/L	[40]
Environmental Protection Agency (EPA) in the United States	40 CFR 435	Upper limit: 72 mg/L for any 24 hr period and 45 mg/L over 30 days.	[41]
North Sea region	Oslo–Paris (OSPAR) Convention	Upper limit:30 mg/L	[2]
OSPAR Commission	Paris Convention	40 mg/L for the offshore fields and 5 mg/L for the on- land fields	[42]
Norway (Norwegian Continental Shelf)	Norwegian Environment Agency and Norwegian Oil and Gas Association	Upper limit: 30 mg/L	[43]
China	Environmental protection law	Upper limit: 10 mg/L	[44]
Department of Environment, Malaysia	Environment Quality Act 1974 in Malaysia	Oil and grease discharge limit: 10 mg/L	[45]
Central Pollution Board of India (CPCB)	Central Pollution Control Board (CPCB), Ministry of Environment and Forestry,	The permissible limit for oil and grease: 35 mg/L	[46]

removed by allowing it to float on the surface of the water [52], while in coagulation, the suspended solids, colloids, and oil particles are destabilized, resulting in aggregation. As they aggregate to form large flocs, their density becomes higher than water density. Afterward, the flocs settle down and are then removed by sedimentation.

Membrane technology has been considered one of the most promising options to treat oily wastewater due to its cost-effectiveness, high treatment efficiency, easy integration, facile operation, and minimum chemical additives to the process [9,53]. Treatment using membranes requires some standards to be met for discharge into the environment [54].

Membranes are separation media for several applications ranging from water desalination to waste treatment in the food, oil, and leather industries [55–57]. Suitable membranes need to suit the operational conditions of the treatment. The application of membrane technology for oily wastewater treatment had bottlenecks due to the presence of foulant constituents in oily wastewater [58]. To tackle this challenge, the oily wastewater undergoes a pretreatment process before it is treated using membrane filtration.

Membranes can be classified based on their pore size. Microfiltration membranes with a pore size less than  $0.1\ \mu\text{m}$  can remove bacteria, suspended solids, and some viruses. UF membranes can remove colloidal particles, viruses, and proteins, while NF membranes are applicable for selective multivalent ions and dissolved compound removal. On the other hand, RO membranes can remove metal ions and aqueous salts including chloride, sodium, lead, copper, etc [2].

Membrane processes can be used for separation purposes either through crossflow filtration or dead-end filtration. In operating the crossflow membrane separation, permeate exits through the pores and then flows over the membrane, while in the dead-end membrane separation, the retentate concentrates on the membrane surface. Hollow fiber or flat sheet membrane can be used for filtration purposes, which depends on the membrane's operating conditions. A hollow fiber membrane makes use of several long narrow porous filaments packed inside a plastic housing, while flat sheet membranes could be used in a plate/frame set-up rolled into spiral-wound modules [59,60].

Oily wastewater treatment using membrane technology can remove the smallest oil droplet with a size of less than  $10\ \mu\text{m}$  [2]. The principle of separation using this technology is anchored on exclusion based on the size of the pollutants through a selective media [61,62]. Most membranes are fabricated from synthetic organic polymers. However, ceramics or inorganic membranes are still used for separation. One of the widely used membrane filtrations for oil/water emulsion and oil removal in the petroleum industry is the UF process. This filtration process is effective for oil separation due to its high oil rejection rate, small space requirement, and low operational cost, while it does not require the addition of chemical additives [58]. However, UF membranes are susceptible to fouling because of high permeate flux. Earlier studies reported that the most efficient way of minimizing the fouling problem is by reducing the surface roughness of the membrane and making the membrane surface hydrophilic [63].

Despite its applicability for oil wastewater treatment, membrane technologies have bottlenecks such as flux reduction, increased energy consumption, and reduction in life span and productivity due to fouling caused by the accumulation of oil droplets on the membrane surface [64]. It is important to note that the membrane's operational conditions and the physico-chemical nature of the membrane are important factors to achieve an efficient separation.

#### 4.1. Mechanism of membrane fouling for oily wastewater treatment

Membrane fouling involves the deposition of a substance which can be either an oil droplet or solid particles on its surface that covers and renders it to become inefficient in the separation process [65]. Fouling reduces the flux rate of the membrane. The fouling mechanism may be classified into four types. Fouling takes place simultaneously during the

filtration process causing the membrane to experience declining flux. The membrane fouling includes; (i) cake filtration, (ii) intermediate fouling-, (iii) standard blocking, and (iv) complete blocking [66].

#### 4.2. Types of fouling mechanisms in oily wastewater treatment

##### 4.2.1. Cake filtration

This is a phenomenon where each foulant oil particle locates on the other deposited particles. Here a layer of a particle forms a cake on the membrane surface. As a result, the layer blocks the membrane pores stopping the water to flow through the pores of the membrane [4].

##### 4.2.2. Intermediate fouling

This type of fouling occurs when each foulant oil particle either settles on other particles that have already deposited on the membrane surface or directly block some membrane area. Here the gradual buildup of a layer of particles creates a constriction or contraction for the water to flow through the membrane pores. It may be considered an intermediate step between cake filtration and complete blocking [4].

##### 4.2.3. Standard blocking

This mechanism refers to conditions under which oil particles are deposited onto the internal pore walls of the membrane. This partial blocking of the pores narrows the channel and reduces the flow rate of water due to the small particle size on the inside wall of the pores leading to a decrease in pore volume [4].

##### 4.2.4. Complete blocking

In complete blocking, each oil foulant particle upon reaching the membrane surface, involves or participates in blocking some pore of the membrane with no superposition of particles. Here the pores are completely blocked by a large particle or particles having sizes comparable to the membrane pore sizes subsequently preventing water from passing through [4]. Fig. 2 shows an illustration of the various fouling mechanism that occurs during oily wastewater separation using a membrane. For a more detailed explanation of the various types of fouling in oily wastewater treatment using membrane filtration, the reader is referred to our published article by Samuel et al., [4].

The fouling mechanism involves oil droplets that form coalescence

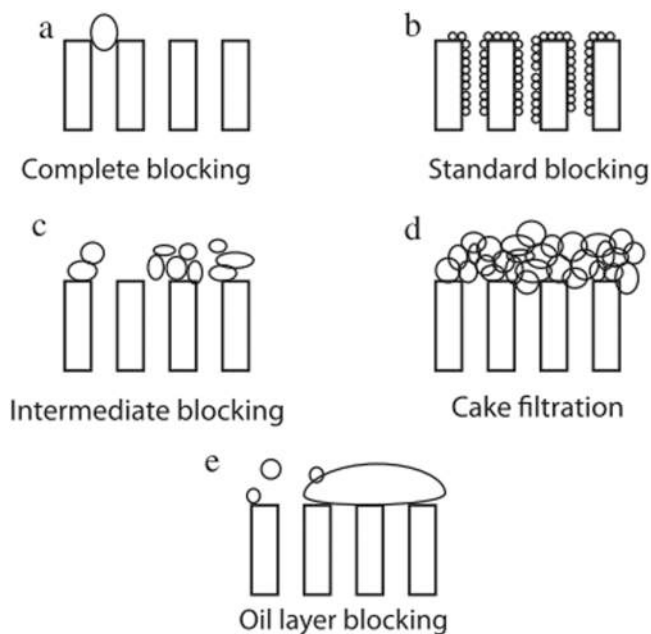


Fig. 2. Schematic diagram representing the various types of fouling mechanisms taking place on the membrane [2].



[67]. As a result, there is a continuous layer of oil on the membrane surface. This is peculiar to the oil-water emulsion and slightly different from the cake filtration process, as the fouling layer does not contain separate particles. In this situation, oil lining could be formed inside the pores and causes a reduction in the pore diameter, which decreases the rejection rate and flux rate [2].

To address this fouling mechanism due to the oil droplets, the use of a photocatalytic membrane, which combines the photocatalytic process and membrane technology in a single unit has been explored to degrade the oil droplet that blocks the membrane pores resulting in flux reduction. The photocatalytic membrane is believed to exhibit self-cleaning and anti-fouling ability, which gives it the ability to self-clean up various pollutants attached to the membrane during treatment. The photocatalyst can either be coated on the surface of the membrane or immobilized into the membrane surface to prevent fouling.

Another way to solve the flux reduction due to fouling is to minimize the interaction between the oily foulants and the membrane surface by improving the latter's hydrophilicity [68,69]. Different nanoscale materials can be used to achieve higher flux and higher rejection rates, as compared to conventional membranes.

#### 4.3. Membrane surface modification

Chemical or physical methods can be used to modify the surface of a membrane. The interaction between the altering substances and the membrane is crucial to be considered. Coating materials can be easily deposited and absorbed into the membrane's surface via secondary interaction (H-bonding, electrostatic interaction, and Van der Waals forces) [70]. Multiple materials can be crosslinked in situ onto the membrane's surface to improve stability and enhance their interactions. The strength of the secondary interaction depends on the type of surface modification and the polymer surface. Plasma treatment and grafting are widely adopted to modify polymer surfaces without the bulk properties being affected [71,72].

Many materials, including TiO<sub>2</sub> nanotubes, graphene oxide (GO), carbon nanotubes (CNTs), and iron oxide particles (IOP), have been employed to modify membrane surfaces. According to Zhang et al., [73] TiO<sub>2</sub> nanotubes were grafted into the channels of an alumina membrane template, which demonstrated good photocatalytic activity on humic acid (HA) photodegradation and significantly reduced membrane fouling. Gao et al., [74] discovered that grafting TiO<sub>2</sub>-GO onto membrane surfaces boosted photocatalytic activity and membrane hydrophilicity.

Photo-induced RAFT-mediated grafting of acrylic acid and TiO<sub>2</sub> photocatalysts could also improve the surface hydrophilicity and anti-fouling ability of polypropylene macroporous membranes [75]. CNTs, serving as electron acceptors by trapping electrons transmitted from semiconductor photocatalysts, were employed to synthesize CNTs-TiO<sub>2</sub>/Al<sub>2</sub>O<sub>3</sub> composite membranes due to their high electron mobility. They slowed the recombination of photogenerated charges and had a reduced photoluminescence intensity and increased photocurrent density, resulting in efficient pollutant degradation and superior anti-fouling properties [76].

Photocatalytic nanofiltration (NF) membranes with double-side active composite TiO<sub>2</sub>, synthesized using a chemical vapor deposition process, have enhanced pollutant photodegradation capacity while reducing pore blockage [77]. To produce high permeability membranes, Goei et al., [78] synthesized a pluronic-based TiO<sub>2</sub> hybrid photocatalytic membrane using an acid-catalyzed sol-gel technique. The membrane had a hierarchical porosity, with Photo-induced super-hydrophilicity which improved the accessibility of organic pollutants to the catalytic sites. The choice of TiO<sub>2</sub> functional groups is influenced by feed parameters (hydrophilic/hydrophobic and electric charge), and therefore a modified membrane with low foulant affinity and high photocatalytic effectiveness is recommended.

Ideally, surface modification minimizes interactions between

undesired molecules in the wastewater to be treated and the membrane, while increasing the selectivity of the filtration system [79]. Physical immobilization can be applied by dipping the membrane into the modifier's colloidal solution. The strength of the interaction between the membrane and the material depends on the secondary interaction [72].

Membrane surface modification to decrease roughness has been associated with reduced membrane fouling and an increase in surface hydrophilicity has been suggested to reduce organic fouling, such as that from oil emulsions [80]. Freeman et al., [80] in their work, coated a polyamide RO membrane with polydopamine and attained a significant improvement in fouling resistance during oil-water separation due to less membrane roughness. Limitations of physical deposition and adsorption include possible leaching of the deposited material over time. As a result, a variety of studies have been conducted to improve the strength of interactions between the membrane and the particles to avoid any loss during the treatment [81–83]. The methods used for membrane surface modification (Table 3) include surface grafting [84, 85], surface coating [86,87], and blending [88,89].

Blending modification (Fig. 3) is widely adopted for polymeric membranes due to its simplicity, versatility in application, cheapness, easy procedure, very efficient, and effective in achieving or obtaining a membrane with the desired properties. This technique is used when the membrane is prepared by the phase inversion method in which the polymer is transformed in a well-coordinated and controlled way from liquid to solids in a selected or chosen solvent thereby allowing the distribution of the polymer uniformly. The chosen modifying material can be added to the polymer casting solution to produce the modified membrane [81,90].

In surface grafting, the membrane is modified by the immobilization of a functional chain onto the membrane surface via covalent interactions as can be seen in Fig. 3. In comparison with the physical deposition method, the grafting method provides considerably longer stability. Fig. 3 shows a schematic diagram of various membrane surface modifications. Table 3 also presents an overview of the various membrane modification techniques during and after membrane fabrication.

#### 4.4. Membrane surface modification using photocatalytic nanomaterials

Photocatalytic nanomaterials are used to modify a membrane with improved hydrophilic, antifouling, and self-cleaning properties. This technique is promising because the photocatalytic nanomaterials are capable of decomposing, degrading, and mineralizing organic contaminants and pollutants into smaller and more biodegradable substances, while not forming secondary pollutants via photocatalysis [79,92,93]. A photocatalyst to be incorporated into a membrane should have excellent photocatalytic activity, lower energy bandgap, and slow  $e^-/h^+$  pair recombination [94]. Important areas of photocatalytic membrane development are the stability of selected membrane material under an oxidative environment, stability of the membrane under UV or visible light irradiation, and the stability of the nanomaterial on the membrane for continuous filtration [95].

With respect to oxidative stability under UV or Visible light irradiation, reactions can take place between photons and the polymeric membrane because photocatalysis generates radicals, which trigger degradation reactions. It is therefore important to utilize materials that do not deteriorate the membrane selectivity and flux when developing a stable photocatalytic membrane under UV or visible light irradiation.

To investigate the oxidative stability of polymeric membranes such as polycarbonates (PC), cellulose acetate (CA), polyvinylidene fluoride (PVDF), polytetrafluoroethylene (PTFE), polyethersulfone (PES), polypropylene (PP), polystyrene (PS) and polyacrylonitrile (PAN), Chin et al. [96] found that PVDF, PTFE and PAN membranes exhibited better stability after 30 days of exposure to UV irradiation. When TiO<sub>2</sub> nanomaterials were added to the treatment system, the deterioration of the PES membrane increased due to the oxidative compounds. They suggested that PVDF and PTFE exhibited better oxidative stability and

**Table 3**  
Various types of membrane modification techniques [19].

Membrane surface modification during fabrication		Membrane surface modification after membrane fabrication			
Blending modification		Bulk modification	Surface grafting	Surface coating	Plasma treatment
Hydrophilic materials incorporation		Hydrophilic functional group incorporation	Chemical attachment of hydrophilic monomers	Hydrophilic layer deposition	Introduction of various functional group
Hydrophilic nanoparticles incorporated into the base polymer	Amphiphilic or hydrophilic polymer incorporation into the base polymer	Bonds enhancement by addition of substituent groups	Covalent bond formation between membrane surface and hydrophilic monomer	Anchored layer: chemical treatment + hydrophilic layer coating	Physical immobilization: spraying, direct adsorption, or dipping of the hydrophilic layer
Examples Carbon nanotubes, SiO <sub>2</sub> , Composite, Fe <sub>2</sub> O <sub>3</sub> , TiO <sub>2</sub> , Al <sub>2</sub> O <sub>3</sub> , etc	Sulfonation polycarbonate, Branched co-polymers, Polymethyl methacrylate, Sulfonated polyether ketone, etc	Carboxylation (dry Ice), Sulfonation (SO <sub>3</sub> , H <sub>2</sub> SO <sub>4</sub> , etc)	<b>Grafting methods:</b> Electron beam radiation, UV radiation, O <sub>3</sub> , □-ray, Plasma treatment. <b>Grafting monomers:</b> Poly(2-hydroxy-ethyl methacrylate), Poly(ethylene glycol) methyl ether methacrylate, etc	<b>Coating materials:</b> Chitosan, Polydopamine, Polyvinyl alcohol, poly(ethylene glycol), etc <b>Chemical treatment (Chemical used):</b> Crosslinking, Sulfonation (H <sub>2</sub> SO <sub>4</sub> )	<b>Coating materials:</b> SiO <sub>2</sub> , Glycerol, TiO <sub>2</sub> , Poly (sodium 4-styrene sulfonate, etc <b>Gas ionization methods:</b> Radiofrequency wave, Microwave. <b>Ionized gases:</b> H <sub>2</sub> , N <sub>2</sub> , H <sub>2</sub> O, He, CO <sub>2</sub> , O <sub>2</sub> , Ne, etc

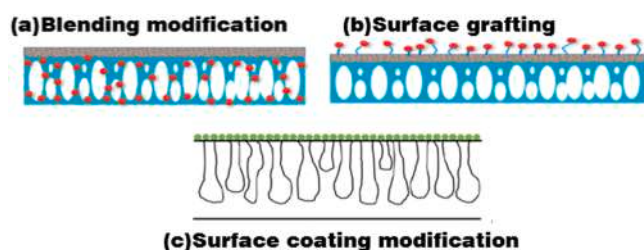


**Fig. 3.** Schematic diagram of common membrane surface modification: (a) Blending [91], (b) Surface grafting [91], (c) Surface coating [62].

higher performance under UV irradiation [96]. The modification affects their stability when added to the membrane. It is therefore essential to ensure the adherence of the nanoparticles to the membrane to enhance their filtration performance while ensuring that they are not lost over time [97]. Fig. 4 shows the cross-section images from EDX analysis of a TiO<sub>2</sub> photocatalyst immobilized membrane showing clearly that the TiO<sub>2</sub> particles have been distributed uniformly on the membrane surface using the co-extrusion technique. Fig. 5 also presents SEM images showing the morphology of a CeO<sub>2</sub> nanoparticles stainless steel coated membrane for oil-water separation. The images present pre and post-coated morphologies of the photocatalytic membrane. The CeO<sub>2</sub> particles were coated on the surface of the membrane as shown in the images.

## 5. Photocatalysis and photocatalytic membrane reactors (PMR)

Over the years, photocatalysis has become a fast-growing field because of its promising application in mineralizing organic pollutants, hydrogen production, water splitting, and CO<sub>2</sub> conversion [100]. "Photocatalysis" refers to the photoactivation of a chemical reaction by absorbing a quantum of light from inorganic or organic material that remains unchanged at the end of the reaction such as the photocatalyst [101–104]. In photocatalysis, \*OH is created by the irradiation of UV or visible light, and this accelerates the oxidation of organic contaminants rapidly and non-selectively [105]. Heterogeneous photocatalysis requires the photoinduced reaction to take place in the presence of a photocatalyst. A PMR is a hybrid unit that combines membrane separation and heterogenous photocatalysis in a single unit. Its basic structure consists of a reactor structure housing the membrane and a light source. Its configuration and design are important factors for its overall

performance [106].

### 5.1. Mechanism of photocatalytic reactions in PMR

Photocatalytic reaction in the presence of semiconductor metal oxides for the degradation of contaminants in wastewater has appeared to be a promising route due to its outstanding performance in degrading oil droplets, inorganic, and recalcitrant organic pollutants [105,107]. The capacity to absorb energy in the UV/Vis region and their high surface-to-mass ratio distinguish the oxide materials. As a result, they have gained popularity for photocatalytic degradation of organic contaminants. As metal oxide semiconductors are non-toxic, they are suitable for water treatment.

A photocatalyst to be incorporated into a membrane is expected to have excellent photocatalytic activity, lower energy band gap, and slow electron/hole pair recombination [94]. Among the various metal oxide semiconductor photocatalyst used for incorporation into photocatalytic membranes, TiO<sub>2</sub> is commonly used due to its high activity under UV light, chemical stability, low-cost, high resistance against photochemical corrosion, and non-toxicity [108]. The catalytic activity of TiO<sub>2</sub> was first reported in 1977 when it was discovered that it can degrade cyanide [109]. After that time, TiO<sub>2</sub> has become a promising photocatalyst for use in photocatalysis for environmental pollution degradation. However, its use in photocatalysis is limited due to some unfavorable properties it exhibits which include poor sensitivity or optical properties in the visible light spectrum of the sun, rapid and fast charge recombination of the photogenerated hole pairs and electrons, and wide energy band gap which make it ineffective in visible light [110]. It is therefore important to note that for efficient and effective treatment and degradation of oily wastewater using PMRs the photocatalyst to be incorporated into the PMRs should exhibit good optical properties, lower band for visible light absorption, and slow charge recombination rate.

Photocatalysis offers advantages such as low cost, its production of non-toxic by-products, and an environmentally friendly process [111–114]. For photocatalysis, several materials could act as a photocatalyst for the degradation of harmful and toxic pollutants without causing secondary pollution [115–117]. Photocatalysis which is a form of advanced oxidation process (AOP) has gained attention because simple aerial oxidation and self-purification processes are no longer efficient to tackle this problem. Photocatalysis involves the use of hydroxyl radicals to completely degrade or mineralize the pollutant [118]. This process has the overall reaction (Eq. (1)):

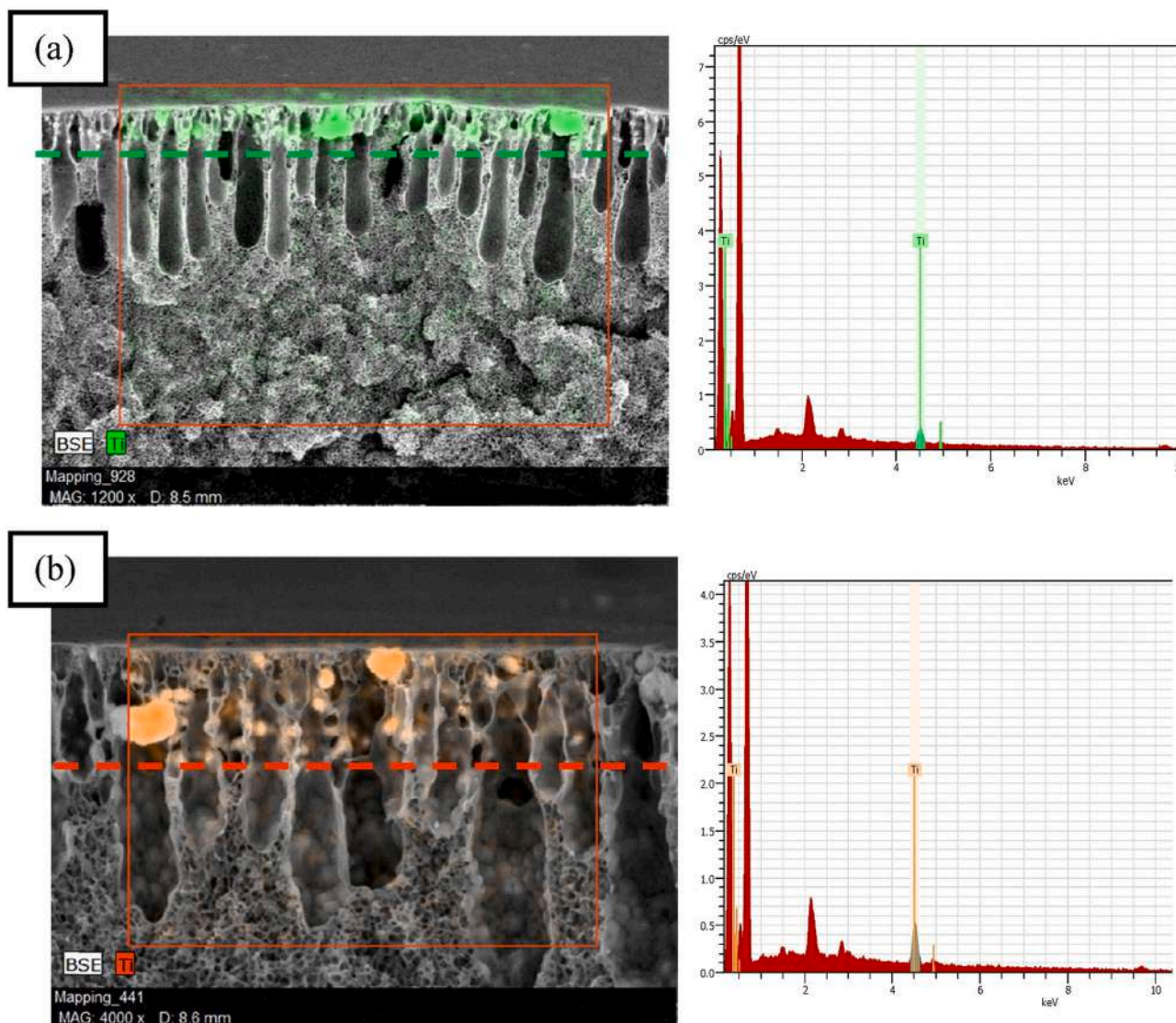
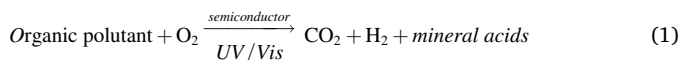
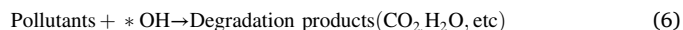
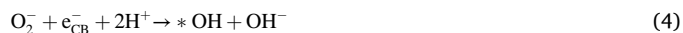


Fig. 4. SEM-EDX images of the (a) DL-PEG/TiO<sub>2</sub> and (b) DL-TiO<sub>2</sub> immobilized membranes with different magnifications. Reprinted with permission Copyright (2017) Elsevier [98].



According to Theerthagiri et al. [117], photocatalyst accelerates the distinct reduction and oxidation process in the presence of UV irradiation of a certain wavelength. The mechanism of photocatalysis involves three stages: (i)  $e^-$  and  $h^+$  separation upon the absorption of light irradiation (movement of electrons from the valence band to the conduction band), (ii) scattering of charge carriers on the photocatalyst's surface, and (iii) the light-driven catalytic reduction and oxidation on the active sites of the photocatalyst.

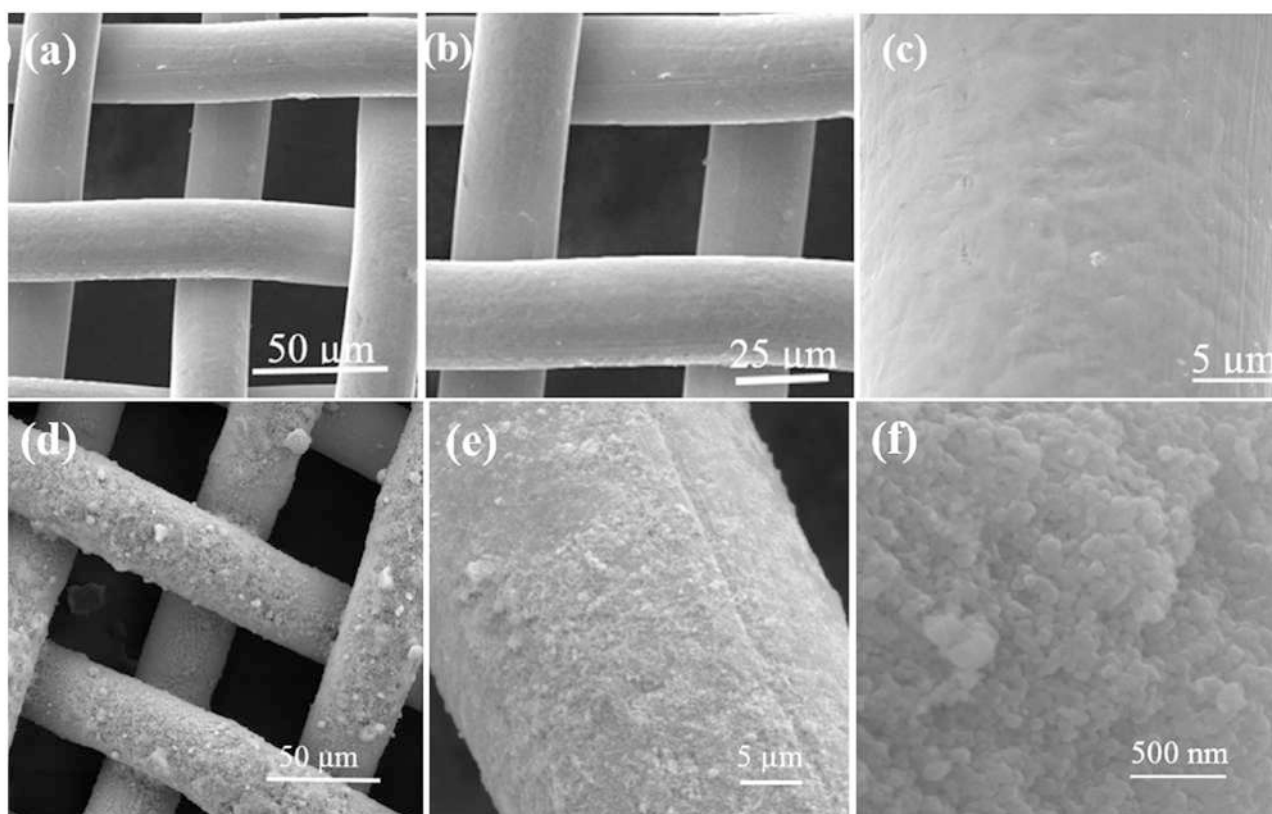
Eqs. (2)–(6) depict the main reaction paths involved in the photocatalytic degradation of the target pollutant (Fig. 6). Eq. (2) shows the simultaneous generations of electrons ( $e^-$ ) and holes ( $h^+$ ) on the photocatalyst upon absorbing light irradiation at the conduction band ( $C_b$ ) and the valence band ( $V_b$ ) respectively. The photogenerated charges are transferred to the surface of the photocatalytic material to initiate the required reduction and oxidation processes. The reaction of  $e^-$  and  $h^+$  with O<sub>2</sub> and H<sub>2</sub>O (Eqs. (3)–(5)), respectively, results in the formation of hydroxyl radical \*OH and O<sub>2</sub><sup>-</sup>. Eq. (6) shows the reaction of the radical species with the organic pollutants, leading to the degradation of target pollutants [118–120].



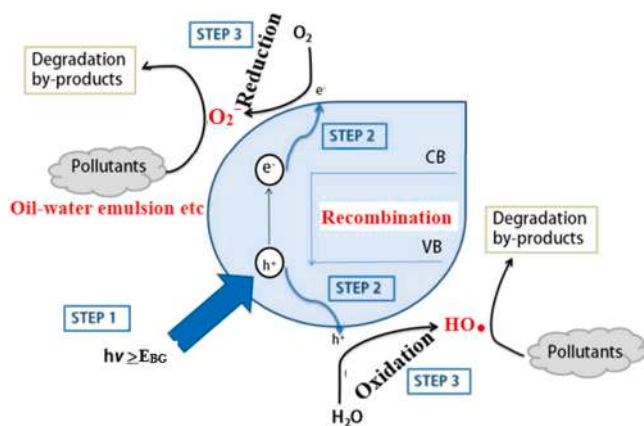
The same mechanism is applicable for the photodegradation of the oily wastewater as the pollutant as presented in Fig. 6.

Table 4 presents the results of earlier studies on the photocatalysis of oily wastewater. Despite high oil degradation, the photocatalytic process could not completely treat the effluents to an acceptable standard. Although the treatment efficiency is less than 90%, it is difficult to separate the photocatalyst from treated effluents. Therefore, the photocatalyst is better immobilized into the membrane to enable better oily wastewater treatment to achieve the required discharge standard.





**Fig. 5.** SEM images of the stainless steel membranes at different magnifications showing the surface morphology (a–c) virgin membrane before deposition (d–f) the surface modified after deposition of ceria nanoparticles. Note the increase in apparent surface roughness after the deposition that contributes to superhydrophobic behavior. Also, the absence of voids between the deposited particles on one of the membrane fibers in the magnified image (f). Reprinted with permission Copyright (2019) Elsevier [99].



**Fig. 6.** Mechanism of photodegradation process [118].

## 5.2. Typical design and configurations of PMR

A photocatalytic membrane incorporates a photocatalyst into a membrane for the photocatalytic reaction. Photocatalytic membrane reactor (PMR) integrates pollutant degradation and separation membrane in the same unit [132]. A supported photocatalysts layer on a porous membrane that facilitates photocatalytic activity under UV or visible light irradiation is referred to as a photocatalytic membrane [133]. During the photocatalytic process, the photocatalyst generates  $\cdot\text{OH}$  to degrade target pollutants into smaller and relatively harmless oxidation by-products without producing secondary pollutants [18]. Energy sources such as visible light, UV light, and heat can trigger

the formation of reactive radicals [134,135]. To improve photocatalytic performance, membrane fouling management, operational and maintenance cost, and light arrangement in PMR setup are critical [136]. Pressure-driven and non-pressure-driven PMR setups are the two main types of setup. PMRs that use MF, UF, NF, or RO separation with photocatalyst suspended or immobilized are known as hydraulic pressure-driven PMRs, while non-hydraulic pressure-driven PMR refers to PMR that uses FO, membrane distillation (MD), pervaporation (PV), or membrane crystallization (MC). In addition, PMR encompasses both suspended (or slurry) and immobilized systems [137].

In terms of membrane fouling tendency, slurry PMRs have more tendency of fouling than the immobilized reactors. Slurry PMR necessitates the separation and recovery of photocatalyst particles, which leads to an increased operational cost [138]. This necessitates the use of an extra container for particle separation and recycling. The immobilized PMR system has a greater advantage in terms of photocatalyst separation than the slurry PMR system. Another disadvantage of the slurry PMR is that photocatalyst particles may induce light scattering, membrane fouling, and clogging in the PMR [134]. To overcome these problems, dosage and particle size need to be determined.

Photocatalytic membranes (PM), which immobilize photocatalysts into/onto membranes have gained considerable interest for an integrative configuration of PMR to reduce photocatalyst loss, membrane fouling, and footprint [139]. Due to the advantage of increased mechanical, physical, and chemical stability, stainless steel and ceramic PM are favored in PMR setups. However, this PMR arrangement has a small light irradiation area than the slurry PMR systems [140].

As a result, the photo-degradation of pollutants was less effective using slurry PMR. Photocatalytic membranes used in immobilized PMR systems are stable when exposed to light. Polymeric membranes with low resistance and photostability to oxidative radicals can be



**Table 4**  
Studies on photocatalytic treatment for oily wastewater from literature.

Type of wastewater	Catalyst	Target pollutant	Treatment Process	Efficiency (%)	References
Synthetic Produced water	ZnO	Petroleum hydrocarbons and partially hydrolyzed polyacrylamide (HPAM)	Photocatalysis	68%, 62%, 56% and 45% removal of 25, 50, 100 and 150 mg/L HPAM were measured by HPLC	[121]
Diesel in seawater	Nano-ZnO	Diesel	UV irradiation	84% removal in 3 h	[122]
Crude oil and contaminated water	Nano-TiO <sub>2</sub>	Oil	Photocatalysis followed by biofilm	90% of oil removal	[123]
Bilgewater	TiO <sub>2</sub> PG500	Oil	Air stripping plus 125-W UV lamp 365 nm	60% removal in 8.5 h	[124]
Crude oil and contaminated water	Nano-TiO <sub>2</sub> loaded on ceramic microbeads	PAHs	Near-UV solar irradiation, 25–50 Wm <sup>-2</sup>	100% removal	[125]
Bilgewater	K-TiO <sub>2</sub>	Oil and COD	Ultrafiltration and UV lamp with a light intensity of 49 W/m <sup>2</sup>	Photocatalysis 100% removal in 2 h	[126]
Artificial water	Nano-TiO <sub>2</sub> -SiO <sub>2</sub>	Naphthenic acid	Fixed-bed system plus sunlight	92% removal after 4 h	[127]
Diesel in Water	Polyurethane foams modified with silver/titanium dioxide/graphene ternary nanoparticles (PU-Ag/P25/G)	Diesel	UV irradiation	72% degradation after 16 h	[128]
Groundwater contaminated by gasoline and diesel	TiO <sub>2</sub> -SiO <sub>2</sub> solution dip-coated on ceramic beads	TPHs, BTEX, TOC	Irradiated by sunlight (1.6 mW/cm <sup>2</sup> measured at 365 nm) with H <sub>2</sub> O <sub>2</sub>	> 70% degradation of BTEX and TPH	[129]
Offshore-produced water	Immobilized TiO <sub>2</sub> on a glass plate	PAHs	8-W UV lamp plus ozone	> 90% in 1 h	[130]
Wastewater from polymer flooding	Nano-TiO <sub>2</sub>	PAM	125-W Hg lamp	80% removal in 1.5 h	[131]

problematic. Hence, in immobilized PMR, stainless steel and ceramic-based membranes are selected [134]. Fig. 7 shows typical configurations of PMR systems.

### 5.3. PMRs for oily wastewater treatment

Treatment of oily wastewater by the PMRs involves a simultaneous filtration and degradation of pollutants in the oily wastewater, which occurs inside the membrane pores, while the permeate passes through the membrane. The degradation of the pollutants happens after the photocatalyst is excited by a light source, while the filtration and separation take place through membrane filtration. For this reason, the membrane act as the irradiated element. As a result, it is vital to use materials resistant to damage due to the effects of OH radicals, which are responsible for the degradation of the pollutants [138].

Normally, photocatalytic reactions are conducted in a suspension of either microscale or nano-sized catalyst particles. Despite the effectiveness of the photocatalytic activity, the separation of the catalyst particles is the key problem of suspension catalyst treatment. Apart from the reusability of the catalyst, the separation is important to minimize the adverse effects of the semiconductor nanoparticles in the absence of light [141]. To promote an efficient photocatalytic reaction, the use of visible-light-driven photocatalytic membranes for oily wastewater treatment needs to be further explored. So far, only a few works have reported its applications using visible light as a light source. In recent years, various studies have reported the use of UV light in PMRs for the treatment of oily wastewater.

Alias et al. [16] synthesized a photocatalytic nanofiber-coated inorganic hollow fiber membrane for oilfield-produced water (OPW) treatment. They fabricated the membrane by coating alumina (Al<sub>2</sub>O<sub>3</sub>) hollow fiber membrane with polyacrylonitrile (PAN) nanofibers combined with graphitic carbon nitride (GCN) photocatalyst. While the porous coating comprised smooth hydrophilic nanofibers for water permeation, it successfully trapped oil droplets, resulting in an improved oil rejection rate. Its sparse mesh prevented oil pollutants from forming a fouling layer on the membrane surface, allowing a high permeate flux to be maintained. For 3 h of crossflow filtration of OPW at 2 bar, a maximum permeates flux of 640 Lm<sup>2</sup>h<sup>-1</sup> and an oil rejection percentage of 99% was obtained, along with a water flux of 816 Lm<sup>-2</sup>h<sup>-1</sup>.

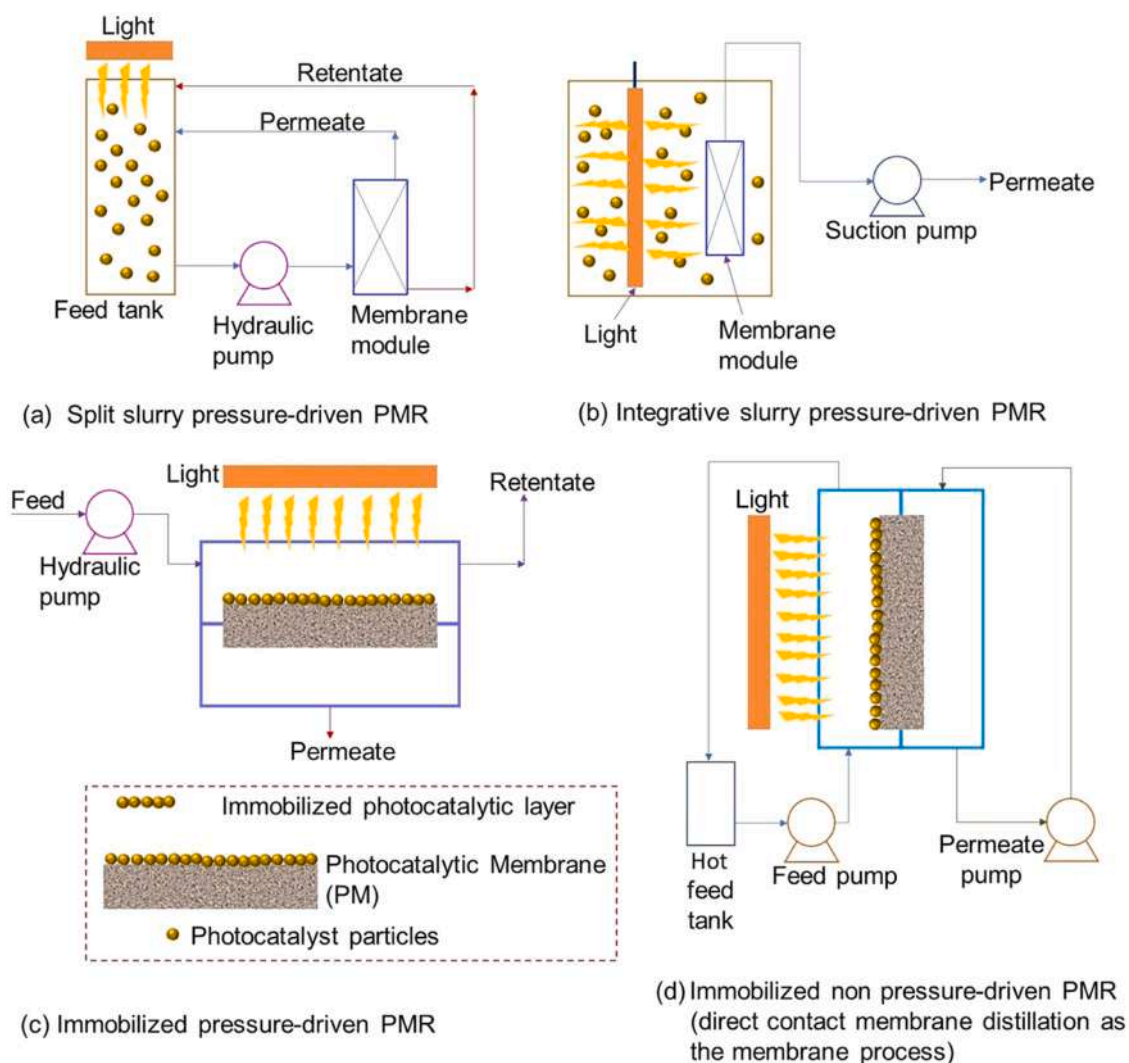
After three cycles of 3 h of filtration, the photocatalytic activity of GCN enabled the coating to degrade the trapped oil on the membrane under UV irradiation, attaining a permeate flux of 577 Lm<sup>-2</sup>h<sup>-1</sup> and oil rejection of 97%. They found that the membrane's fouling resistance and cleaning capabilities are beneficial for a long-term filtering operation. The SEM images of the membrane using bare Al<sub>2</sub>O<sub>3</sub>, NF/Al<sub>2</sub>O<sub>3</sub>, NF-bGCN/Al<sub>2</sub>O<sub>3</sub>, and NF-nsGCN/Al<sub>2</sub>O<sub>3</sub> are displayed in Fig. 8. While oil covered the surface of the membranes, the NF-nsGCN/Al<sub>2</sub>O<sub>3</sub> attained a better permeate flux. The membrane surface was not totally covered with oil droplets due to the presence of the photocatalyst.

Fig. 9 shows the oil droplet size distribution in the oilfield produced water (OPW) feed and permeate solution produced by bare Al<sub>2</sub>O<sub>3</sub> and NF-nsGCN/Al<sub>2</sub>O<sub>3</sub> membranes after 3 h. The figure also displays a higher particle size distribution in the bare Al<sub>2</sub>O<sub>3</sub> membrane than in the NF-nsGCN/Al<sub>2</sub>O<sub>3</sub> membrane, indicating a higher degradation of the target contaminant by the latter.

In another work, Veréb et al., [142] prepared TiO<sub>2</sub> and TiO<sub>2</sub>/carbon nanotubes (CNT) composite modified PVDF membranes to purify oil-in-water emulsions. They found that the combination of the photocatalytic nanomaterial TiO<sub>2</sub> with 1 wt% CNT resulted in the highest flux and lowest resistance. The enhanced photocatalytic degradation by the composite resulted from the presence of the photocatalytic nanomaterials. The membrane exhibited the ability to regenerate during the photocatalytic process, thereby exhibiting self-cleaning properties, leading to a longer period of treatment cycles.

Zangeneh et al., [143] prepared a photocatalytic self-cleaning PES nanofiltration membrane that incorporated triple metal-nonmetal doped TiO<sub>2</sub> (K-B-N-TiO<sub>2</sub>) for post-treatment of palm oil mill effluent. They found that the addition of K-B-N-TiO<sub>2</sub> nanoparticles (0.5 wt%) improved the modified membranes' water flux, due to their hydrophilicity and increased photocatalytic activities of the photocatalyst. They also reported that the highest permeation flux, dye, and COD removal efficiency were around 27 kg/m<sup>2</sup> h, 98%, and 90%, respectively.

Fig. 10a displays the SEM images of the surface of the mixed matrix PES membrane with 0.5% (w/w), K-B-N-TiO<sub>2</sub> which gave a better permeate flux due to the presence of finger-like pores in the modified membrane. The authors also reported that the degradation of the fouling agents on the surface of the membrane and the improved removal of COD and color from the biologically treated POME was attributed to the



**Fig. 7.** Schematic diagram of typical PMR: (a) split slurry pressure-driven PMR, (b) integrative slurry pressure-driven (submerged) PMR, (c) pressure-driven immobilized PMR, and (d) non-pressure-driven immobilized PMR (photocatalytic-direct contact membrane distillation as an example) Reprinted with permission Copyright (2022) Elsevier [21].

super hydrophilic impact and the increasing nanoparticles (NPs) reusability of the modified membranes after UV Visible light irradiation on the K-B-N-TiO<sub>2</sub>/PES modified membranes increased flux recovery ratio (FRR).

They also characterized the modified membrane using Atomic Force Microscopy (AFM). As can be seen from Fig. 10b, they presented the 3D AFM images of the blended and unfilled PES membrane surfaces. It could be seen from the images that the valleys or pores of the membrane are shown in dark patches, and the brighter region displayed the largest membrane surface. They reported that the surface roughness of the unfilled PES membrane is the highest, and it can be decreased by adding K-B-N-TiO<sub>2</sub> nanoparticles at concentrations between 0.1 and 0.5 wt%. As reported in other studies, it is known that decreasing surface roughness of the modified membrane limits foulant entrapment or adsorption in the valleys and adhesion at peaks, which reduces membrane fouling [144,145]. However, as the nanoparticle content increased from 0.5 to 1 wt%, the surface roughness also increased. This is because the hydrophilic nanoparticles agglomerated or accumulated on the membrane surface. Due to foulant deposition in the "valleys" of the rough membrane surface, it has been discovered that membrane fouling can become more severe as roughness increases [146].

Zangeneh et al., [143] also reported the reusability of the bare PES and the modified membrane after three (3) cycles of filtration which

lasted for 60 min. They found that after 60 min of visible or UV cleaning, the FRR values for the post-treatment of the biologically treated Palm oil mill effluent (POME) for the 0.5 wt% TiO<sub>2</sub> modified and unmodified membranes cleaned by visible light irradiation showed a reduction in FRR value after three regeneration cycles of approximately 2.6% and 12.5%, respectively. However, when UV irradiation was used, this value was attained at roughly 1% and 5.2% respectively. According to Fig. 10c (i & ii) the 0.5 wt% TiO<sub>2</sub> modified nanocomposite membrane's UV/Vis cleaning efficiency was still high after three cycles. It shows that doping TiO<sub>2</sub> with K, B, and N was able to reduce the band gap, increase visible-light absorption with a decrease in the rate of recombination, and function as a powerful photocatalyst for the degradation of fouling agents and xenobiotic compounds during membrane filtration.

They also investigated the stability of the membrane under visible and UV irradiation by examining the permeation flux variations of the unmodified and the 0.5 wt% TiO<sub>2</sub> modified membranes. They reported that after three regeneration cycles with visible light cleaning, it was discovered that the permeation flux of unmodified and 0.5 wt% modified membrane was reduced by around 29.8% and 6.40%, respectively, while the loss of permeation flux values were about 17.3% and 3% with UV irradiation cleaning. Additionally, after three regeneration cycles, neither the unmodified nor the 0.5% TiO<sub>2</sub> modified membranes' ability to remove COD was altered. After three regeneration cycles with Vis/UV

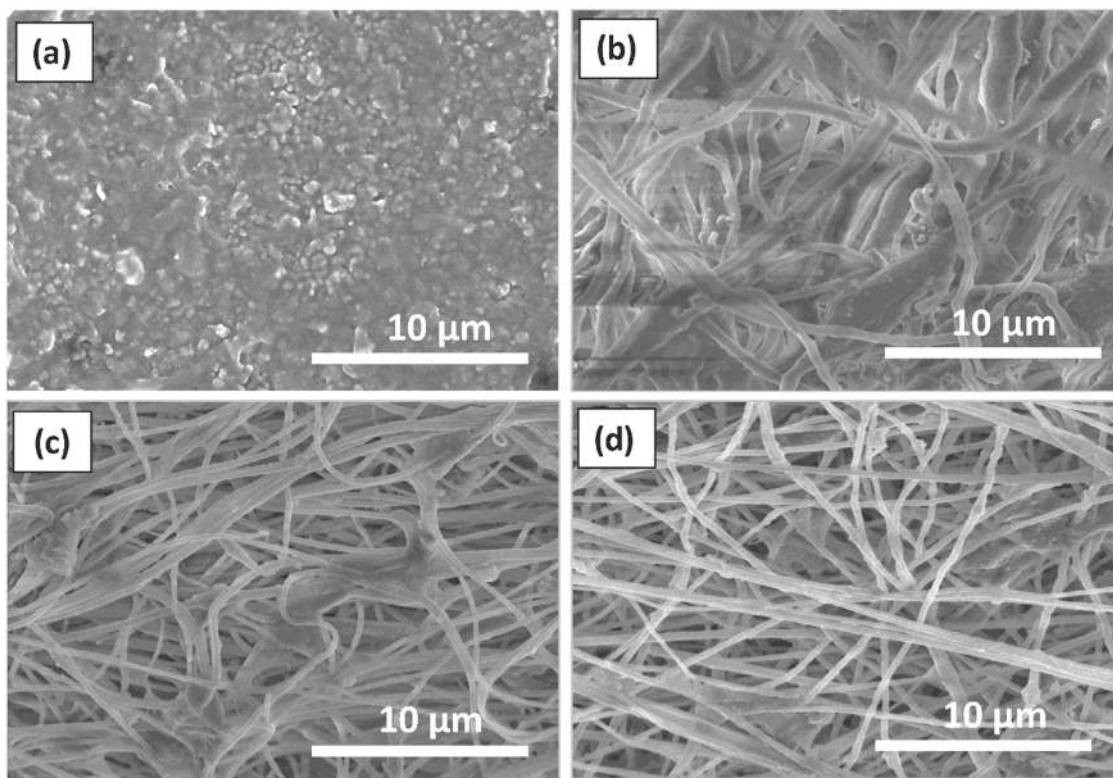


Fig. 8. Surface SEM micrographs of (a) bare  $\text{Al}_2\text{O}_3$ , (b)  $\text{NF}/\text{Al}_2\text{O}_3$ , (c)  $\text{NF-bGCN}/\text{Al}_2\text{O}_3$ , and (d)  $\text{NF-nsGCN}/\text{Al}_2\text{O}_3$  membranes after 180 min OPW filtration. Reprinted with permission Copyright (2019) Elsevier [16].

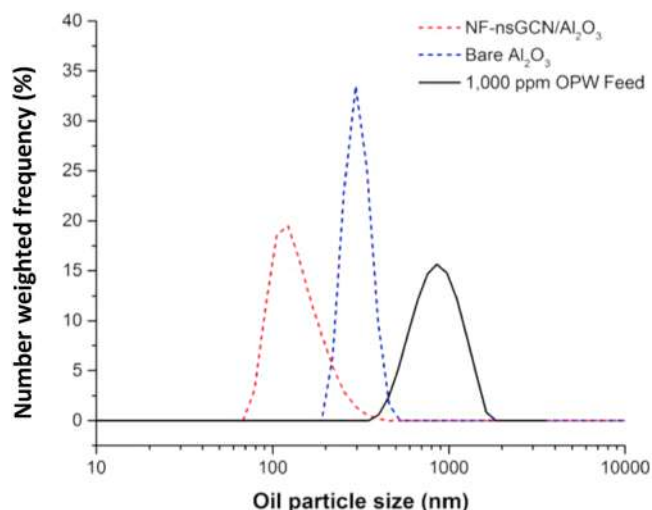


Fig. 9. Oil droplets size distribution in OPW feed and permeate solutions produced by bare  $\text{Al}_2\text{O}_3$  and  $\text{NF-nsGCN}/\text{Al}_2\text{O}_3$  membranes after 3 h. Reprinted with permission Copyright (2019) Elsevier [16].

light cleaning, the results demonstrated that membrane degradation had not occurred.

The photographic images of the surface of unmodified PES and the 0.5 wt%  $\text{TiO}_2$  modified membranes after three cycles of filtration under various cleaning conditions are shown in Fig. 11. According to Fig. 11, the 0.5 wt%  $\text{TiO}_2$  modified membrane is lighter in color than the unmodified membrane after cleaning. This suggested that the triple-doped  $\text{TiO}_2$  NP addition increased the PES's ability to clean itself and be reused.

In separate work, Moslehyani et al. [147] fabricated a PVDF/MWCNT

nanocomposite photocatalytic membrane system for the treatment of petroleum refinery wastewater. They reported that the photocatalytic process resulted in over 90% of pollutant degradation and the UF permeation cell eliminated all contaminants. They reported that the nanocomposite membrane with 1% (w/w) oxidized MWCNTs incorporated into the PVDF matrix was the best nanocomposite membrane for filtration purposes among all of the fabricated membranes.

Lou et al., [148] fabricated a functional PVDF/rGO/ $\text{TiO}_2$  nanofiber web for the removal of oil from water. This was done by incorporating rGO/ $\text{TiO}_2$  nanoparticles into the electrospun solution. In that study, they reported that the PVDF/rGO/ $\text{TiO}_2$  nanofibers with rGO/ $\text{TiO}_2$  concentration of 3% gave the best oil removal from the oil-water emulsion. They reported a removal efficiency of 98.46% under UV light irradiation. They attributed this to the presence of the photocatalytic nanoparticles which aided the degradation of the oil from the oil-water mixture.

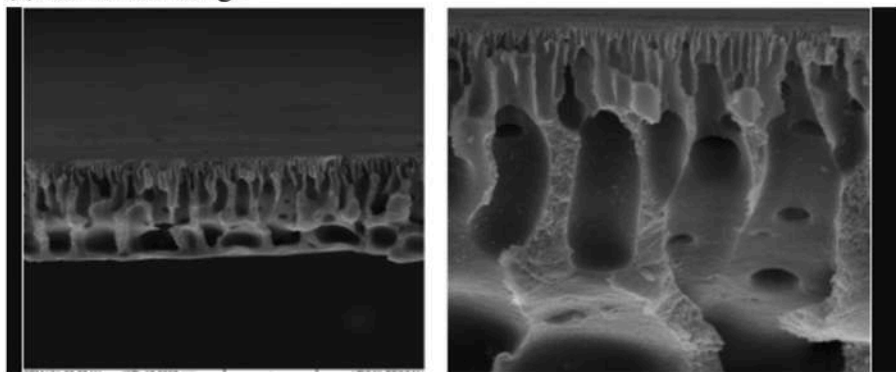
Alias et al., [149] synthesized a photocatalytic graphitic carbon nitride embedded in electrospun polyacrylonitrile nanofibers for the degradation of OPW. They reported that under visible light irradiation, the photocatalytic nanofiber gave 85.4% OPW degradation which was enhanced to 96.6% under UV light. They attributed the photodegradation efficiency to the ability of the PAN nanofibers to adsorb the oil and GCNs ability for photodegradation of the oil. The synergic effect gave rise to effective photodegradation by the photocatalytic nanofiber for the OPW.

Chen et al., [150] fabricated a photocatalytic cellulose acetate membrane decorated by RGO-Ag- $\text{TiO}_2$  for the photodegradation of dye-oil water emulsion. They reported over 99% dye-oil rejection from the oil-water emulsion after six (6) cycles of photodegradation under visible light irradiation. They also reported that the membrane demonstrated a relatively stable dye-oil-water permeation flux of about  $27.5 \text{ L m}^{-2} \text{ h}^{-1}$ .

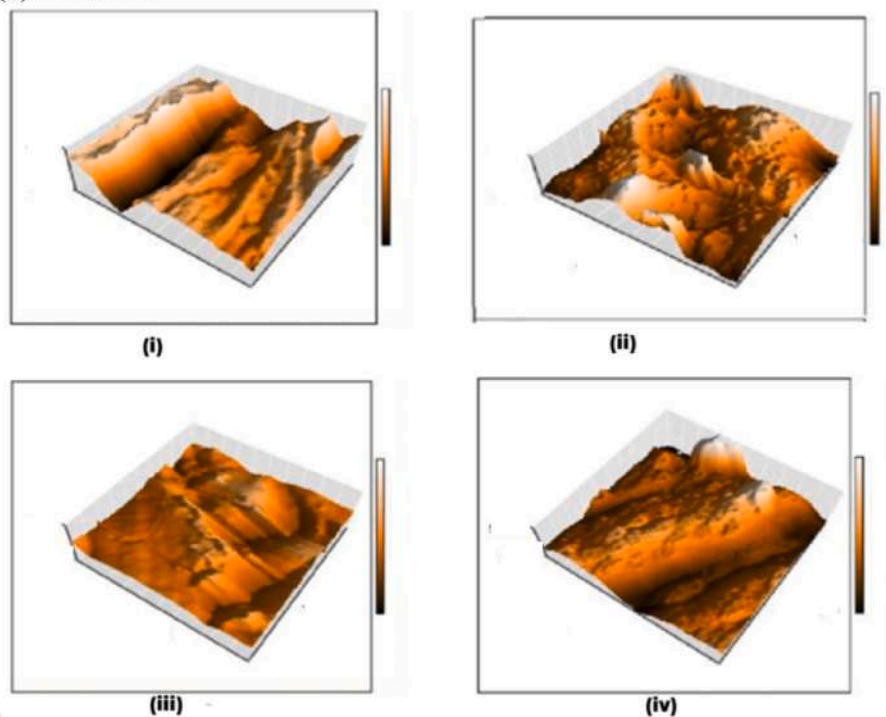
Table 5 presents various studies reported on photocatalytic membranes for oily wastewater treatment. It is evident from Table 5 that the



(a) the SEM image



(b) the AFM



(c) the FRR

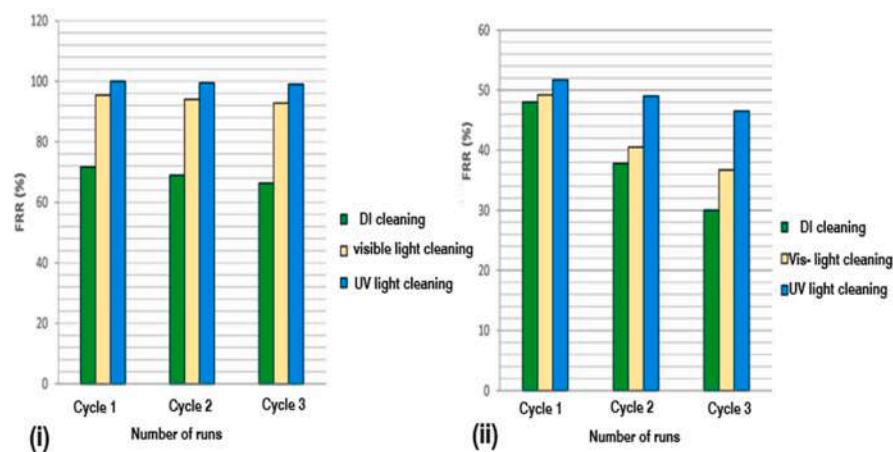


**Fig. 10.** a. The SEM cross-section images of the mixed matrix PES membranes with 0.5% (w/w) K-B-N-TiO<sub>2</sub>. Reprinted with permission Copyright (2018) Elsevier [143]. b- AFM images of modified PES membranes with different weight fractions of the K-B-N-TiO<sub>2</sub> nanocomposite (i) bare PES, (ii) 0.1 wt%, (iii) 0.5 wt %, (iv) 1 wt%. Reprinted with permission Copyright (2018) Elsevier [143]. c-. FRR values of the unmodified membrane (i), 0.5% TiO<sub>2</sub> modified membrane (ii) membranes after reusability tests using distilled water (DI), distilled water and visible light cleaning (DI + VIS), and distilled water and UV light cleaning (DI + UV) irradiation for 60 min. Reprinted with permission Copyright (2018) Elsevier [143].>

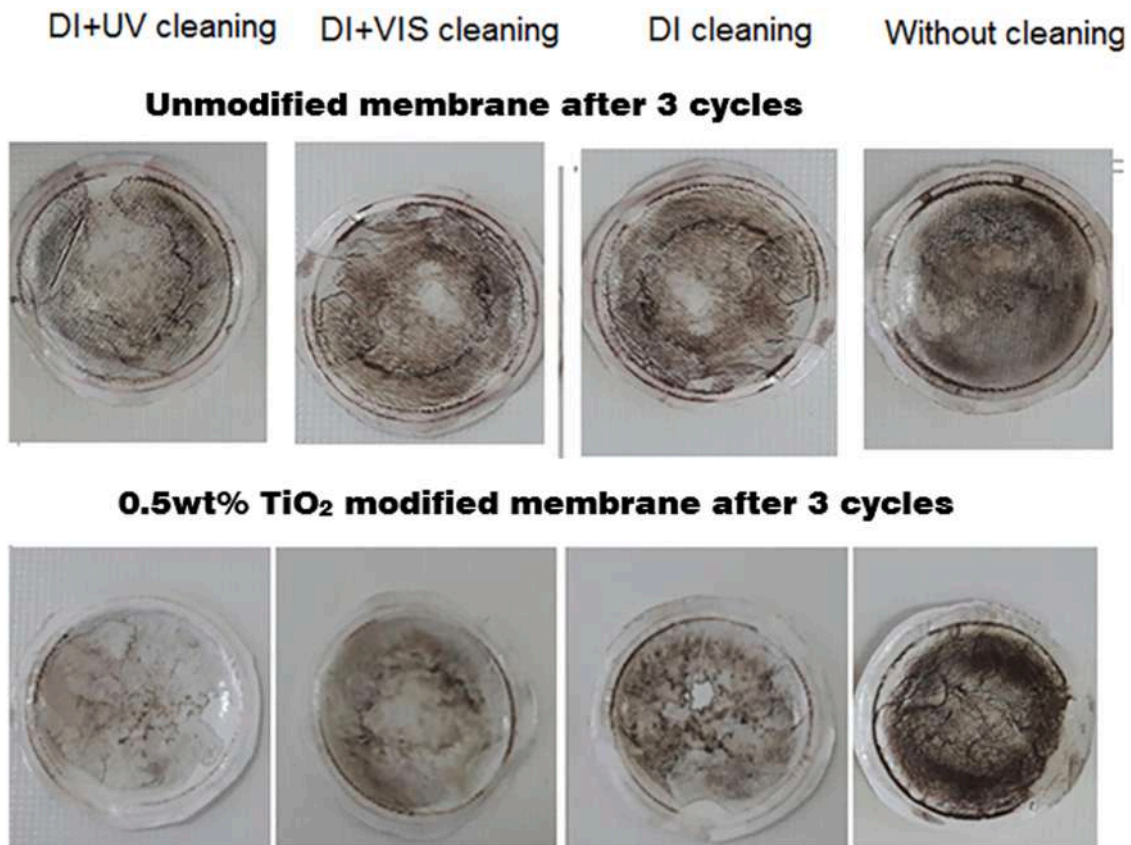


Fig. 11. Digital camera images of the unmodified and the 0.5 wt% TiO<sub>2</sub> modified membranes after three cycles of filtration with various cleaning conditions Reprinted with permission Copyright (2018) Elsevier [143].

various photocatalytic membrane reactors attained over 90% removal of the pollutants present in the oily wastewater. Both the UV and visible light aided the degradation of oil and targeted contaminants in the oily wastewater. When the membrane has a high surface area, it provides additional sites for the photocatalyst to occupy and contribute to efficient degradation. Overall, the combination of the photocatalytic process with membrane filtration gives a synergic effect, which contributes to the efficient treatment of oily wastewater. It is important to note that the light source, configuration, and design of the photocatalyst are important to attain an efficient degradation of target pollutants in oily wastewater.

#### 5.4. PMR separation kinetic for stabilized oil-water emulsion and trace oil contaminants

The fundamental issue, which can cause an irreversible drop in the permeate flux in a membrane, is membrane fouling by suspended or dissolved organic compounds. To tackle this problem, photocatalytic materials can be introduced into the membranes which when exposed to light, can break down these organic compounds formed on the surface of the membrane. Even though these photocatalytic membranes have shown they can restore their original permeability, less is known about how photocatalysis affects the permeate flux's kinetics. Water can selectively pass through a photocatalytic membrane while being repelled by it [159].

It is postulated that the degree of permeate flux recovery in response to light illumination is influenced by a number of experimental factors, including the photocatalytic degradation rate ( $k_p$ ), the active surface area ( $A$ ) of the photocatalytic membrane coating, and the incident light intensity ( $I$ ) [160]. Adsorption, desorption, and photocatalytic degradation of oil molecules are the three main chemical reactions that can

occur when the surface of a photocatalytic membrane used for oily wastewater treatment is exposed to UV or visible light [161,162].

Panchanathan et al., [163] in their work showed that the three reactions above obey the first order kinetics. Now for F-SiO<sub>2</sub> not photocatalytic [164], and N-TiO<sub>2</sub> photocatalytic [165], the following differential equation can be obtained describing a time-dependent photocatalysis-driven evolution of the area fraction of the surface of the membrane contaminated with oil ( $f_c(t_i)$ ):

$$\frac{d}{dt} f_c(t_i) = f_T X \frac{d}{dt} f_{c(T)}(t_i) + f_F X \frac{d}{dt} f_{c(F)}(t_i) \quad (7)$$

where  $f_{(F)}$  and  $f_{(T)}$  are the area fraction of F-SiO<sub>2</sub> and N-TiO<sub>2</sub> respectively. The subscripts F and T and symbolize F-SiO<sub>2</sub> and N-TiO<sub>2</sub> respectively. Solving Eq. (7) by substituting

$$\frac{d}{dt} f_{c(F)}(t_i) = k_{a(F)} f_{nc(F)} - k_{d(F)} f_{c(F)} \quad (8)$$

and

$$\frac{d}{dt} f_{c(T)}(t_i) = k_{a(T)} f_{nc(T)} - k_{d(T)} f_{c(T)} - k_{p(T)} f_{c(T)} \quad (9)$$

where  $k_a$ ,  $k_d$ , and  $k_p$  are the rate constant values for adsorption, desorption, and photocatalytic degradation of oil respectively, on a particular phase (e.g., F-SiO<sub>2</sub> N-TiO<sub>2</sub>), and

$$f_{nc(F)} = 1 - f_{c(F)} \quad (10)$$

and

$$f_{nc(T)} = 1 - f_{c(T)} \quad (11)$$

(i.e., the non-contaminated area fraction of each phase,  $f_{nc(F)}$  or  $f_{nc(T)}$ )

**Table 5**  
Summary of the different photocatalytic membranes for treatment of oily wastewater.

Photocatalyst	Membrane	Light source	Reactor	Water source	Oil rejection (%)	Membrane preparation Technique	Reference
GCN	NF-GCN/Al <sub>2</sub> O <sub>3</sub>	UV	Photocatalytic membrane	Produced water	94	electrospinning	[16]
TiO <sub>2</sub>	TiO <sub>2</sub> /PVDF	UV	Photocatalytic membrane	Produced water	67	Dry-wet spinning	[151]
TiO <sub>2</sub> + HNT	TiO <sub>2</sub> /HNT/PVDF	UV	Photoreactor (TiO <sub>2</sub> ) + filtration (HNT)	Bilge water	98	Phase inversion	[152]
TiO <sub>2</sub>	TiO <sub>2</sub> /PVDF	UV	Filtration + photocatalytic cleaning	Crude oil-water emulsion	96	Physical deposition	[153]
TiO <sub>2</sub> + CNT	TiO <sub>2</sub> /CNT/PVDF	UV	Filtration + photocatalytic cleaning	Crude oil-water emulsion	92	Physical deposition	[142]
RGO-Ag-TiO <sub>2</sub>	RGO-Ag-TiO <sub>2</sub> /CA	Visible light	Photocatalytic membrane	Dye oil-water emulsion	99	Physical deposition	[150]
HMO-TiO <sub>2</sub>	HMO-TiO <sub>2</sub> /PES	UV	Filtration + photocatalytic cleaning	palm oil-water emulsion	99	Phase inversion	[143]
TiO <sub>2</sub> /Fe <sub>2</sub> O <sub>3</sub>	TiO <sub>2</sub> /Fe <sub>2</sub> O <sub>3</sub> /CA	UV	Filtration + photocatalytic cleaning	Surfactant-stabilized oil-water emulsion	100	Physical deposition	[154]
ZnO	PVDF@PDA@ZnO	UV	Filtration + photocatalytic cleaning	Stable oil-water emulsion	99	Facial phase inversion	[155]
TiO <sub>2</sub>	TiO <sub>2</sub> /PVDF/MWCNT	UV	Photocatalytic reactor (TiO <sub>2</sub> ) + filtration (MWCNT)	Petroleum refinery water	99	Phase inversion	[147]
RGO/PDA/g-C <sub>3</sub> N <sub>4</sub>	RGO/PDA/g-C <sub>3</sub> N <sub>4</sub> /CA	Visible light	Photocatalytic membrane	Diesel, gasoline, soybean oil emulsion	100	Physical deposition	[156]
Graphitic carbon nitride (GCN)	Graphitic carbon nitride (GCN) coated on Alumina (Al <sub>2</sub> O <sub>3</sub> )	UV and Vis	Photocatalytic membrane	Produced water	97 - UV (180 min), 85-Vis	Electrospinning	[149]
TiO <sub>2</sub>	PVDF/TiO <sub>2</sub>	UV	Photocatalytic membrane	Produced water	67 (focused on surfactant removal)	Dry-wet spinning	[151]
α-Fe <sub>2</sub> O <sub>3</sub>	Al <sub>2</sub> O <sub>3</sub> /YSZ	Vis	Photocatalytic membrane	Synthetic oily wastewater	98	Phase inversion	[157]
GCN	PAN nanofibers	UV	Photocatalytic membrane	Produced water	90 (partially hydrolyzed polyacrylamide (HPAM))	Electrospinning	[158]
rGO/TiO <sub>2</sub>	PVDF nanofiber webs	UV	Photocatalytic membrane	Oil-water emulsion	98	Electrospinning	[148]

results in:

$$f_{c(i)} = \left\{ \frac{k_{a(T)}}{K_{(T)}} - \left( \frac{k_{a(T)}}{K_{(T)}} - f_{c(T)}(t_i = 0) \right) e^{-K_{(T)} t_i} \right\} X f_{(T)} + \left\{ \frac{k_{a(F)}}{K_{(F)}} - \left( \frac{k_{a(F)}}{K_{(F)}} - f_{c(F)}(t_i = 0) \right) e^{-K_{(F)} t_i} \right\} X f_{(F)} \quad (12)$$

where  $f_{c(F)}(t_i = 0)$  and  $f_{c(T)}(t_i = 0)$  are the initial area fraction of the contaminated regions for F-SiO<sub>2</sub> and N-TiO<sub>2</sub> at the start of visible light illumination respectively, which are assumed to be zero.

Here  $K_{(T)}$  and  $K_{(F)}$  are defined as

$$K_{(F)} = k_{a(F)} + k_{d(F)} \quad (13)$$

and

$$K_{(T)} = k_{a(T)} + k_{d(T)} + k_{p(T)} \quad (14)$$

respectively.

The time-dependent flux of the water-rich permeate under visible light illumination ( $J_{(i)}$ ) can be written as

$$J_{(i)} = \Delta P \left\{ r_m + \frac{R_c}{A} \left( 1 - f_{c(i)} \right) \mu \right\} \quad (15)$$

where  $A$  and  $\Delta P$  are the total surface area of the membrane and the transmembrane pressure respectively.  $R_c$  and  $r_m$  are the oil contamination and the resistance per unit area of the membrane to the permeation of the water-rich permeate originating from the membrane itself respectively.  $\mu$  is the dynamic viscosity of the water-rich permeate (approximately 0.953 mPa-s) [159,166]. The above equation represents the time-dependent evolution of the water-rich permeate flux through the membrane exposed to oil-water upon illumination by visible light.

### 5.5. Influencing parameters for PMRs in water treatment

Photocatalysis is a crucial step in the decomposition of oil and oily wastewater via the PMRs. Several studies have been conducted in recent years to determine the operational parameters for an efficient photodegradation process. The goal of investigating the parameters is to find out optimum conditions for maximizing the photodegradation of target contaminants. Light intensity, pH, the dose of photocatalyst, and substrate concentration are the operational parameters studied [106].

#### 5.5.1. Effect of photocatalyst dosage on photodegradation efficiency

To enhance photodegradation, the amount of photocatalyst available on the photocatalytic membrane is critical. As the photocatalyst's dose increases, its surface area increases as well. The presence of additional active sites on the membrane surface is indicated by the availability of a



large surface area on the membrane. This results in additional reactive-OH and  $O_2$  to complete mineralization.

The photocatalyst dose and degradation rate have a corresponding relationship. When the photocatalyst dose exceeds its optimum level, the degradation rate may be slowed down due to the inhibition of light that penetrates the solution [167]. The optimal loading of  $TiO_2$  in a slurry PMR was 1.5 g/L. When the loading exceeds it, the flux declines due to fouling and this results in a lower treatment efficiency because of the agglomeration of  $TiO_2$  on the membrane [168].

### 5.5.2. Effect of light intensity and quantum efficiency on photodegradation efficiency

Photocatalytic reaction rates can be boosted by light intensity. Beyond the ideal intensity, the photon energy distribution determines the reaction rate [169,170]. Therefore, high quantum efficiency is critical in PMR. The quantum efficiency depends on the rate of radiant energy absorption and the radiative field distribution. The amount of

light that reaches the photocatalyst surface is determined by the photocatalyst loading and the reactor geometry. Therefore PMR's rational design is critical to achieving optimum quantum efficiency.

Jia et al. [171] used  $TiO_2$ /activated carbon to study the photodegradation rate of phenol under a UV light irradiation at pH 7.5 with 40 mg/L of initial phenol concentration. The light intensity ranged from 0.875 to 2.625 W/L. When the light intensity increased, the photocatalytic degradation improved. The photon energy was limited at low light intensities. Therefore, only a few reactive radicals were formed. As the intensity of the light grew, the production of free radicals increased because of the large number of excited  $e^-/h^+$  pairs. When the light intensity exceeded 1.75 W/L, the increase in photodegradation performance was negligible. [172].

As a result, the reaction between target molecules and the active sites became faster, increasing the photodegradation rate. When light intensity exceeded its optimum level, it was no longer a limiting factor in the rate of photodegradation [173]. Due to the increasing temperature,

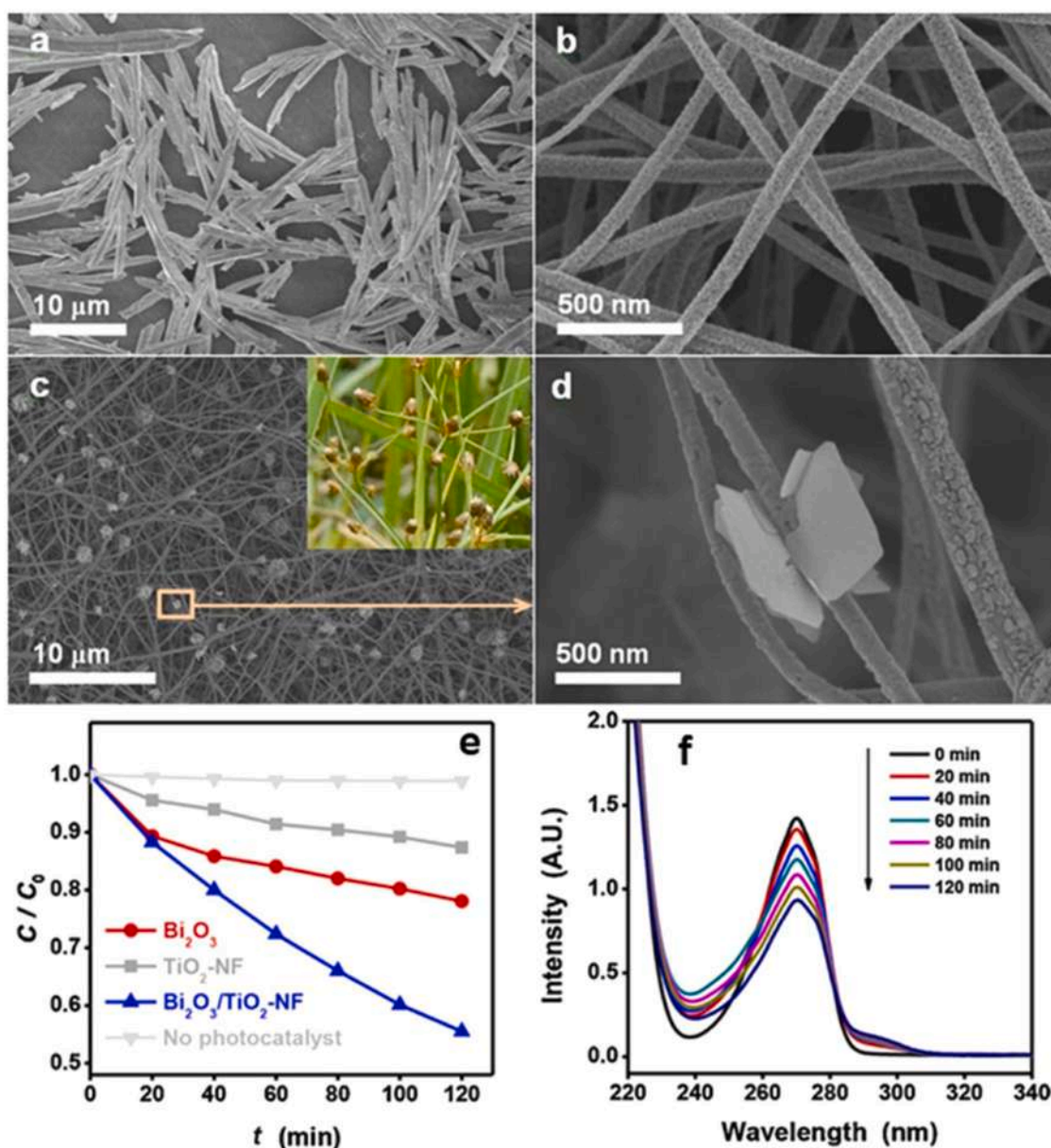


Fig. 12. Field emission SEM images of (a)  $Bi_2O_3$ , (b)  $TiO_2$  nanofiber, and (c) and (d) hierarchical  $Bi_2O_3/TiO_2$  fibrous composite; (e) phenol photodegradation curves using  $Bi_2O_3$ ,  $TiO_2$  nanofibers, and  $Bi_2O_3/TiO_2$  fibrous composite; (f) temporal evolution of the UV spectra of the phenol solution using  $Bi_2O_3/TiO_2$  fibrous composite. Reprinted with permission Copyright (2020) Elsevier [175].

the excessive light intensity would cause  $e^-/h^+$  pair recombination, which decreased photocatalytic activities [174].

### 5.5.3. Effect of catalyst morphology on photodegradation efficiency

Morphological structures determine the specific surface area for contaminants' adsorption on photocatalyst surfaces. High specific surface areas are achieved using a hierarchical structure to improve photocatalytic activities. Rongan et al. [175] reported that a hierarchical  $\text{Bi}_2\text{O}_3/\text{TiO}_2$  fibrous composite had a specific surface area of  $51 \text{ m}^2/\text{g}$ , while pure  $\text{Bi}_2\text{O}_3$  had  $4 \text{ m}^2/\text{g}$ . The  $\text{Bi}_2\text{O}_3/\text{TiO}_2$  fibrous composite with 4–60 nm mesopores demonstrated an outstanding phenol photodegradation among the other three photocatalysts due to its slit-like mesoporous hierarchical structure (Fig. 12(a)–(d)). (pure  $\text{Bi}_2\text{O}_3$ ,  $\text{TiO}_2$  nanofiber, and  $\text{Bi}_2\text{O}_3/\text{TiO}_2$  fibrous composite) (Fig. 12 (e) and (f)).

Photocatalyst physical and chemical stability are critical to boosting photocatalytic performance. The photocatalysts' stability is ensured by their resistance to deactivation due to light irradiation and the hostile environment (acid or basic pH). The stability of the chosen photocatalyst depends on pore size and crystalline structures [176].

### 5.5.4. Effect of pH of the solution on photodegradation efficiency

Due to the effect of the pH solution, the properties of the surface charge or zeta potential on photocatalyst, adsorption behavior, and the aggregate size formation of the compounds may change [177]. pH has a relationship with membrane charge or zeta potential. At high pH, the membrane pore surface becomes more negative and this is due to the type of material used in the membrane fabrication [178,179]. The redox reaction is affected by changes in surface potential. When the pH rises, the amount of  $\text{OH}^-$  in the solution increases, improving the pollutant's removal.

Emam & Aboul-Gheit [177] studied the photocatalytic degradation of oil in seawater using  $\text{TiO}_2$ . They found that pH influenced the degradation rate of the oil. Khezrianjoo & Revanasiddappa [180] reported a photodegradation of *m*-cresol utilizing ZnO and found that the photodegradation rate was affected by the number of  $\text{OH}^-$  in solution and the electrostatic attraction between catalysts and substrates.

ZnO has a  $\text{pH}_{\text{pzc}}$  (point of zero charges) of 9.0 [181]. Khodja et al. [182] reported that the catalytic activity of ZnO is adversely affected at  $\text{pH} < 4$ , as the catalyst is photodecomposed. Under alkaline conditions, the repulsive electrostatic contact between the negatively charged catalyst surface and the anionic dye became stronger. The repulsive force between them became important as the  $\text{pH} > \text{pH}_{\text{pzc}}$ , resulting in a reduction in the amount of adsorbed substrate [183]. Consequently, this had a negative impact on the photodegradation rate.

## 6. Self-cleaning and anti-fouling properties of PMRs in oily wastewater treatment

During the filtration process, impurities accumulate onto the membrane's surface and in its pores, causing fouling. Suspended inorganic solids (inorganic fouling), organic colloids, soluble inorganic chemicals (scaling), living/growing microbes (biofouling), and organic macromolecules (organic fouling) contribute to fouling [9,184–186].

In oil-polluted water, scaling is induced by hydroxide and salt precipitation, whereas oil droplets are the cause of fouling in the pores and surface blockage [186]. The characteristics such as physico-chemical properties and concentrations, membrane properties like hydrophilicity, charge properties, and surface roughness, and operational conditions like temperature, applied transmembrane pressure, flow velocity, and recovery can affect the fouling layer [187,188].

Electrostatic and Van der Waals forces of interactions between the membrane surface and colloidal particles determine the fouling mechanism [189–191]. Ionic strength, droplet size, pH, temperature, and emulsifier concentration also influence the interactions between the contaminant and the surface of the membrane during the treatment of oil-contaminated water [2,153]. It is, therefore, necessary to investigate

the variation, as they influence membrane efficiency, performance, pore, and fouling [192–195].

Contaminants in oily wastewater can form a hydrophobic layer, resulting in a barrier to water on the surface of the membrane and causing a declining flux, decreased life span, and difficulty in cleaning. This increases energy consumption and treatment cost [31]. Several studies have been carried out to address these issues to make membrane technology for the treatment of oily wastewater become efficient.

Membrane modification, enhanced cleaning processes, hydrodynamic surface shearing, and application of pretreatment are useful to prevent membrane fouling [184,196]. Another way to cope with flux decline is to improve the membrane's hydrophilicity, which reduces sticky contacts between the membrane surface and the foulants. Sulfonation, carboxylation, grafting, and plasma treatments are examples of the techniques used [13,69,80,197].

The use of hydrophilic materials in membrane modification is another strategy to prevent oil droplets from adhering to the membrane's surface and maintain low-level filtration resistance. Hydrophilicity is defined by the contact angle  $\alpha$  between the membrane surface and a droplet of water. A lower contact angle indicates more hydrophilicity [81]. Membrane materials are hydrophobic, which interferes with the interactions between the surface of the membrane and water molecules, and prevent water from passing through the membrane. The hydrophobic nature of membrane materials induces fouling by allowing hydrophobic molecules to attach to the membrane's surface, forming a thick layer on the boundary [68,81].

It is therefore significant to increase the membrane hydrophilicity by modifying their properties. Regular shutdowns of filtration for cleaning the membrane and recovery of permeability tend to increase the cost of the membrane filtration, while chemical consumption in the filtration reduces the lifespan of the membrane. Consequently, this increases the costs of the filtration process [196].

For this reason, the development of membranes with excellent antifouling and self-cleaning properties from hydrophilic photocatalytic nanomaterials is a promising technique, as the organic foulant can be effectively decomposed or degraded. In most cases producing non-toxic substances without producing any secondary pollutants using solar irradiation [79,92,93,198]. The self-cleaning and photocatalytic mechanisms work altogether to prevent deposition of adsorb foulants, and degrading them using a photocatalyst (Fig. 13) [199,200].

Excellent antifouling and self-cleaning ability of membranes are crucial for the treatment of oily wastewater due to the oil-in-water emulsion process. Zhang et al. [201] synthesized a hydrophilic photo-Fenton-like catalyst. The GO/Fe MOF-assembled polyacrylonitrile (SPAN) nanofibrous membrane with self-cleaning and anti-fouling properties was used to inhibit the accumulation of oil droplets on the membrane surface. They reported that the membrane had a permeation ranging from 920 to 7083  $\text{Lm}^{-2}\text{h}^{-1}$  and separation efficiency of 96%. They also observed that the membrane had a flux recovery ratio of  $> 96\%$ . This indicates that the membrane exhibited anti-fouling and self-cleaning properties during the filtration cycle.

Cai et al. [26] prepared a series of visible-light-driven self-cleaning 2D heterojunctions performing heterostructured membranes for oil-in-water emulsion separation. The presence of g-CN and  $\text{Bi}_2\text{O}_3\text{CO}_3$  (BOC) heterojunction also referred to as BOC with visible light catalytic properties efficiently avoided a sharp decrease in permeation flux and membrane fouling. They tested the self-cleaning ability of the CN@BOC heterojunction by degrading 1000 mg/L of soybean oil-in-water emulsion for 1 h under simulated light and found that the white emulsion turned into a colorless solution after 1 h of irradiation. The oil and water contact angles for the fabricated GO/PG/CN@BOC heterojunction membrane and other prepared membranes as determined are shown in Fig. 14a. Since for waste-water treatment, the membrane surface's wettability is crucial, they, therefore, tested the wettability of the fabricated GO/PG/CN@BOC heterojunction membranes by measuring the contact angles of organic solvent and water in the air and the organic

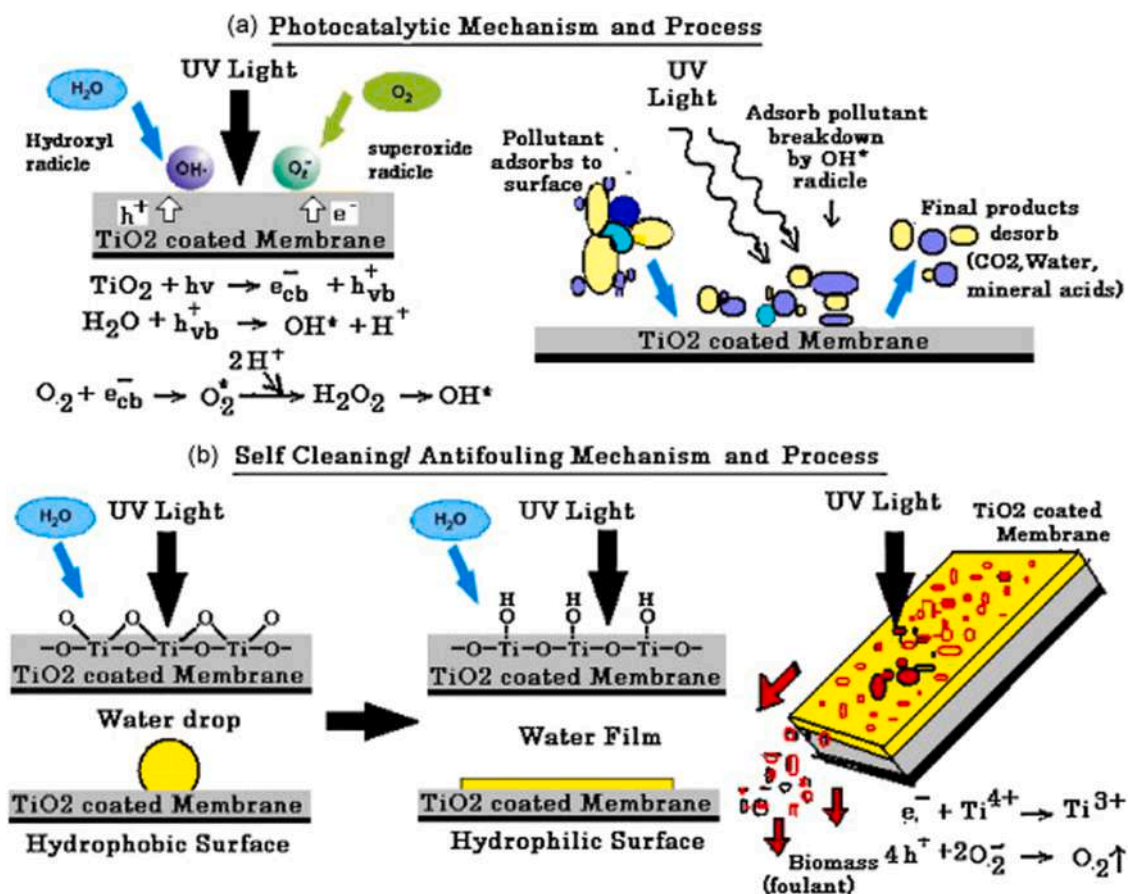


Fig. 13. (a) Photocatalytic mechanism and process. (b) Self-cleaning/antifouling mechanism and process of PVDF/TiO<sub>2</sub> membrane. Reprinted with permission Copyright (2009) Elsevier [200].

solvent's contact angle underwater.

They claimed that the fabricated 2D heterojunction membrane had superoleophobic properties underwater but was both lipophilic and hydrophilic in air. The water contact angle (WCA) of the GO/PG membrane was less than that of the GO/PG/CN membrane because of the more hydrophilic nature of GO/PG than g-CN. But as the amount of the CN@BOC heterojunction grew, the contact angle with water reduced due to the high hydrophilicity of Bi<sub>2</sub>O<sub>2</sub>CO<sub>3</sub> (Fig. 14a). The GO/PG/CN@BOC-3 and GO/PG/water CN@BOC-4's contact angles declined by 10° in just 2 min, and both values fell below 10° in just 15 min.

According to their findings, the fabricated 2D heterojunction membrane exhibited superoleophobic properties when underwater but was both lipophilic and hydrophilic in air. They observed that GO/PG membrane had a smaller water contact angle than the GO/PG/CN membrane because GO/PG is more hydrophilic than g-CN. However, due to the high hydrophilicity of Bi<sub>2</sub>O<sub>2</sub>CO<sub>3</sub>, the contact angle with water decreases with an increase in the amount of CN@BOC heterojunction (Fig. 14a). Additionally, they observed that within 2 min, the water contact angles (WCAs) of the GO/PG/CN@BOC-4 and GO/PG/CN@BOC-3 membrane decreased by 10° and the contact angle for both membranes fell below 10° in 15 min.

They also investigated the stability of the fabricated GO/PG/CN@BOC heterojunction membrane and reported that significantly, the fabricated GO/PG/CN@BOC membranes were free-standing, flexible, and continuous after the substrate was dissolved by dimethylacetamide (Fig. 14c).

Additionally, they presented a schematic view of the oil contact angle (OCA) underwater for the original GO/PG/CN@BOC-3 membrane, OCA after contamination with soybean oil and after further

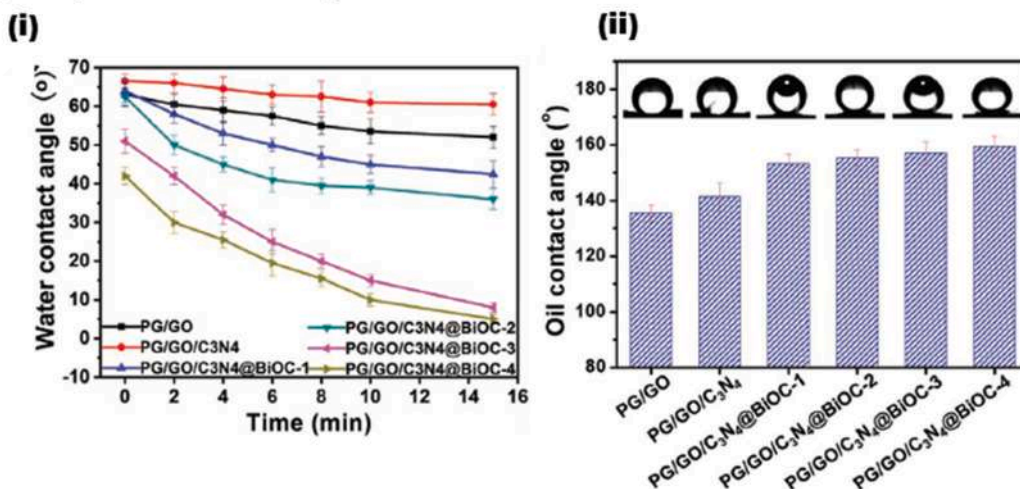
irradiation by sunlight. Following the fouling by oil, they found out that the OCA of the CN@BOC membrane decreased from 160° to 95° (Fig. 14b), indicating a loss of superoleophobicity. After exposure to the light for 1 h underwater, the membrane regained superoleophobicity. The results supported the heterojunction's high photodegradation performance over the GO membrane, indicating the anti-fouling and self-cleaning ability of the membrane.

Wang et al. [202] prepared a novel and multifunctional polyvinylidene fluoride-co-hexafluoro propylene (PVDF-HFP)/catechol-polyethyleneimine (CA-PEI)/Ag/3-glycidyloxy propyltrimethoxy silane (KH560) tubular nanofiber membrane (TNM) for dye degradation and oil/water separation. They used Ag nanoparticles on the surface of the nanofiber to improve the membrane's catalytic capacity for the degradation of Congo red and methylene blue (MB). They found that the modified KH560 membrane with 3% (w/w) became more hydrophilic and could catalytically separate oil-water emulsion over ten (10) cycles of the test without any decay in the membrane. This performance indicates its self-cleaning capability.

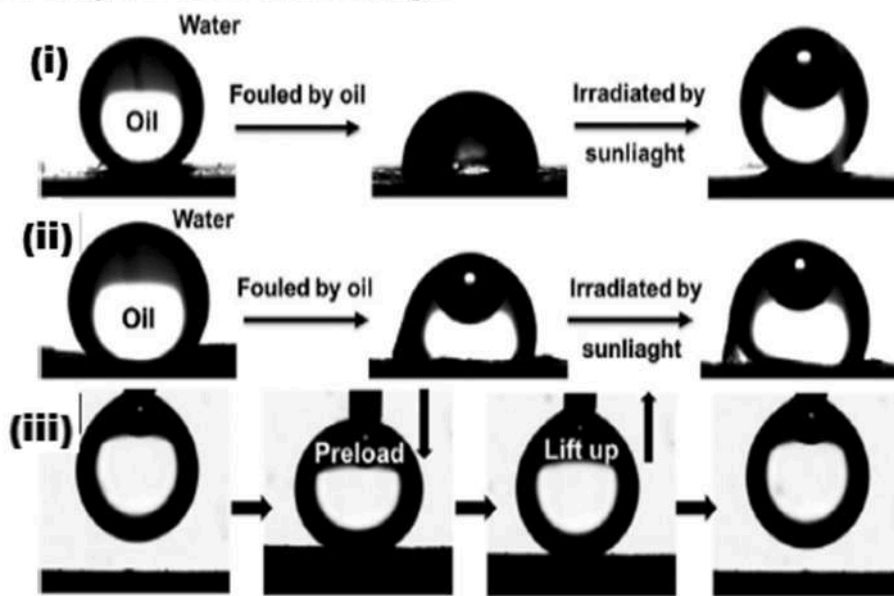
Liu et al. [203] fabricated a super hydrophilic composite photocatalytic membrane with self-cleaning and degradation ability based on LDH and g-C<sub>3</sub>N<sub>4</sub> photocatalyst. For photocatalytic degradation and pollutant separation, the PVDF/LDH@g-C<sub>3</sub>N<sub>4</sub>@PDA/GO composite membrane performed excellently. They reported a degradation rate of 93%, 97%, 92%, 95%, and 100% for the diesel, gasoline, petroleum ether, rhodamine B (RhB), and MB, respectively. The fabricated membrane exhibited high efficiency and stability with high flux and rejection for the pollutants over ten (10) cycles of filtration. This suggests that the photocatalytic degradation demonstrated a superior photocatalytic, self-cleaning, and anti-fouling ability. Liu et al., [152] synthesized a sunlight-driven 2D heterostructure photocatalytic membrane with



(a) the plot of contact angle



(b) the diagram of the contact angle



(c) the photographic picture

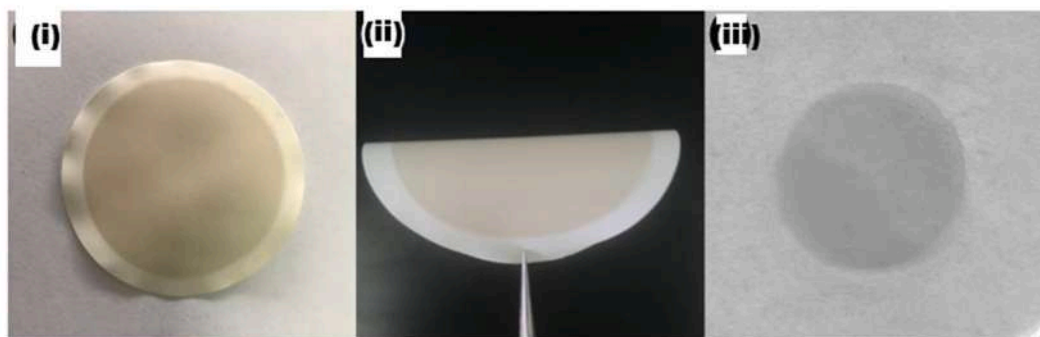


Fig. 14. a -(i) Water contact angle in air; (ii) Oil contact angle underwater for GO/PG/CN@BOC 2D heterostructure membranes. [26]. b - Oil contact angle underwater: (i) original GO/PG/CN@BOC-3 membrane (left), the membrane after contamination with soybean oil (middle), and the membrane after further irradiation by sunlight (right); (ii) original GO membrane (left), the membrane after contamination with soybean oil (middle), and the membrane after irradiation by sunlight (right). (iii) Oil adhesion test after self-cleaning of membrane underwater [26]. c -The photograph of (i) the fabricated GO/PG/CN@BOC heterojunction membrane (ii) the flexible (iii); the stability after dissolved by dimethylacetamide [26].

self-cleaning ability for efficient oil-water separation. When the fabricated membrane was used for oil-water separation, it had an initial permeate flux of  $4536 \text{ Lm}^{-2}\text{h}^{-1}\text{bar}^{-1}$ . With continuous filtration, however, the flux decreased due to the adsorption of oil droplets on the surface of the membrane, while after exposure of the membrane to sunlight, the membrane maintained a flux recovery ratio (FRR) of higher than 95% after ten (10) cycles of the filtration process. This reveals excellent anti-fouling and self-cleaning properties under sunlight irradiation.

Table 6 summarizes the ability of fabricated membranes to exhibit anti-fouling and self-cleaning properties. Due to its hydrophilic and photocatalytic properties on the same surface,  $\text{TiO}_2$  is good support for self-cleaning photocatalytic membranes [204]. The fabricated membranes had high flux depending on the oil content in the oil-water emulsion. With light oils, the flux was higher than that with heavy oils. Table 6 also shows that most of the membranes had over 90% oil

rejection rate during the separation of oil-water emulsion. They exhibited a high flux of recovery ratio after several filtration cycles under UV Vis irradiation. With proper design and fabrication methods, the membranes can do self-cleaning and be re-used for several cycles of filtration with high efficiency.

## 7. Influencing factors for Scale-up of PMR

There have not been any noteworthy large-scale applications of PMRs in the field of water/wastewater treatment despite intensive study on a number of features of PMRs and their well-known characteristics. A thorough evaluation of the three potential technological components (membranes, light source, and photocatalysts,) and their interactions indicates that each technological readiness level (TRL) is currently low (at about ; 4–5); as a result, significant developmental work is needed to

**Table 6**  
Summary of PMRs with self-cleaning and anti-fouling properties for oily wastewater treatment.

Membrane	Feed concentration/ operating conditions	Pure water flux ( $\text{L.m}^{-2}$ $\text{h}^{-1}\text{bar}^{-1}$ )	Application (Foulant)	Rejection rate %	Light source	Flux recovery ratio (%)	Reference
GO/MCU- $\text{C}_3\text{N}_4$ /PVDF	Ddf Oil = 100 ppm, SDS= 0.2 mg/L Pressure = 1 bar, with 4 cycles of filtration	1281	Oil/water emulsion	> 98	Visible	92.36	[205]
SPAN@GO/M88A	Oil= 2 ML, Water = 200 ML, SDS= 50 ppm, with 3 cycles of filtration	920–7083	Oil/water (diesel/water)	99	UV-Vis	> 96	[201]
MXene@CS/TA- FeOOH	Span-80(0.1 g), oil: water (1:99), pressure= 1 bar	500.38–1022.7	Oil/water emulsion ( petroleum ether crude oil)	100	UV-Vis	> 96%	[206]
N- $\text{BiO}_2\text{CO}_3$ @MXene/ PES	Oil: water (1:100), SDS= 0.15 mg/mL Pressuere= 0.1Mpa with 5 cycles of filtration,	815.3	Oil/water emulsion	> 99	Visible	> 95%,	[207]
GO/PG/g- $\text{C}_3\text{N}_4\text{OBi}_2\text{O}_2\text{CO}_3$	Oil= 1000 ppm, SDS= 0.1 g, with filtration time of 1 hr.	420	Oil-water emulsion separation	–	Vis	> 96%	[26]
PVDF-HFP	Tween80 = 0.5 g, 500 g water, 5 g oil, Pressure 0.02Mpa, with 10 cycles of filtration	799	Oil and water separation/ dye degradation.	98	UV/Vis	> 95%	[208]
PVDF/LDH@g- $\text{C}_3\text{N}_4$ @PDA/GO	SDS = 0.2 mg/m, oil:water (1:100), lPressure 0.1Mpa, with 10 cycles of filtration.	397.14	Gasoline, diesel, and petroleum ether removal	96.74, 93.22, and 92.35, respectively.	UV light	> 90%	[203]
GO/g- $\text{C}_3\text{N}_4$ @ $\text{TiO}_2$	Oil/SDS= 1000 ppm,With 10 cycles of filtration	Reached 4536	Oil-water separation	99	Visible	> 95	[152]
FP- $\text{Fe}_2\text{O}_3$ -STA	Water = 20 g, Oil(toluene) = 20 g, With 6 cycles of separation	80	Oil/water (toluene, trichloromethane, and n- hexane)	> 89	UV	> 80%	[209]
ZIF-8 @GSH/PI	Oil: water (1:50), Span 80 (0.1 wt%), 10 cycles of filtration	5632.98	Oil/water (Kerosene, Toulene, hexane)	> 99	UV	> 90%	[210]
Nanostructured $\text{TiO}_2$ mesh membrane	Oil/water mixture (50% v/ v), with 10 cycles of filtration	16954	Oil/water (Heavy and light oil)	> 99	UV	> 99.2	[211]
Carbon Cloth (CC) @ $\text{TiO}_2$ @Ag	Oil dyed with Sudan III= 5 mL, Water= 5 mL with 60 cycles of filtration. (Low viscosity oil)	8840–9008 (Soyabean oil, diesel), 9729–10682	Oil/water (Soyabean, diesel, light oils)	99	Visible	> 90%	[212]
Stereocomplex Polyactide (GTsc) -GA- $\text{TiO}_2$ coated scPLA(GTsc)	Oil= 1 mL, water = 100 mL, SDS= 20 mg, with 15 cycles of filtration	$4200 \text{ Lm}^{-2}\text{h}^{-1}$	Oil/water (n-hexane/ water mixture)	> 99	UV	> 97%	[213]
PKCN/PVDF (carbon nitride membrane)	Oil: water (1:99), Tween 8 0 = 10 mg, pressure = 1 bar, With 10 cycles of filtration	129	Oil/water	> 99	Visible	96.5	[214]
PANI/ $\text{TiO}_2$ modified mesh	Oil:water (1:1) = 80 mL, with 100 cycles of filtration.	46,000–176,000	Oil/water (diesel, toluene, etc)	100	UV-Vis	> 90%	[215]
CC@ $\text{TiO}_2$ -Cu	Oil = 5 mL dyed with Sudan III, water = 5 mL, with 80 cycles of filtration	6.64 (Soyabean), 7.00 (1,2-dichloroethane, 8.97 (Petroleum ether, 8.57 (Toulene)	Oil/water (Soyabean, petroleum ether, 1–2- di- chloroethane, toluene)	99.6%	Visible	> 99%	[216]
CNT@CS/TA-FeOOH	Oil = 10 g, water = 1 L, Tween 80 = 0.1 g, Pressure = 0.5 bar	4300–5700	Oil/water	> 99%	Sunlight irradiation	> 97%	[217]

make PMR systems appealing and prepared for commercialization (with  $TRL = 9$ ). The need to create cutting-edge, environmentally friendly, and socially responsible technology should serve as the driving force behind these efforts. Considerable research and development (R&D) is needed to move the PMR process toward commercialization, with a focus on testing and demonstration in real environment and pilot plants to improve important design and performance parameters such as hydraulic residence time, concentration, type of photocatalyst, and apparent quantum efficiency,

It is important that in PMRs scale-up, technical challenges be given priority in R&D. It will be feasible to accurately identify environmental indicators (such as environmental footprint/ $CO_2$ , total processed water unit cost) and process economic following PMR pilot-scale testing/demonstration. In general, no substantial scale-up challenges are anticipated due to the modular nature of PMR components, and the stages toward PMR full-scale development seem simple. However, since such a novel hybrid process would compete in the market for a place that is characterized by well-entrenched conventional processes and conservatism, operating with reasonable reliability for an extended period of time, the pilot PMR data must be reasonably accurate and the various performance indicators must be attractive.

However, a few distinct merits of the PMR technology over conventional methods, particularly in regard to the overall environmental performance highlighted in recent years including lack of addition of oxidants and minimization or elimination of side reactions or streams, may prove to be a deciding factor in favor of large-scale PMR applications [218].

## 7.1. Economic issues

### 7.1.1. Equipment-capital expenses

For PMR process researchers and developers, a fairly thorough and trustworthy economic analysis of an industrial-size PMR system that links construction, operation, and process equipment design to respective cost parameters (primarily treated water per unit cost) is essential because it makes it easier to evaluate and prioritize those aspects and problems of the technology which need to be addressed to achieve the desired advancement. For a novel PMR process, the same technique that applies to typical process engineering projects can also be applied. The fundamental work is designing equipment, specifying it, and estimating costs; as a result, the kind of equipment utilized and its accessibility on the market plays a key role in the development of new processes. Additionally, in comparison to the conventional membrane separation process, more related uncertainties and significant design issues exist in PMRs which have a negative impact on cost estimation [219].

Overall, it is anticipated that data obtained from a novel PMR pilot plant operated under practical conditions would help to considerably reduce those uncertainties that may exist and will enable fair and reliable estimations of operating and capital expenses. The modular design of both membrane and UV/Visible light equipment will also make it easier to scale up from pilot to full scale, making it easier to estimate capital costs.

### 7.1.2. Operating expenses

The specific cost items, such as the cost of energy, membrane, chemicals, capital, UV/Visible lamp replacement, and personnel (including maintenance and supervision) are pretty well defined when it comes to operating expenses, which are converted into total treated water unit cost ( $\text{€ m}^{-3}$ ). Pearce, [220] reported that considering experience with comparable water treatment processes, it is anticipated that the main cost components for any module of PMRs will be capital expenditures and membrane stability (membrane replacement and performance restoration) with the biggest source of uncertainty relating to energy use [219,220]. Generally, the challenges surrounding the most effective system geometric configuration in conjunction with the effective use of UV/Visible light, are prevalent in all types of PMR and

demand top priority in the task relating to its technological development.

## 7.2. Technical issues

### 7.2.1. Photocatalytic system morphology and design

The configuration and morphology of the system have a significant impact on whether the primary goal of PMR technological development and process design, i.e., minimizing specific energy consumption (SEC), treatment cost measured in terms of a unit volume of purified water, and overall environmental impact, is achieved. Indeed, the latter has a direct impact on operating costs, capital costs, and energy efficiency (in the use of solar and artificial light). Choosing the best photocatalytic system's morphology is therefore a fundamental task in the technological development and scale-up of the PMR and this is given top priority in the order of steps for process design [218].

The two basic types of PMR design or configuration based on photocatalyst usage are PMRs that utilize photocatalysts immobilized on a substrate material such as stainless steel, polymers, and ceramic, and PMRs that employ powdered photocatalysts dispersed in water or liquid. The most prevalent systems discussed in the literature are those PMR with dispersed photocatalysts because they have more active surface area accessible than immobilized systems, which may make them more effective. Their configuration, therefore, affects the effectiveness of the system which in turn affects the possibility of scale-up [21,218].

### 7.2.2. Mode of operation of the PMR

The preferred mode of operating PMR system for industrial purposes is continuous, with the primary operating conditions including energy requirements pollutants removal rate, and treated water volumetric throughput, which is essentially constant. However, there can be situations of interest such as for small treatment operations where batch or semi-batch operations are used. The primary problems when trying to maintain continuous PMR operations are connected to membrane degradation caused by material aging such as pinhole development and as well fouling results in decreased separation effectiveness and increased operating pressure respectively. As a result, measures to control or mitigate these operating problems with proper performance assessment techniques are required [221,222].

Another issue is the cleaning of the UV light sources employed for the PMR which are commercially accessible as mercury lamps housed inside cylindrical glass sleeves for water applications. Standard ways are available to clean up those sleeves from potential deposits automatically [223]. Such a periodically used cleaning technique was found to be efficient in removing deposited photocatalyst particles from UV lamp sleeves, preserving constant UV light emission, in a recent PMR pilot [224]. The heat release and corresponding rise in treated water's temperature caused by UV power utilization in a PMR system are problems that could have an adverse overall impact, especially in applications needing long hydraulic residence times (HRT).

Another crucial aspect of the operation of the PMR system is air bubbling or aeration. Two primary purposes of air bubbling are to maintain the concentration of dissolved oxygen in the treated water and to produce agitation of fluid close to the surfaces of the membrane, particularly in the case of the submerged membranes, which causes fluid shear stresses that typically reduce fouling [221,222]. However, practical experience with submerged UF membranes in a bit to optimize aeration rate, shows that increased nonoptimized aeration can greatly increase water treatment unit cost. Some research has substituted sparging oxygen for air bubbling; nevertheless, it is unlikely that doing so will improve photocatalytic processes [225].

These important issues have not received sufficient attention thus far and ought to be a research and development item for inclusion in practical pilot projects. A critical investigation based on the variation of the main values of operating parameters, largely through permeate quantitative and qualitative studies, can be made in the operation of



plants indirectly by assessing the photocatalyst performance or efficiency to identify stability and efficiency in contaminant degradation.

### 7.3. Sustainability issues

Recent years have seen the acceptance of the "triple bottom line" (TBL) technique for sustainability, i.e., considering social, environmental, and economic criteria, to determine the best water and wastewater treatment technology for a given application. This is crucial when making investments in large-scale operations since the used technologies should satisfy specific and connected sustainability "pillars" within the allotted amounts of time and space. Literature has described PMR as a sustainable and green technology that can compete with other traditional and cutting-edge water treatment methods.

This evaluation is mostly based on the environmental performance of the technology exclusively in laboratory-scale studies, without taking other pertinent effects, like social and economic into account. However, assessment of the PMR social impact and economic performance is an essential component of the sustainability assessment for future studies considering promising PMR technology, providing scientific backing in the choice of the best among competing sustainable technologies [219].

A project for water treatment should be evaluated for sustainability from a sufficiently broad regional and temporal viewpoint. Regarding the latter, all project-related actions and factors should be taken into account, including planning, designing, building, commissioning plants, operating them, and even decommissioning. Spatially, a study should take into account potential consequences that may be felt outside the immediate region of the plant, as is the case with "greenhouse gases" released in connection with the disposal of plant effluents and energy consumption. Various techniques now employed to evaluate the effects of water/wastewater treatment facilities, include the driver- pressure-state-impact-response (DPSIR) method, best available technology (BAT), life cycle assessment (LCA), and the environmental impact assessment (EIA)[226].

Therefore, in a complex, dynamic, and uncertain environment where water and wastewater treatment operations would be done, PMR technology can be seen as a viable and logical choice, maintaining a minimum variation in its sustainability performance.

### 8. Future direction of research of PMR

The degree of mineralization of contaminants and the kind and toxicity of side products due to incomplete degradation are key issues to be confronted in every PMR system implementation. Relevant R&D projects should be given top priority, both at the basic level and in pilot plants. To enable evaluation of the performance of both entire innovative PMR systems and photocatalysts individually, appropriate ISO standards development should be pursued. Scaling up of equipment and the assessment of environmental, economic, and technical PMR performance metrics are anticipated to be simple once the aforementioned scientific and technological challenges have been effectively addressed and the associated uncertainties have been eliminated.

Research on photocatalysis applications for oily wastewater has intensified. Effective catalysts with longer stability and durability are essential to boost their performance. For application in larger-scale systems, extensive research is necessary. To maximize their removal efficiencies, in-depth studies on the interaction between the nature of water molecules, oil droplets on the membrane surface, and surface change during photocatalysis are required. For the enhanced performance of the photocatalytic membranes for oily wastewater treatment, future PMR studies need to consider: (i) developing antifouling and self-cleaning photocatalytic membranes with stable properties for long-term operations, (ii) the ability to absorb a wide spectrum of visible light; (iii) applications at a larger scale, (iv) real samples of oilfield-produced and other wastewater, (v) simple methods for synthesizing photocatalyst with a long lifetime, (vi) the identification of intermediate compounds

during treatment, and (vii) the effects of vapor phase on PMR photocatalytic performance at high temperature.

### 9. Conclusion

It is difficult to treat oily wastewater because of its complex constituents and the presence of oil droplets, oil-water emulsion, and other components. Conventional membrane technology suffers from drawbacks such as its inability to treat tiny oil droplets, which accumulate on the surface of the membrane. This decreases its flux and reduces its efficiency while increasing treatment cost. Minimizing the contact between membrane surface and oily foulants by enhancing the membrane's hydrophilicity is critical to overcoming the flux reduction problems. Therefore, a hybrid process that involves photocatalysis and conventional membrane filtration is a promising option. PMR technology offers effective mineralization of tiny oil droplets and emulsion in water, heavy metal detoxication, and mineral recovery in oily wastewater.

It was conclusively evident from a literature survey of 226 published articles (1976–2022) that individual treatment either photocatalysis or membrane technology alone could not maximize its treatment performance for oil-water separation. Synergizing the two separate systems could overcome the drawbacks of the individual treatment. The PMRs attained over 96% removal of the pollutants in oily wastewater which was shown that in most cases meet the regulatory standard of a maximum of 40 ppm of allowable oil discharge into the environment or water body. Both the UV and visible light aided the degradation of oil in the wastewater. When the membrane has a high surface area, it provides additional sites for the photocatalyst to occupy, contributing to an efficient degradation. Concludingly, PMRs can exhibit a high flux of recovery ratio after several filtration cycles under UV/Vis irradiation resulting in low filtration cost, lower energy requirements, and required level of oil in water before discharge or reuse. Therefore, with proper design and fabrication methods, the PMR can exhibit self-cleaning and be re-used for several cycles of filtration with high efficiency.

### Declaration of Competing Interest

The authors declare that they have no known competing financial interests or personal relationships that could have appeared to influence the work reported in this paper.

### Data availability

Data will be made available on request.

### Acknowledgments

The authors gratefully acknowledge the financial support from Ministry of Higher Education Malaysia for the funding through the Higher Institution Centre of Excellence Scheme (Project Number: R. J090301.7809.4J430). The authors also would like to thank the JICA Technical Cooperation Project for ASEAN University Network/ Southeast Asia Engineering Education Development Network (JICA Project for AUN/SEED-Net) via Collaborative Education Program for Water and Wastewater Treatment Engineering Research Consortium (Program Contract No: UTM CEP 2102a/Project Number: R. J130000.7309.4B647) and Universiti Teknologi Malaysia for the research grants namely the UTM High Impact Research (UTMHIR) (Project number: Q. J130000.2409.08G34) and Industry/International Incentive Grant (IIIG) (Project number: Q. J130000.3609.03M17). The authors would also like to thank the Research Management Centre, Universiti Teknologi Malaysia for technical support. The first author acknowledges the Tertiary Education Trust Fund (tetfund) Nigeria for study scholarship.

## References

- [1] X. Zhu, A. Dudchenko, X. Gu, D. Jassby, Surfactant-stabilized oil separation from water using ultrafiltration and nanofiltration, *J. Memb. Sci.* 529 (2017) 159–169, <https://doi.org/10.1016/j.memsci.2017.02.004>.
- [2] J.M. Dickhout, J. Moreno, P.M. Biesheuvel, L. Boels, R.G.H. Lammertink, W.M. de Vos, Produced water treatment by membranes: A review from a colloidal perspective, *J. Colloid Interface Sci.* 487 (2017) 523–534, <https://doi.org/10.1016/j.jcis.2016.10.013>.
- [3] E.N. Tummans, V.V. Tarabara, J.W. Chew, A.G. Fane, Behavior of oil droplets at the membrane surface during crossflow microfiltration of oil-water emulsions, *J. Memb. Sci.* 500 (2016) 211–224, <https://doi.org/10.1016/j.memsci.2015.11.005>.
- [4] O. Samuel, M.H.D. Othman, R. Kamaludin, O. Sinsamphanh, H. Abdullah, M. H. Puteh, T.A. Kurniawan, T. Li, A.F. Ismail, M.A. Rahman, J. Jaafar, T. El-badawy, S. Chinedu Mamah, Oilfield-produced water treatment using conventional and membrane-based technologies for beneficial reuse: A critical review, *J. Environ. Manag.* 308 (2022), 114556, <https://doi.org/10.1016/j.jenvman.2022.114556>.
- [5] A. Fakhru'l-Razi, A. Pendashteh, L.C. Abdullah, D.R.A. Biak, S.S. Madaeni, Z. Z. Abidin, Review of technologies for oil and gas produced water treatment, *J. Hazard. Mater.* 170 (2009) 530–551, <https://doi.org/10.1016/j.jhazmat.2009.05.044>.
- [6] J. Neff, K. Lee, E.M. DeBlois, Produced Water: Overview of Composition, Fates, and Effects BT - Produced Water: Environmental Risks and Advances in Mitigation Technologies, in: K. Lee, J. Neff (Eds.), *Prod. Water*, Springer, New York, New York, NY, 2011, pp. 3–54, [https://doi.org/10.1007/978-1-4614-0046-2\\_1](https://doi.org/10.1007/978-1-4614-0046-2_1).
- [7] B. Petroleum, Statistical Review of World Energy globally consistent data on world energy markets. and authoritative publications in the field of energy, *BP Energy Outlook 2021* 70 (2021) 8–20.
- [8] D. O'Rourke, S. Connolly, Just oil? The distribution of environmental and social impacts of oil production and consumption, *Annu. Rev. Environ. Resour.* 28 (2003) 587–617, <https://doi.org/10.1146/annurev.energy.28.050302.105617>.
- [9] Y. Zhu, D. Wang, L. Jiang, J. Jin, Recent progress in developing advanced membranes for emulsified oil-water separation, *NPG Asia Mater.* 6 (2014), <https://doi.org/10.1038/am.2014.23>.
- [10] M.S. Muhamad, M.R. Salim, W.J. Lau, Z. Yusop, A review on bisphenol A occurrences, health effects and treatment process via membrane technology for drinking water, *Environ. Sci. Pollut. Res.* 23 (2016) 11549–11567, <https://doi.org/10.1007/s11356-016-6357-2>.
- [11] N.F.D. Junaidi, N.H. Othman, N.S. Fuzil, M.S. Mat Shayuti, N.H. Alias, M. Z. Shahrudin, F. Marpani, W.J. Lau, A.F. Ismail, N.F.D. Aba, Recent development of graphene oxide-based membranes for oil-water separation: A review, *Sep. Purif. Technol.* 258 (2021), 118000, <https://doi.org/10.1016/j.seppur.2020.118000>.
- [12] H. Yasuda, M. Gazicki, Biomedical applications of plasma polymerization and plasma treatment of polymer surfaces, *Biomaterials* 3 (1982) 68–77, [https://doi.org/10.1016/0142-9612\(82\)90036-9](https://doi.org/10.1016/0142-9612(82)90036-9).
- [13] S. Ahn, X. Cong, C.B. Lebrilla, S. Gronert, Zwitterion formation in gas-phase cyclodextrin complexes, *J. Am. Soc. Mass Spectrom.* 16 (2005) 166–175, <https://doi.org/10.1016/j.jasms.2004.10.007>.
- [14] W. Yu, M. Brown, N.J.D. Graham, Prevention of PVDF ultrafiltration membrane fouling by coating MnO<sub>2</sub> nanoparticles with ozonation, *Sci. Rep.* 6 (2016), <https://doi.org/10.1038/srep30144>.
- [15] W. Yu, L.C. Campos, N. Graham, Application of pulsed UV-irradiation and pre-coagulation to control ultrafiltration membrane fouling in the treatment of micro-polluted surface water, *Water Res* 107 (2016) 83–92, <https://doi.org/10.1016/j.watres.2016.10.058>.
- [16] N.H. Alias, J. Jaafar, S. Samitsu, T. Matsuura, A.F. Ismail, M.H.D. Othman, M. A. Rahman, N.H. Othman, N. Abdullah, S.H. Paiman, N. Yusof, F. Aziz, Photocatalytic nanofiber-coated alumina hollow fiber membranes for highly efficient oilfield produced water treatment, *Chem. Eng. J.* 360 (2019) 1437–1446, <https://doi.org/10.1016/j.cej.2018.10.217>.
- [17] S. Riaz, S.J. Park, An overview of TiO<sub>2</sub>-based photocatalytic membrane reactors for water and wastewater treatments, *J. Ind. Eng. Chem.* 84 (2020) 23–41, <https://doi.org/10.1016/j.jiec.2019.12.021>.
- [18] S. Leong, A. Razmjou, K. Wang, K. Hapgood, X. Zhang, H. Wang, TiO<sub>2</sub> based photocatalytic membranes: A review, *J. Memb. Sci.* 472 (2014) 167–184, <https://doi.org/10.1016/j.memsci.2014.08.016>.
- [19] É. Nascimben Santos, Z. László, C. Hodúr, G. Arthanareeswaran, G. Veréb, Photocatalytic membrane filtration and its advantages over conventional approaches in the treatment of oily wastewater: A review, *Asia-Pac. J. Chem. Eng.* 15 (2020) 1–29, <https://doi.org/10.1002/apj.2533>.
- [20] G. Nie, Y. Bai, Y. Xu, L. Ye, Photocatalytic Membranes for Oily Wastewater Treatment, in: *Oil–Water Mix. Emuls.* Vol. 1 Membr. Mater. Sep. Treat., American Chemical Society, 2022: pp. 217–246 SE–6. <https://doi.org/doi:10.1021/bk-2022-1407.ch006>.
- [21] L. Chen, P. Xu, H. Wang, Photocatalytic membrane reactors for produced water treatment and reuse: Fundamentals, affecting factors, rational design, and evaluation metrics, *J. Hazard. Mater.* 424 (2022), 127493, <https://doi.org/10.1016/j.jhazmat.2021.127493>.
- [22] A.A. Cerqueira, in: M.R. da, C.M.E.-J.S. Gomes (Eds.), *Electrolytic Treatment of Wastewater in the Oil Industry*, IntechOpen, Rijeka, 2012, <https://doi.org/10.5772/50712>.
- [23] K. Ighilahriz, M. Taleb Ahmed, H. Djelal, R. Maachi, Efficiency of an electrocoagulation treatment of water contaminated by hydrocarbons in a continuous mode powered by photovoltaic solar modules, *Environ. Eng. Manag. J.* 17 (2018) 1521–1529, <https://doi.org/10.30638/eeemj.2018.151>.
- [24] J. Beyer, H.C. Trannum, T. Bakke, P.V. Hodson, T.K. Collier, Environmental effects of the Deepwater Horizon oil spill: A review, *Mar. Pollut. Bull.* 110 (2016) 28–51, <https://doi.org/10.1016/j.marpolbul.2016.06.027>.
- [25] J.P. Guyer, *An Introduction to Industrial Wastewater Collection and Treatment*, 2013.
- [26] Y. Cai, D. Chen, N. Li, Q. Xu, H. Li, J. He, J. Lu, A. Self-Cleaning Heterostructured, Membrane for efficient oil-in-water emulsion separation with stable flux, *Adv. Mater.* 32 (2020), 2001265, <https://doi.org/10.1002/adma.202001265>.
- [27] T. Ahmad, C. Guria, A. Mandal, A review of oily wastewater treatment using ultrafiltration membrane: A parametric study to enhance the membrane performance, *J. Water Process Eng.* 36 (2020), 101289, <https://doi.org/10.1016/j.jwpe.2020.101289>.
- [28] O.B. Akpor, D.A. OTOhinoyi, Pollutants in wastewater effluents: impacts and remediation processes, *Int. J. Environ. Res. Earth Sci.* 27 (2014) 249–253, <https://doi.org/10.1007/s10162-014-0441-4>.
- [29] L. Hui, W. Yan, W. Juan, L. Zhongming, A review: recent advances in oily wastewater treatment, *Recent Innov. Chem. Eng. (Former. Recent Pat. Chem. Eng.* 7 (2015) 17–24, <https://doi.org/10.2174/2211334707666140415222545>.
- [30] R.P. Côté, N.R.C.C.A.C. on S.C. for E. Quality, The Effects of Petroleum Refinery Liquid Wastes on Aquatic Life, with Special Emphasis on the Canadian Environment, National Research Council of Canada, Associate Committee on Scientific Criteria for Environmental Quality, 1976. (<https://books.google.com.my/books?id=yJ63lyH6eAIC>).
- [31] J. Tang, M. Wang, F. Wang, Q. Sun, Q. Zhou, Eco-toxicity of petroleum hydrocarbon contaminated soil, *J. Environ. Sci.* 23 (2011) 845–851, [https://doi.org/10.1016/S1001-0742\(10\)60517-7](https://doi.org/10.1016/S1001-0742(10)60517-7).
- [32] H.I. Abdel-Shafy, M.S.M. Mansour, A review on polycyclic aromatic hydrocarbons: Source, environmental impact, effect on human health and remediation, *Egypt. J. Pet.* 25 (2016) 107–123, <https://doi.org/10.1016/j.ejpe.2015.03.011>.
- [33] T.L. Tasker, W.D. Burgos, P. Piotrowski, L. Castillo-Meza, T.A. Blewett, K. B. Ganow, A. Stallworth, P.L.M. Delompré, G.G. Goss, L.B. Fowler, J.P. Vanden Heuvel, F. Dorman, N.R. Warner, Environmental and Human Health Impacts of Spreading Oil and Gas Wastewater on Roads, *Environ. Sci. Technol.* 52 (2018) 7081–7091, <https://doi.org/10.1021/acs.est.8b00716>.
- [34] S. Putatunda, S. Bhattacharya, D. Sen, C. Bhattacharjee, A review on the application of different treatment processes for emulsified oily wastewater, *Int. J. Environ. Sci. Technol.* 16 (2019) 2525–2536, <https://doi.org/10.1007/s13762-018-2055-6>.
- [35] Y.F. AlJaberi, A.B. Abdulmajeed, A.A. Hassan, L.M. Ghadban, Assessment of an Electrocoagulation Reactor for the Removal of Oil Content and Turbidity from Real Oily Wastewater Using Response Surface Method, *Recent Innov. Chem. Eng.* 13 (2020) 55–71, <https://doi.org/10.2174/2405520412666190830091842>.
- [36] S.J. Maguire-Boyle, A.R. Barron, A new functionalization strategy for oil/water separation membranes, *J. Memb. Sci.* 382 (2011) 107–115, <https://doi.org/10.1016/j.memsci.2011.07.046>.
- [37] O. Tahiri Alaoui, Q.T. Nguyen, C. Mbareck, T. Rhilou, Elaboration and study of poly(vinylidene fluoride)-anatase TiO<sub>2</sub> composite membranes in photocatalytic degradation of dyes, *Appl. Catal. A Gen.* 358 (2009) 13–20, <https://doi.org/10.1016/j.apcata.2009.01.032>.
- [38] C. Zhao, J. Zhou, Y. Yan, L. Yang, G. Xing, H. Li, P. Wu, M. Wang, H. Zheng, Application of coagulation/flocculation in oily wastewater treatment: A review, *Sci. Total Environ.* 765 (2021), 142795, <https://doi.org/10.1016/j.scitotenv.2020.142795>.
- [39] M. Han, J. Zhang, W. Chu, J. Chen, G. Zhou, Research Progress and prospects of marine Oily wastewater treatment: A review, *Water (Switz.)* 11 (2019) 1–29, <https://doi.org/10.3390/w11122517>.
- [40] H.A. Tayim, A.H. Al-Yazouri, Industrial Wastewater Treatment Using Local Natural Soil in Abu Dhabi, U.A.E., *Am. J. Environ. Sci.* 1 (2005) 190–193, <https://doi.org/10.3844/ajessp.2005.190.193>.
- [41] A.S.C. Chen, J.T. Flynn, R.G. Cook, A.L. Casaday, Removal of oil, grease, and suspended solids from produced water with ceramic crossflow microfiltration, *SPE Prod. Eng.* 6 (1991) 131–136, <https://doi.org/10.2118/20291-PA>.
- [42] R.G. Holdich, I.W. Cumming, I.D. Smith, Crossflow microfiltration of oil in water dispersions using surface filtration with imposed fluid rotation, *J. Memb. Sci.* 143 (1998) 263–274, [https://doi.org/10.1016/S0376-7388\(98\)00023-4](https://doi.org/10.1016/S0376-7388(98)00023-4).
- [43] H.J. Tanudjaja, C.A. Hejase, V.V. Tarabara, A.G. Fane, J.W. Chew, Membrane-based separation for oily wastewater: A practical perspective, *Water Res* 156 (2019) 347–365, <https://doi.org/10.1016/j.watres.2019.03.021>.
- [44] L. Yu, M. Han, F. He, A review of treating oily wastewater, *Arab. J. Chem.* 10 (2017) S1913–S1922, <https://doi.org/10.1016/j.arabjc.2013.07.020>.
- [45] W.L. Liew, M.A. Kassim, K. Muda, S.K. Loh, A.C. Affam, Conventional methods and emerging wastewater polishing technologies for palm oil mill effluent treatment: A review, *J. Environ. Manag.* 149 (2015) 222–235, <https://doi.org/10.1016/j.jenvman.2014.10.016>.
- [46] F. Luis, G. Moncayo, Ambient Air, Automobiles, Fuels, Industries and Noise: Pollution and Control Law Series PCL/4/2000–2001, 2000. Central Pollution Control Board (CPCB), Ministry of Environment and Forestry, 2000, (n.d.).
- [47] K. Abuhasel, M. Kchaou, M. Alquraish, Y. Munusamy, Y.T. Jeng, Oily Wastewater Treatment: Overview of Conventional and Modern Methods, Challenges, and Future Opportunities, *Water* 13 (2021), <https://doi.org/10.3390/w13070980>.

- [48] A.A. El-Samakh, D. Ponnamm, M.K. Hassan, A. Ammar, S. Adham, M.A.A. Al-Maadeed, A. Karim, Designing Flexible and Porous Fibrous Membranes for Oil Water Separation-A Review of Recent Developments, *Polym. Rev.* 60 (2020) 671–716, <https://doi.org/10.1080/15583724.2020.1714651>.
- [49] D.L. Zhao, S. Japip, Y. Zhang, M. Weber, C. Maletzko, T.S. Chung, Emerging thin-film nanocomposite (TFN) membranes for reverse osmosis: A review, *Water Res* 173 (2020), 115557, <https://doi.org/10.1016/j.watres.2020.115557>.
- [50] M. Lu, Z. Zhang, W. Yu, W. Zhu, Biological treatment of oilfield-produced water: A field pilot study, *Int. Biodeterior. Biodegrad.* 63 (2009) 316–321, <https://doi.org/10.1016/j.ibiod.2008.09.009>.
- [51] K.R. Mofokeng, M.F. Yahaya, J.O. Madu, F.N. Chukwudi, S. Ojo, F.V. Adams, Modified Clay Filters for Purification of Petroleum Products Contaminated Water, *Eng. Innov. Address Soc. Chall.* 107 (2021) 55–63, <https://doi.org/10.4028/www.scientific.net/ast.107.55>.
- [52] M. Çakmakce, N. Kayaalp, I. Koyuncu, Desalination of produced water from oil production fields by membrane processes, *Desalination* 222 (2008) 176–186, <https://doi.org/10.1016/j.desal.2007.01.147>.
- [53] M. Golphur, M. Pakizeh, Development of a new nanofiltration membrane for removal of kinetic hydrate inhibitor from water, *Sep. Purif. Technol.* 183 (2017) 237–248, <https://doi.org/10.1016/j.seppur.2017.04.011>.
- [54] W.I. Syarifah Nazirah, Y. Norhaniza, A. Farhana, M. Nurasyikin, Ulasan mengenai rawatan sisa medan minyak menggunakan teknologi membran penapisan berbanding teknologi konvensional, *Malays. J. Anal. Sci.* 21 (2017) 643–658, <https://doi.org/10.17576/mjas-2017-2103-14>.
- [55] S.C. Mamah, P.S. Goh, A.F. Ismail, L.T. Yogarathinam, N.D. Suzaimi, A.C. Opia, S. Ojo, N.E. Ngwana, Bio-polymer modified nanoclay embedded forward osmosis membranes with enhanced desalination performance, *J. Appl. Polym. Sci.* 139 (2022) 1–15, <https://doi.org/10.1002/app.52473>.
- [56] I.G. Wenten, Recent development in membrane science and its industrial applications, *J. Sci. Technol.* 24 (2003) 1009–1024.
- [57] M. Cheryan, N. Rajagopalan, Membrane processing of oily streams. Wastewater treatment and waste reduction, *J. Memb. Sci.* 151 (1998) 13–28, [https://doi.org/10.1016/S0376-7388\(98\)00190-2](https://doi.org/10.1016/S0376-7388(98)00190-2).
- [58] E.T. Igunu, G.Z. Chen, Produced water treatment technologies, *Int. J. Low-Carbon Technol.* 9 (2014) 157–177, <https://doi.org/10.1093/ijlct/cts049>.
- [59] S. Judd, *The MBR Book: Principles and Applications of Membrane Bioreactors for Water and Wastewater Treatment*. Elsevier Science, 2010. (<https://books.google.com.my/books?id=SYI2FAAM04kC>).
- [60] A. Rahimpour, S.F. Seyedpour, S. Aghapour Aktij, M. Dadashi Firouzjaei, A. Zirehpour, A. Arabi Shamsabadi, S. Khoshhal Salestan, M. Jabbari, M. Soroush, Simultaneous Improvement of Antimicrobial, Antifouling, and Transport Properties of Forward Osmosis Membranes with Immobilized Highly-Compatible Polyrhodanine Nanoparticles, *Environ. Sci. Technol.* 52 (2018) 5246–5258, <https://doi.org/10.1021/acs.est.8b00804>.
- [61] M.R. Rahimpour, N.M. Kazerooni, M. Parhoudeh, Water treatment by renewable energy-driven membrane distillation, in: *Curr. Trends Futur. Dev. Membr. Renew. Energy Integr. with Membr. Oper.*, Elsevier, 2018, pp. 179–211, <https://doi.org/10.1016/B978-0-12-813545-7.00008-8>.
- [62] Y. Wen, J. Yuan, X. Ma, S. Wang, Y. Liu, Polymeric nanocomposite membranes for water treatment: a review, *Environ. Chem. Lett.* 17 (2019) 1539–1551, <https://doi.org/10.1007/s10311-019-00895-9>.
- [63] S. Wang, Z. yang Wang, J. zhong Xia, X. mao Wang, Polyethylene-supported nanofiltration membrane with in situ formed surface patterns of millimeter size in resisting fouling, *J. Memb. Sci.* 620 (2021), 118830, <https://doi.org/10.1016/j.memsci.2020.118830>.
- [64] D. Zhao, C. Su, G. Liu, Y. Zhu, Z. Gu, Performance and autopsy of nanofiltration membranes at an oil-field wastewater desalination plant, *Environ. Sci. Pollut. Res.* 26 (2019) 2681–2690, <https://doi.org/10.1007/s11356-018-3797-x>.
- [65] X. Du, Y. Shi, V. Jegatheesan, I. Ul Haq, A review on the mechanism, impacts and control methods of membrane fouling in MBR system, 2020. <https://doi.org/10.3390/membranes10020024>.
- [66] M. Abbasi, A. Taheri, Modeling of permeation flux decline during oily wastewater treatment by MF - PAC hybrid process using mullite ceramic, *Membr., Indian J. Chem. Technol.* 21 (2014) 49–55.
- [67] J. Hermia, Constant pressure blocking filtration law application to powder-law non-newtonian fluid, *Trans. Inst. Chem. Eng.* 60 (1982) 183–187. (<https://cir.nii.ac.jp/crid/1572261549984044160>).
- [68] B. Van der Bruggen, Chemical modification of polyethersulfone nanofiltration membranes: a review, *J. Appl. Polym. Sci.* 114 (2009) 630–642.
- [69] D. Rana, T. Matsuura, Surface modifications for antifouling membranes, *Chem. Rev.* 110 (2010) 2448–2471, <https://doi.org/10.1021/cr800208y>.
- [70] A. Momoh, F.V. Adams, O. Samuel, O.P. Bolade, P.A. Olubambi, Corrosion Prevention: The Use of Nanomaterials BT - Modified Nanomaterials for Environmental Applications: Electrochemical Synthesis, in: O.M. Ama, S. Sinha Ray, P. Ogbemudia Osifo (Eds.), *Characterization, and Properties*, Springer International Publishing, Cham, 2022, pp. 91–105, [https://doi.org/10.1007/978-3-030-85555-0\\_5](https://doi.org/10.1007/978-3-030-85555-0_5).
- [71] M. Padaki, R. Surya Murali, M.S. Abdullah, N. Misdan, A. Moselehyani, M. A. Kassim, N. Hilal, A.F. Ismail, Membrane technology enhancement in oil-water separation. A review, *Desalination* 357 (2015) 197–207, <https://doi.org/10.1016/j.desal.2014.11.023>.
- [72] D.J. Miller, D.R. Dreyer, C.W. Bielawski, D.R. Paul, B.D. Freeman, Surface Modification of Water Purification Membranes, *Angew. Chem. Int. Ed.* 56 (2017) 4662–4711, <https://doi.org/10.1002/anie.201601509>.
- [73] X. Zhang, A.J. Du, P. Lee, D.D. Sun, J.O. Leckie, Grafted multifunctional titanium dioxide nanotube membrane: Separation and photodegradation of aquatic pollutant, *Appl. Catal. B Environ.* 84 (2008) 262–267, <https://doi.org/10.1016/j.apcatb.2008.04.009>.
- [74] Y. Gao, M. Hu, B. Mi, Membrane surface modification with TiO<sub>2</sub>-graphene oxide for enhanced photocatalytic performance, *J. Memb. Sci.* 455 (2014) 349–356, <https://doi.org/10.1016/j.memsci.2014.01.011>.
- [75] S. Yang, J.S. Gu, H.Y. Yu, J. Zhou, S.F. Li, X.M. Wu, L. Wang, Polypropylene membrane surface modification by RAFT grafting polymerization and TiO<sub>2</sub> photocatalysts immobilization for phenol decomposition in a photocatalytic membrane reactor, *Sep. Purif. Technol.* 83 (2011) 157–165, <https://doi.org/10.1016/j.seppur.2011.09.081>.
- [76] H. Zhao, H. Li, H. Yu, H. Chang, X. Quan, S. Chen, CNTs-TiO<sub>2</sub>/Al<sub>2</sub>O<sub>3</sub> composite membrane with a photocatalytic function: Fabrication and energetic performance in water treatment, *Sep. Purif. Technol.* 116 (2013) 360–365, <https://doi.org/10.1016/j.seppur.2013.06.007>.
- [77] G.E. Romanos, C.P. Athanasekou, F.K. Katsaros, N.K. Kanellopoulos, D. D. Dionysiou, V. Likodimos, P. Falaras, Double-side active TiO<sub>2</sub>-modified nanofiltration membranes in continuous flow photocatalytic reactors for effective water purification, *J. Hazard. Mater.* 211–212 (2012) 304–316, <https://doi.org/10.1016/j.jhazmat.2011.09.081>.
- [78] R. Goei, Z. Dong, T.T. Lim, High-permeability pluronic-based TiO<sub>2</sub> hybrid photocatalytic membrane with hierarchical porosity: Fabrication, characterizations and performances, *Chem. Eng. J.* 228 (2013) 1030–1039, <https://doi.org/10.1016/j.cej.2013.05.068>.
- [79] M. Ulbricht, Advanced functional polymer membranes, *Polym. (Guildf.)* 47 (2006) 2217–2262, <https://doi.org/10.1016/j.polymer.2006.01.084>.
- [80] S. Kasemset, A. Lee, D.J. Miller, B.D. Freeman, M.M. Sharma, Effect of polydopamine deposition conditions on fouling resistance, physical properties, and permeation properties of reverse osmosis membranes in oil/water separation, *J. Memb. Sci.* 425–426 (2013) 208–216, <https://doi.org/10.1016/j.memsci.2012.08.049>.
- [81] F. Liu, N.A. Hashim, Y. Liu, M.R.M. Abed, K. Li, Progress in the production and modification of PVDF membranes, *J. Memb. Sci.* 375 (2011) 1–27, <https://doi.org/10.1016/j.memsci.2011.03.014>.
- [82] A.K. Fard, G. McKay, A. Buekenhoudt, H. Al Sulaiti, F. Motmans, M. Khraisheh, M. Atieh, Inorganic membranes: Preparation and application for water treatment and desalination, *Mater. (Basel)* 11 (2018), <https://doi.org/10.3390/ma11010074>.
- [83] G. dong Kang, Y. ming Cao, Development of antifouling reverse osmosis membranes for water treatment: A review, *Water Res* 46 (2012) 584–600, <https://doi.org/10.1016/j.watres.2011.11.041>.
- [84] J. Gao, J. Miao, P.Z. Li, W.Y. Teng, L. Yang, Y. Zhao, B. Liu, Q. Zhang, A p-type Ti (iv)-based metal-organic framework with visible-light photo-response, *Chem. Commun.* 50 (2014) 3786–3788, <https://doi.org/10.1039/c3cc49440c>.
- [85] H. Zhang, H. Kou, J. Yang, D. Huang, H. Nan, J. Li, Microstructure evolution and tensile properties of Ti-6.5Al-2Zr-Mo-V alloy processed with thermo hydrogen treatment, *Mater. Sci. Eng. A* 619 (2014) 274–280, <https://doi.org/10.1016/j.msea.2014.09.104>.
- [86] L. Ni, J. Meng, X. Li, Y. Zhang, Surface coating on the polyamide TFC RO membrane for chlorine resistance and antifouling performance improvement, *J. Memb. Sci.* 451 (2014) 205–215, <https://doi.org/10.1016/j.memsci.2013.09.040>.
- [87] S. Zou, E.D. Smith, S. Lin, S.M. Martin, Z. He, Mitigation of bidirectional solute flux in forward osmosis via membrane surface coating of zwitterion functionalized carbon nanotubes, *Environ. Int.* 131 (2019), 104970, <https://doi.org/10.1016/j.envint.2019.104970>.
- [88] Y.Q. Wang, Y.L. Su, Q. Sun, X. Le Ma, Z.Y. Jiang, Generation of anti-biofouling ultrafiltration membrane surface by blending novel branched amphiphilic polymers with polyethersulfone, *J. Memb. Sci.* 286 (2006) 228–236, <https://doi.org/10.1016/j.memsci.2006.09.040>.
- [89] Y. Liu, Y. Su, X. Zhao, Y. Li, R. Zhang, Z. Jiang, Improved antifouling properties of polyethersulfone membrane by blending the amphiphilic surface modifier with crosslinked hydrophobic segments, *J. Memb. Sci.* 486 (2015) 195–206, <https://doi.org/10.1016/j.memsci.2015.03.045>.
- [90] J. Kim, B. Van Der Bruggen, The use of nanoparticles in polymeric and ceramic membrane structures: Review of manufacturing procedures and performance improvement for water treatment, *Environ. Pollut.* 158 (2010) 2335–2349, <https://doi.org/10.1016/j.envpol.2010.03.024>.
- [91] W. Sun, J. Shi, C. Chen, N. Li, Z. Xu, J. Li, H. Lv, X. Qian, L. Zhao, A review on organic-inorganic hybrid nanocomposite membranes: A versatile tool to overcome the barriers of forward osmosis, *RSC Adv.* 8 (2018) 10040–10056, <https://doi.org/10.1039/c7ra12835e>.
- [92] J. Saïen, H. Nejati, Enhanced photocatalytic degradation of pollutants in petroleum refinery wastewater under mild conditions, *J. Hazard. Mater.* 148 (2007) 491–495, <https://doi.org/10.1016/j.jhazmat.2007.03.001>.
- [93] X. Yu, Q. Ji, J. Zhang, Z. Nie, H. Yang, Photocatalytic degradation of diesel pollutants in seawater under visible light, *Reg. Stud. Mar. Sci.* 18 (2018) 139–144, <https://doi.org/10.1016/j.rmsa.2018.02.006>.
- [94] R. Molinari, C. Lavorato, P. Argurio, Recent progress of photocatalytic membrane reactors in water treatment and in synthesis of organic compounds. A review, *Catal. Today* 281 (2017) 144–164, <https://doi.org/10.1016/j.cattod.2016.06.047>.
- [95] H. Dzinun, M.H.D. Othman, A.F. Ismail, T. Matsuura, M.H. Puteh, M.A. Rahman, J. Jaafar, Stability study of extruded dual layer hollow fibre membranes in a long operation photocatalysis process, *Polym. Test.* 68 (2018) 53–60, <https://doi.org/10.1016/j.polymertesting.2018.03.048>.



- [96] S.S. Chin, K. Chiang, A.G. Fane, The stability of polymeric membranes in a TiO<sub>2</sub> photocatalysis process, *J. Memb. Sci.* 275 (2006) 202–211, <https://doi.org/10.1016/j.memsci.2005.09.033>.
- [97] J. Yin, B. Deng, Polymer-matrix nanocomposite membranes for water treatment, *J. Memb. Sci.* 479 (2015) 256–275, <https://doi.org/10.1016/j.memsci.2014.11.019>.
- [98] H. Dzinun, M.H.D. Othman, A.F. Ismail, M.H. Puteh, M.A. Rahman, J. Jaafar, Performance evaluation of co-extruded microporous dual-layer hollow fiber membranes using a hybrid membrane photoreactor, *Desalination* 403 (2017) 46–52, <https://doi.org/10.1016/j.desal.2016.05.029>.
- [99] U. Baig, A. Matin, M.A. Gondal, S.M. Zubair, Facile fabrication of superhydrophobic, superoleophilic photocatalytic membrane for efficient oil-water separation and removal of hazardous organic pollutants, *J. Clean. Prod.* 208 (2019) 904–915, <https://doi.org/10.1016/j.jclepro.2018.10.079>.
- [100] John Moma, Jeffrey Baloyi, Modified Titanium Dioxide for Photocatalytic Applications, *Photocatal. - Appl. Attrib. IntechOpen* (2018) 37–56. (<https://www.intechopen.com/books/advanced-biometric-technologies/liveness-detection-in-biometrics>).
- [101] S.E. Braslavsky, A.M. Braun, A.E. Cassano, A.V. Emeline, M.I. Litter, L. Palmisano, V.N. Parmon, N. Serpone, Glossary of terms used in photocatalysis and radiation catalysis (IUPAC recommendations 2011), *Pure Appl. Chem.* 83 (2011) 931–1014, <https://doi.org/10.1351/PAC-REC-09-09-36>.
- [102] N. Serpone, A. Salinaro, Terminology, relative photonic efficiencies and quantum yields in heterogeneous photocatalysis. Part I: Suggested protocol (Technical Report), *Pure Appl. Chem.* 71 (1999) 303–320, <https://doi.org/10.1351/pac199971020303>.
- [103] U. Diebold, The surface science of titanium dioxide, *Surf. Sci. Rep.* 48 (2002) 53–229. (<http://linkinghub.elsevier.com/retrieve/pii/S0167572902001000>).
- [104] M. Coha, G. Farinelli, A. Tiraferri, M. Minella, D. Vione, Advanced oxidation processes in the removal of organic substances from produced water: Potential, configurations, and research needs, *Chem. Eng. J.* 414 (2021), 128668, <https://doi.org/10.1016/j.cej.2021.128668>.
- [105] O. Samuel, M.H.D. Othman, R. Kamaludin, O. Sinsamphanh, H. Abdullah, M. H. Puteh, T.A. Kurniawan, WO<sub>3</sub>-based photocatalysts: A review on synthesis, performance enhancement and photocatalytic memory for environmental applications, *Ceram. Int.* (2021), <https://doi.org/10.1016/j.ceramint.2021.11.158>.
- [106] W.S. Koe, J.W. Lee, W.C. Chong, Y.L. Pang, L.C. Sim, An overview of photocatalytic degradation: photocatalysts, mechanisms, and development of photocatalytic membrane, *Environ. Sci. Pollut. Res.* 27 (2020) 2522–2565, <https://doi.org/10.1007/s11356-019-07193-5>.
- [107] K. Rajeshwar, *Solar Energy Conversion and Environmental Remediation Using*, *J. Phys. Chem.* (2011) 1301–1309.
- [108] C.N.C. Hitam, A.A. Jalil, A review on exploration of Fe<sub>2</sub>O<sub>3</sub> photocatalyst towards degradation of dyes and organic contaminants, *J. Environ. Manag.* 258 (2020), 110050, <https://doi.org/10.1016/j.jenvman.2019.110050>.
- [109] A.F.A. Rahman, A.A. Jalil, S. Triwahyono, A. Ripin, F.F.A. Aziz, N.A.A. Fatah, N. F. Jaafar, C.N.C. Hitam, N.F.M. Salleh, N.S. Hassan, Strategies for introducing titania onto mesostructured silica nanoparticles targeting enhanced photocatalytic activity of visible-light-responsive Ti-MSN catalysts, *J. Clean. Prod.* 143 (2017) 948–959, <https://doi.org/10.1016/j.jclepro.2016.12.026>.
- [110] O. Samuel, M.H.D. Othman, R. Kamaludin, O. Sinsamphanh, H. Abdullah, M. H. Puteh, T.A. Kurniawan, WO<sub>3</sub>-based photocatalysts: A review on synthesis, performance enhancement and photocatalytic memory for environmental applications, *Ceram. Int.* 48 (2022) 5845–5875, <https://doi.org/10.1016/j.ceramint.2021.11.158>.
- [111] M. Tayebi, B.K. Lee, Recent advances in BiVO<sub>4</sub> semiconductor materials for hydrogen production using photoelectrochemical water splitting, *Renew. Sustain. Energy Rev.* 111 (2019) 332–343, <https://doi.org/10.1016/j.rser.2019.05.030>.
- [112] D.W. Kolpin, E.T. Furlong, M.T. Meyer, E.M. Thurman, S.D. Zaugg, L.B. Barber, H. T. Buxton, Pharmaceuticals, Hormones, and Other Organic Wastewater Contaminants in U.S. Streams, 1999–2000: A National Reconnaissance, *Environ. Sci. Technol.* 36 (2002) 1202–1211, <https://doi.org/10.1021/es011055j>.
- [113] N.M. Mahmoodi, M. Arami, Degradation and toxicity reduction of textile wastewater using immobilized titania nanophotocatalysis, *J. Photochem. Photobiol. B Biol.* 94 (2009) 20–24, <https://doi.org/10.1016/j.jphotobiol.2008.09.004>.
- [114] M.A. Fox, M.T. Dulay, Heterogeneous photocatalysis, *Chem. Rev.* 93 (1993) 341–357, <https://doi.org/10.1021/cr00017a016>.
- [115] S. Gautam, H. Agrawal, M. Thakur, A. Akbari, H. Sharda, R. Kaur, M. Amini, Metal oxides and metal organic frameworks for the photocatalytic degradation: A review, *J. Environ. Chem. Eng.* 8 (2020), 103726, <https://doi.org/10.1016/j.jece.2020.103726>.
- [116] R. Li, T. Li, Q. Zhou, Impact of titanium dioxide (TiO<sub>2</sub>) modification on its application to pollution treatment—a review, 2020. <https://doi.org/10.3390/catal10070804>.
- [117] J. Theerthagiri, S. Chandrasekaran, S. Salla, V. Elakkiya, R.A. Senthil, P. Nithyadharseni, T. Maiyalagan, K. Micheal, A. Ayeshamariam, M.V. Arasu, N. A. Al-Dhabi, H.S. Kim, Recent developments of metal oxide based heterostructures for photocatalytic applications towards environmental remediation, *J. Solid State Chem.* 267 (2018) 35–52, <https://doi.org/10.1016/j.jssc.2018.08.006>.
- [118] M.S.S. Danish, L.L. Estrella, I.M.A. Alemeida, A. Lisin, N. Moiseev, M. Ahmadi, M. Nazari, M. Wali, H. Zahab, T. Senjyu, Photocatalytic applications of metal oxides for sustainable environmental remediation, *Met. (Basel)* 11 (2021) 1–25, <https://doi.org/10.3390/met11010080>.
- [119] Z. Dai, A. Yang, X. Bao, R. Yang, Facile Non-Enzymatic Electrochemical Sensing for Glucose Based on Cu<sub>2</sub>O-BSA Nanoparticles Modified GCE, *MDPI-Sens.* 19 (2019), <https://doi.org/10.3390/s19122824>.
- [120] Y. Li, Y. Fu, M. Zhu, Green synthesis of 3D tripyramidal TiO<sub>2</sub> architectures with assistance of aloe extracts for highly efficient photocatalytic degradation of antibiotic ciprofloxacin, *Appl. Catal. B Environ.* 260 (2020), <https://doi.org/10.1016/j.apcatb.2019.118149>.
- [121] J. Al-Sabahi, T. Bora, M. Claereboudt, M. Al-Abri, J. Dutta, Visible light photocatalytic degradation of HPAM polymer in oil produced water using supported zinc oxide nanorods, *Chem. Eng. J.* 351 (2018) 56–64, <https://doi.org/10.1016/j.cej.2018.06.071>.
- [122] X. Yu, D. Hu, J. Chen, X. Jin, X. Zheng, Study on the photocatalytic degradation of diesel pollutants in seawater by a prepared nano Ag-doped Zinc Oxide, *Key Eng. Mater.* 609 (2014) 311–316, <https://doi.org/10.4028/www.scientific.net/KEM.609-610.311>.
- [123] M. Yeber, E. Paul, C. Soto, Chemical and biological treatments to clean oily wastewater: optimization of the photocatalytic process using experimental design, *Desalin. Water Treat.* 47 (2012) 295–299, <https://doi.org/10.1080/19443994.2012.696413>.
- [124] D. Cazoir, L. Fine, C. Ferronato, J.M. Chovelon, Hydrocarbon removal from bilgewater by a combination of air-stripping and photocatalysis, *J. Hazard. Mater.* 235–236 (2012) 159–168, <https://doi.org/10.1016/j.jhazmat.2012.07.037>.
- [125] I.-H. Cho, Y.-G. Kim, J.-K. Yang, N.-H. Lee, S.-M. Lee, Solar-Chemical Treatment of Groundwater Contaminated with Petroleum at Gas Station Sites: Ex Situ Remediation Using Solar/TiO<sub>2</sub> Photocatalysis and Solar Photo-Fenton, *J. Environ. Sci. Heal. Part A* 41 (2006) 457–473, <https://doi.org/10.1080/10934520500428336>.
- [126] K. Karakulski, W.A. Morawski, J. Grzechulska, Purification of bilge water by hybrid ultrafiltration and photocatalytic processes, *Sep. Purif. Technol.* 14 (1998) 163–173, [https://doi.org/10.1016/S1383-5866\(98\)00071-9](https://doi.org/10.1016/S1383-5866(98)00071-9).
- [127] A.D. McQueen, C.M. Kinley, R.L. Kiekhaefer, A.J. Calomeni, J.H. Rodgers, J. W. Castle, Photocatalysis of a commercial naphthenic acid in water using fixed-film TiO<sub>2</sub>, *Water Air. Soil Pollut.* 227 (2016), <https://doi.org/10.1007/s11270-016-2835-x>.
- [128] L. Ni, Y. Li, C. Zhang, L. Li, W. Zhang, D. Wang, Novel floating photocatalysts based on polyurethane composite foams modified with silver/titanium dioxide/graphene ternary nanoparticles for the visible-light-mediated remediation of diesel-polluted surface water, *J. Appl. Polym. Sci.* 133 (2016), <https://doi.org/10.1002/app.43400>.
- [129] I.-H. Cho, L.-H. Kim, K.-D. Zoh, J.-H. Park, H.-Y. Kim, Solar photocatalytic degradation of groundwater contaminated with petroleum hydrocarbons, *Environ. Prog.* 25 (2006) 99–109, <https://doi.org/10.1002/ep.10124>.
- [130] B. Liu, B. Chen, B. Zhang, J. Zheng, Jisi and Liang, Toxicity and biodegradability study on enhanced photocatalytic oxidation of polycyclic aromatic hydrocarbons in offshore produced water, in: *Can. Soc. Civ. Eng. Annu. Gen. Conf.*, Vancouver, Canada, 2017: pp. 1–2.
- [131] B. Wang, Y. Chen, S. Liu, H. Wu, H. Song, Photocatalytic visbreaking of wastewater produced from polymer flooding in oilfields, *Colloids Surf. A Physicochem. Eng. Asp.* 287 (2006) 170–174, <https://doi.org/10.1016/j.colsurfa.2006.03.051>.
- [132] I. Horovitz, D. Avisar, M.A. Baker, R. Grilli, L. Lozzi, D. Di Camillo, H. Mamane, Carbamazepine degradation using a N-doped TiO<sub>2</sub> coated photocatalytic membrane reactor: Influence of physical parameters, *J. Hazard. Mater.* 310 (2016) 98–107, <https://doi.org/10.1016/j.jhazmat.2016.02.008>.
- [133] D.D.C.J. Zhang X, D.K. Wang, Recent progresses on fabrication of photocatalytic membranes for water treatment, *Catal. Today* 230 (2014) 47–54.
- [134] R. Molinari, P. Argurio, K. Szymański, D. Darowna, S. Mozia, Chapter 4 - Photocatalytic membrane reactors for wastewater treatment, in: A. Basile, A.B.T.-C.T. and F.D. on (Bio-) M. Comite (Eds.), *Elsevier*, 2020: pp. 83–116. <https://doi.org/10.1016/B978-0-12-816823-3.00004-6>.
- [135] O. Samuel, A. Taofeek Ayodele, A. Anna Solomon, Predictive Performance of Hargreaves Model in Estimating Solar Radiation in Yola, Adamawa State Nigeria Using Minimum Climatological Data, *J. Eng. Res. Rep.* (2018) 1–8, <https://doi.org/10.9734/jerr/2018/v1i129801>.
- [136] S. Mozia, A. Heciak, D. Darowna, A.W. Morawski, A novel suspended/supported photoreactor design for photocatalytic decomposition of acetic acid with simultaneous production of useful hydrocarbons, *J. Photochem. Photobiol. A Chem.* 236 (2012) 48–53, <https://doi.org/10.1016/j.jphotochem.2012.03.017>.
- [137] S. Mozia, M. Tomaszewska, A.W. Morawski, A new photocatalytic membrane reactor (PMR) for removal of azo-dye Acid Red 18 from water, 59 (2005) 131–137. <https://doi.org/10.1016/j.apcatb.2005.01.011>.
- [138] S. Mozia, Photocatalytic membrane reactors (PMRs) in water and wastewater treatment. A review, *Sep. Purif. Technol.* 73 (2010) 71–91, <https://doi.org/10.1016/j.seppur.2010.03.021>.
- [139] R. Molinari, C. Lavorato, P. Argurio, K. Szymański, D. Darowna, S. Mozia, Overview of photocatalytic membrane reactors in organic synthesis, energy storage and environmental applications, *Catalysts* 9 (2019) 1–39, <https://doi.org/10.3390/catal9030239>.
- [140] P. Wang, A.G. Fane, T.T. Lim, Evaluation of a submerged membrane vis-LED photoreactor (sMPR) for carbamazepine degradation and TiO<sub>2</sub> separation, *Chem. Eng. J.* 215–216 (2013) 240–251, <https://doi.org/10.1016/j.cej.2012.10.075>.
- [141] W.-F. Ma, Y. Zhang, L.-L. Li, L.-J. You, P. Zhang, Y.-T. Zhang, J.-M. Li, M. Yu, J. Guo, H.-J. Lu, C.-C. Wang, Tailor-Made Magnetic Fe<sub>3</sub>O<sub>4</sub>@mTiO<sub>2</sub> Microspheres with a Tunable Mesoporous Anatase Shell for Highly Selective and Effective Enrichment of Phosphopeptides, *ACS Nano* 6 (2012) 3179–3188, <https://doi.org/10.1021/nm3009646>.

- [142] G. Veréb, V. Kálmán, T. Gyulavári, S. Kertész, S. Beszedés, G. Kovács, K. Hernádi, Z. Pap, C. Hodúr, Z. László, Advantages of TiO<sub>2</sub>/carbon nanotube modified photocatalytic membranes in the purification of oil-in-water emulsions, *Water Sci. Technol. Water Supply* 19 (2019) 1167–1174, <https://doi.org/10.2166/ws.2018.172>.
- [143] H. Zangeneh, A.A. Zinatizadeh, S. Zinadini, M. Feysi, D.W. Bahnemann, A novel photocatalytic self-cleaning PES nanofiltration membrane incorporating triple metal-nonmetal doped TiO<sub>2</sub> (K-B-N-TiO<sub>2</sub>) for post treatment of biologically treated palm oil mill effluent, *React. Funct. Polym.* 127 (2018) 139–152, <https://doi.org/10.1016/j.reactfunctpolym.2018.04.008>.
- [144] Z. Rahimi, A.A.L. Zinatizadeh, S. Zinadini, Preparation of high antibiofouling amino functionalized MWCNTs/PES nanocomposite ultrafiltration membrane for application in membrane bioreactor, *J. Ind. Eng. Chem.* 29 (2015) 366–374, <https://doi.org/10.1016/j.jiec.2015.04.017>.
- [145] M. Safarpour, V. Vatanpour, A. Khataee, Preparation and characterization of graphene oxide/TiO<sub>2</sub> blended PES nanofiltration membrane with improved antifouling and separation performance, *Desalination* 393 (2016) 65–78, <https://doi.org/10.1016/j.desal.2015.07.003>.
- [146] L. Shen, X. Bian, X. Lu, L. Shi, Z. Liu, L. Chen, Z. Hou, K. Fan, Preparation and characterization of ZnO/polyethersulfone (PES) hybrid membranes, *Desalination* 293 (2012) 21–29, <https://doi.org/10.1016/j.desal.2012.02.019>.
- [147] A. Moslehiani, A.F. Ismail, M.H.D. Othman, T. Matsuura, Design and performance study of hybrid photocatalytic reactor-PVDF/MWCNT nanocomposite membrane system for treatment of petroleum refinery wastewater, *Desalination* 363 (2015) 99–111, <https://doi.org/10.1016/j.desal.2015.01.044>.
- [148] L. Lou, R.J. Kendall, E. Smith, S.S. Ramkumar, Functional PVDF/rGO/TiO<sub>2</sub> nanofiber webs for the removal of oil from water, *Polym. (Guildf.)* 186 (2020), 122028, <https://doi.org/10.1016/j.polymer.2019.122028>.
- [149] N.H. Alias, J. Jaafar, S. Samitsu, N. Yusof, M.H.D. Othman, M.A. Rahman, A. F. Ismail, F. Aziz, W.N.W. Salleh, N.H. Othman, Photocatalytic degradation of oilfield produced water using graphitic carbon nitride embedded in electrospun polyacrylonitrile nanofibers, *Chemosphere* 204 (2018) 79–86, <https://doi.org/10.1016/j.chemosphere.2018.04.033>.
- [150] Q. Chen, Z. Yu, F. Li, Y. Yang, Y. Pan, Y. Peng, X. Yang, G. Zeng, A novel photocatalytic membrane decorated with RGO-Ag-TiO<sub>2</sub> for dye degradation and oil-water emulsion separation, *J. Chem. Technol. Biotechnol.* 93 (2018) 761–775, <https://doi.org/10.1002/jctb.5426>.
- [151] H. Rawindran, J.W. Lim, P.S. Goh, M.N. Subramaniam, A.F. Ismail, N.M. Radi bin Nik, M. Daud, M. Rezaei-Dasht Arzhandi, Simultaneous separation and degradation of surfactants laden in produced water using PVDF/TiO<sub>2</sub> photocatalytic membrane, *J. Clean. Prod.* 221 (2019) 490–501, <https://doi.org/10.1016/j.jclepro.2019.02.230>.
- [152] Y. Liu, Y. Su, J. Guan, J. Cao, R. Zhang, M. He, K. Gao, L. Zhou, Z. Jiang, 2D Heterostructure Membranes with Sunlight-Driven Self-Cleaning Ability for Highly Efficient Oil–Water Separation, *Adv. Funct. Mater.* 28 (2018), 1706545, <https://doi.org/10.1002/adfm.201706545>.
- [153] I. Kovács, G. Veréb, S. Kertész, C. Hodúr, Z. László, Fouling mitigation and cleanability of TiO<sub>2</sub> photocatalyst-modified PVDF membranes during ultrafiltration of model oily wastewater with different salt contents, *Environ. Sci. Pollut. Res.* 25 (2018) 34912–34921, <https://doi.org/10.1007/s11356-017-0998-7>.
- [154] B.Y.L. Tan, J. Juay, Z. Liu, D. Sun, Flexible Hierarchical TiO<sub>2</sub>/Fe<sub>2</sub>O<sub>3</sub> Composite Membrane with High Separation Efficiency for Surfactant-Stabilized Oil-Water Emulsions, *Chem. – Asian J.* 11 (2016) 561–567, <https://doi.org/10.1002/asia.201501203>.
- [155] T. Wang, L. li Jiang, L. Lu Huang, L. Guang Wu, C. Juan Li, J. Cai, Photo-induced antifouling polyvinylidene fluoride ultrafiltration membrane driven by weak visible light, *J. Ind. Eng. Chem.* 89 (2020) 476–484, <https://doi.org/10.1016/j.jiec.2020.06.027>.
- [156] F. Li, Z. Yu, H. Shi, Q. Yang, Q. Chen, Y. Pan, G. Zeng, L. Yan, A Mussel-inspired, method to fabricate reduced graphene oxide/g-C<sub>3</sub>N<sub>4</sub> composites membranes for catalytic decomposition and oil-in-water emulsion separation, *Chem. Eng. J.* 322 (2017) 33–45, <https://doi.org/10.1016/j.cej.2017.03.145>.
- [157] S.H. Paiman, M.A. Rahman, T. Uchikoshi, N.A.H. Md Nordin, N.H. Alias, N. Abdullah, K.H. Abas, M.H.D. Othman, J. Jaafar, A.F. Ismail, In situ growth of α-Fe<sub>2</sub>O<sub>3</sub> on Al<sub>2</sub>O<sub>3</sub>/YSZ hollow fiber membrane for oily wastewater, *Sep. Purif. Technol.* 236 (2020), <https://doi.org/10.1016/j.seppur.2019.116250>.
- [158] N.H. Alias, J. Jaafar, S. Samitsu, A.F. Ismail, M.H.D. Othman, M.A. Rahman, N. H. Othman, N. Yusof, F. Aziz, T.A.T. Mohd, Efficient removal of partially hydrolysed polyacrylamide in polymer-flooding produced water using photocatalytic graphitic carbon nitride nanofibres, *Arab. J. Chem.* 13 (2020) 4341–4349, <https://doi.org/10.1016/j.arabjc.2019.08.004>.
- [159] B. Shrestha, M. Ezazi, S.V. Rad, G. Kwon, Predicting kinetics of water-rich permeate flux through photocatalytic mesh under visible light illumination, *Sci. Rep.* 11 (2021) 1–9, <https://doi.org/10.1038/s41598-021-00607-w>.
- [160] H. Mamane, I. Horovitz, L. Lozzi, D. Di Camillo, D. Avisar, The role of physical and operational parameters in photocatalysis by N-doped TiO<sub>2</sub> sol-gel thin films, *Chem. Eng. J.* 257 (2014) 159–169, <https://doi.org/10.1016/j.cej.2014.07.018>.
- [161] P.S. Foran, C. Boxall, K.R. Denison, Photoinduced Superhydrophilicity: A Kinetic Study of Time Dependent Photoinduced Contact Angle Changes on TiO<sub>2</sub> Surfaces, *Langmuir* 28 (2012) 17647–17655, <https://doi.org/10.1021/la3026649>.
- [162] A. Mills, J. Wang, D.F. Ollis, Dependence of the kinetics of liquid-phase photocatalyzed reactions on oxygen concentration and light intensity, *J. Catal.* 243 (2006) 1–6, <https://doi.org/10.1016/j.jcat.2006.06.025>.
- [163] D. Panchanathan, G. Kwon, T.F. Qahtan, M.A. Gondal, K.K. Varanasi, G. H. McKinley, Kinetics of Photoinduced Wettability Switching on Nanoporous Titania Surfaces under Oil, *Adv. Mater. Interfaces* 4 (2017), 1700462, <https://doi.org/10.1002/admi.201700462>.
- [164] B. Shrestha, M. Ezazi, G. Kwon, Engineered nanoparticles with decoupled photocatalysis and wettability for membrane-based desalination and separation of oil-saline water mixtures, *Nanomaterials* 11 (2021), <https://doi.org/10.3390/nano11061397>.
- [165] S.M. Wetterer, D.J. Lavrich, T. Cummings, S.L. Bernasek, G. Scoles, Energetics and Kinetics of the Physisorption of Hydrocarbons on Au(111), *J. Phys. Chem. B* 102 (1998) 9266–9275, <https://doi.org/10.1021/jp982338>.
- [166] J.R. Cooper, Q. Mary, M.E. Road, S.I. Associates, The International Association for the Properties of Water and Steam Release on the IAPWS Formulation 2008 for the Thermodynamic Properties of Water and Steam., 2008: 1–19.
- [167] R. Saravanan, F. Gracia, A. Stephen, in: M.M. Khan, D. Pradhan, Y. Sohn (Eds.), *Basic Principles, Mechanism, and Challenges of Photocatalysis BT - Nanocomposites for Visible Light-induced Photocatalysis*, Springer International Publishing, Cham, 2017, pp. 19–40, [https://doi.org/10.1007/978-3-319-62446-4\\_2](https://doi.org/10.1007/978-3-319-62446-4_2).
- [168] S. Mozia, D. Darowna, K. Szymański, S. Grondzewska, K. Borchert, R. Wróbel, A. W. Morawski, Performance of two photocatalytic membrane reactors for treatment of primary and secondary effluents, *Catal. Today* 236 (2014) 135–145, <https://doi.org/10.1016/j.cattod.2013.12.049>.
- [169] D.M. Blake, J. Webb, C. Turchi, K. Magrini, Kinetic and mechanistic overview of TiO<sub>2</sub>-photocatalyzed oxidation reactions in aqueous solution, *Sol. Energy Mater.* 24 (1991) 584–593, [https://doi.org/10.1016/0165-1633\(91\)90092-Y](https://doi.org/10.1016/0165-1633(91)90092-Y).
- [170] D. Chen, Y. Cheng, N. Zhou, P. Chen, Y. Wang, K. Li, S. Huo, P. Cheng, P. Peng, R. Zhang, L. Wang, H. Liu, Y. Liu, R. Ruan, Photocatalytic degradation of organic pollutants using TiO<sub>2</sub>-based photocatalysts: A review, *J. Clean. Prod.* 268 (2020), 121725, <https://doi.org/10.1016/j.jclepro.2020.121725>.
- [171] G. Jia, G. Wang, Y. Zhang, L. Zhang, Effects of light intensity and H<sub>2</sub>O<sub>2</sub> on photocatalytic degradation of phenol in wastewater using TiO<sub>2</sub>/ACF, *Proc. - 2010 Int. Conf. Digit. Manuf. Autom. ICDMA 2010. 1*, 2010: 623–626. <https://doi.org/10.1109/ICDMA.2010.431>.
- [172] X. Chen, S.S. Mao, Titanium dioxide nanomaterials: synthesis, properties, modifications, and applications, *Chem. Rev.* 107 (2007) 2891–2959, <https://doi.org/10.1021/cr0500535>.
- [173] S.M. Lam, J.C. Sin, A.R. Mohamed, Parameter effect on photocatalytic degradation of phenol using TiO<sub>2</sub>-P25/activated carbon (AC), *Korean J. Chem. Eng.* 27 (2010) 1109–1116, <https://doi.org/10.1007/s11814-010-0169-8>.
- [174] A. G.P. Kumar, A Review on the Factors Affecting the Photocatalytic Degradation of Hazardous Materials, *Mater. Sci. Eng. Int. J.* 1 (2017), <https://doi.org/10.15406/mseij.2017.01.00018>.
- [175] H. Rongan, L. Haijuan, L. Huimin, X. Difa, Z. Liuyang, S-scheme photocatalyst Bi<sub>2</sub>O<sub>3</sub>/TiO<sub>2</sub> nanofiber with improved photocatalytic performance, *J. Mater. Sci. Technol.* 52 (2020) 145–151, <https://doi.org/10.1016/j.jmst.2020.03.027>.
- [176] J. Liqiang, S. Xiaojun, C. Weimin, X. Zili, D. Yaoguo, F. Honggang, The preparation and characterization of nanoparticle TiO<sub>2</sub>/Ti films and their photocatalytic activity, *J. Phys. Chem. Solids* 64 (2003) 615–623, [https://doi.org/10.1016/S0022-3697\(02\)00362-1](https://doi.org/10.1016/S0022-3697(02)00362-1).
- [177] E.A. Emam, N.A.K. Aboul-Gheit, Photocatalytic degradation of oil-emulsion in water/seawater using titanium dioxide, *Energy Sources, Part A Recover. Util. Environ. Eff.* 36 (2014) 1123–1133, <https://doi.org/10.1080/15567036.2010.544154>.
- [178] C. Van Chung, N.Q. Bui, N.H. Chau, Influence of surface charge and solution pH on the performance characteristics of a nanofiltration membrane, *Sci. Technol. Adv. Mater.* 6 (2005) 246–250, <https://doi.org/10.1016/j.stam.2005.02.025>.
- [179] P.M. Williams, in: E. Drioli, L. Giorno (Eds.), *Membrane Charge (Zeta Potential) Effect BT - Encyclopedia of Membranes*, Springer Berlin Heidelberg, Berlin, Heidelberg, 2016, pp. 1–2, [https://doi.org/10.1007/978-3-642-40872-4\\_1003-1](https://doi.org/10.1007/978-3-642-40872-4_1003-1).
- [180] S. Khezriano, H.D. Revanasiddappa, Effect of operational parameters and kinetic study on the photocatalytic degradation of m-cresol purple using irradiated ZnO in aqueous medium, *Water Qual. Res. J. Can.* 51 (2016) 69–78, <https://doi.org/10.2166/wqrj.2015.028>.
- [181] S. Anandan, Y. Ikuma, K. Niwa, An overview of semi-conductor photocatalysis: Modification of TiO<sub>2</sub> nanomaterials, *Solid State Phenom.* 162 (2010) 239–260, <https://doi.org/10.4028/www.scientific.net/SSP.162.239>.
- [182] A.A. Khodja, T. Sehili, J.F. Pilichowski, P. Boule, Photocatalytic degradation of 2-phenylphenol on TiO<sub>2</sub> and ZnO in aqueous suspensions, *J. Photochem. Photobiol. A Chem.* 141 (2001) 231–239, [https://doi.org/10.1016/S1010-6030\(01\)00423-3](https://doi.org/10.1016/S1010-6030(01)00423-3).
- [183] I.K. Konstantinou, T.A. Albanis, TiO<sub>2</sub>-assisted photocatalytic degradation of azo dyes in aqueous solution: Kinetic and mechanistic investigations: A review, *Appl. Catal. B Environ.* 49 (2004) 1–14, <https://doi.org/10.1016/j.apcatb.2003.11.010>.
- [184] L. Li, R. Lee, Purification of produced water by ceramic membranes: material screening, process design and economics, *Sep. Sci. Technol.* 44 (2009) 3455–3484, <https://doi.org/10.1080/01496390903253395>.
- [185] C.K. Kim, M.J. Yoo, G. Y. Yoo, Development of combined fouling model in a membrane bioreactor, *Asia-Pac. J. Chem. Eng.* 6 (2011) 423–432, <https://doi.org/10.1002/apj>.
- [186] S. Alzahrani, A.W. Mohammad, Challenges and trends in membrane technology implementation for produced water treatment: A review, *J. Water Process Eng.* 4 (2014) 107–133, <https://doi.org/10.1016/j.jwpe.2014.09.007>.
- [187] N.M. Syarifah Nazirah Wan Ikhshan, Norhaniza Yusof, Farhana Aziz, A review of oilfield wastewater treatment using Membrane filtration over conventional technology, *Malays. J. Anal. Sci.* 21 (2017) 643–658.

- [188] C.Y. Tang, T.H. Chong, A.G. Fane, Colloidal interactions and fouling of NF and RO membranes: A review, *Adv. Colloid Interface Sci.* 164 (2011) 126–143, <https://doi.org/10.1016/j.cis.2010.10.007>.
- [189] H.J. Tanudjaja, J.W. Chew, Assessment of oil fouling by oil-membrane interaction energy analysis, *J. Memb. Sci.* 560 (2018) 21–29, <https://doi.org/10.1016/j.memsci.2018.05.008>.
- [190] W. JD, W. Wei, L. SH, Q. Zhong, F. Liu, Z. JH, W. JP, The effect of membrane surface charges on demulsification and fouling resistance during emulsion separation, *J. Memb. Sci.* 563 (2018) 126–133, <https://doi.org/10.1016/j.memsci.2018.05.065>.
- [191] Y. Liu, Y. Su, J. Cao, J. Guan, R. Zhang, M. He, L. Fan, Q. Zhang, Z. Jiang, Antifouling, high-flux oil/water separation carbon nanotube membranes by polymer-mediated surface charging and hydrophilization, *J. Memb. Sci.* 542 (2017) 254–263, <https://doi.org/10.1016/j.memsci.2017.08.018>.
- [192] L. Han, Y.Z. Tan, T. Netke, A.G. Fane, J.W. Chew, Understanding oily wastewater treatment via membrane distillation, *J. Memb. Sci.* 539 (2017) 284–294, <https://doi.org/10.1016/j.memsci.2017.06.012>.
- [193] S. Velioglu, L. Han, C. JW, Understanding membrane pore-wetting in the membrane distillation of oil emulsions via molecular dynamics simulations, *J. Memb. Sci.* 551 (2018) 76–84, <https://doi.org/10.1016/j.memsci.2018.01.027>.
- [194] Z. Wang, Y. Chen, F. Zhang, S. Lin, Significance of surface excess concentration in the kinetics of surfactant-induced pore wetting in membrane distillation, *Desalination* 450 (2019) 46–53, <https://doi.org/10.1016/j.desal.2018.10.024>.
- [195] Y.Z. Tan, S. Velioglu, L. Han, B.D. Joseph, L.G. Unnithan, J.W. Chew, Effect of surfactant hydrophobicity and charge type on membrane distillation performance, *J. Memb. Sci.* 587 (2019), 117168, <https://doi.org/10.1016/j.memsci.2019.117168>.
- [196] P. Srijaroonrat, E. Julien, Y. Aurelle, Unstable secondary oil/water emulsion treatment using ultrafiltration: Fouling control by backflushing, *J. Memb. Sci.* 159 (1999) 11–20, [https://doi.org/10.1016/S0376-7388\(99\)00044-7](https://doi.org/10.1016/S0376-7388(99)00044-7).
- [197] Z. Yang, H. Peng, W. Wang, T. Liu, Crystallization behavior of poly( $\epsilon$ -caprolactone)/layered double hydroxide nanocomposites, *J. Appl. Polym. Sci.* 116 (2010) 2658–2667, <https://doi.org/10.1002/app>.
- [198] O. Samuel, M. Baba, A. Thlimabari, The Ecological, Economical and Social Impact of Adopting Solar Cooking in Mubi Metropolis Adamawa State, Nigeria, *J. Sci. Res. Rep.* 18 (2018) 1–6, <https://doi.org/10.9734/jsrr/2018/37401>.
- [199] Z. Xu, T. Wu, J. Shi, K. Teng, W. Wang, M. Ma, J. Li, X. Qian, C. Li, J. Fan, Photocatalytic antifouling PVDF ultrafiltration membranes based on synergy of graphene oxide and TiO<sub>2</sub> for water treatment, *J. Memb. Sci.* 520 (2016) 281–293, <https://doi.org/10.1016/j.memsci.2016.07.060>.
- [200] R.A. Damodar, S.J. You, H.H. Chou, Study the self cleaning, antibacterial and photocatalytic properties of TiO<sub>2</sub> entrapped PVDF membranes, *J. Hazard. Mater.* 172 (2009) 1321–1328, <https://doi.org/10.1016/j.jhazmat.2009.07.139>.
- [201] L. Zhang, Y. He, P. Luo, L. Ma, S. Li, Y. Nie, F. Zhong, Y. Wang, L. Chen, Photocatalytic GO/M88A “interceptor plate” assembled nanofibrous membrane with photo-Fenton self-cleaning performance for oil/water emulsion separation, *Chem. Eng. J.* 427 (2022), <https://doi.org/10.1016/j.cej.2021.130948>.
- [202] X. Wang, C. Xiao, H. Liu, M. Chen, H. Xu, W. Luo, F. Zhang, Robust functionalization of underwater superoleophobic PVDF-HFP tubular nanofiber membranes and applications for continuous dye degradation and oil/water separation, *J. Memb. Sci.* 596 (2020), 117583, <https://doi.org/10.1016/j.memsci.2019.117583>.
- [203] Y. Liu, Z. Yu, X. Li, L. Shao, H. Zeng, Super hydrophilic composite membrane with photocatalytic degradation and self-cleaning ability based on LDH and g-C<sub>3</sub>N<sub>4</sub>, *J. Memb. Sci.* 617 (2021), 118504, <https://doi.org/10.1016/j.memsci.2020.118504>.
- [204] O. Carp, C.L. Huisman, A. Reller, Photoinduced reactivity of titanium dioxide, *Prog. Solid State Chem.* 32 (2004) 33–177, <https://doi.org/10.1016/j.progsolidstchem.2004.08.001>.
- [205] Y. Shi, J. Huang, G. Zeng, W. Cheng, J. Hu, L. Shi, K. Yi, Evaluation of self-cleaning performance of the modified g-C<sub>3</sub>N<sub>4</sub> and GO based PVDF membrane toward oil-in-water separation under visible-light, *Chemosphere* 230 (2019) 40–50, <https://doi.org/10.1016/j.chemosphere.2019.05.061>.
- [206] J. Hu, Y. Zhan, G. Zhang, Q. Feng, W. Yang, Y.H. Chiao, S. Zhang, A. Sun, Durable and super-hydrophilic/underwater super-oleophobic two-dimensional MXene composite lamellar membrane with photocatalytic self-cleaning property for efficient oil/water separation in harsh environments, *J. Memb. Sci.* 637 (2021), 119627, <https://doi.org/10.1016/j.memsci.2021.119627>.
- [207] Q. Lin, G. Zeng, G. Yan, J. Luo, X. Cheng, Z. Zhao, H. Li, Self-cleaning photocatalytic MXene composite membrane for synergistically enhanced water treatment: Oil/water separation and dyes removal, *Chem. Eng. J.* 427 (2022), 131668, <https://doi.org/10.1016/j.cej.2021.131668>.
- [208] F. Wang, X. Xiao, C. Liu, H. Chen, M. Xu, H. Luo, W. Zhang, Robust functionalization of underwater superoleophobic PVDF-HFP tubular nanofiber membranes and applications for continuous dye degradation and oil/water separation, *J. Memb. Sci.* 596 (2020).
- [209] Z. Yin, F. Yuan, M. Li, M. Xue, D. Zhou, Y. Chen, X. Liu, Y. Luo, Z. Hong, C. Xie, J. Ou, Self-cleaning, underwater writable, heat-insulated and photocatalytic cellulose membrane for high-efficient oil/water separation and removal of hazardous organic pollutants, *Prog. Org. Coat.* 157 (2021), 106311, <https://doi.org/10.1016/j.porgcoat.2021.106311>.
- [210] W. Ma, Y. Li, M. Zhang, S. Gao, J. Cui, C. Huang, G. Fu, Biomimetic Durable Multifunctional Self-Cleaning Nanofibrous Membrane with Outstanding Oil/Water Separation, Photodegradation of Organic Contaminants, and Antibacterial Performances, *ACS Appl. Mater. Interfaces* 12 (2020) 34999–35010, <https://doi.org/10.1021/acsami.0c09059>.
- [211] H. Kang, Z. Cheng, H. Lai, H. Ma, Y. Liu, X. Mai, Y. Wang, Q. Shao, L. Xiang, X. Guo, Z. Guo, Superlyophobic anti-corrosive and self-cleaning titania robust mesh membrane with enhanced oil/water separation, *Sep. Purif. Technol.* 201 (2018) 193–204, <https://doi.org/10.1016/j.seppur.2018.03.002>.
- [212] Y. Song, J. Lang, J. Guo, Q. Zhang, Q. Han, H. Fan, M. Gao, M. Wei, J. Yang, Z. Sheng, Preparation of carbon cloth membrane with visible light induced self-cleaning performance for oil-water separation, *Surf. Coat. Technol.* 403 (2020), 126372, <https://doi.org/10.1016/j.surfcoat.2020.126372>.
- [213] Z.M. Zhang, Z.Q. Gan, R.Y. Bao, K. Ke, Z.Y. Liu, M.B. Yang, W. Yang, Green and robust superhydrophilic electrospun stereocomplex polylactide membranes: Multifunctional oil/water separation and self-cleaning, *J. Memb. Sci.* 593 (2020), 117420, <https://doi.org/10.1016/j.memsci.2019.117420>.
- [214] R. Yue, M. Saifur Rahman, Hydrophilic and underwater superoleophobic porous graphitic carbon nitride (g-C<sub>3</sub>N<sub>4</sub>) membranes with photo-Fenton self-cleaning ability for efficient oil/water separation, *J. Colloid Interface Sci.* 608 (2022) 1960–1972, <https://doi.org/10.1016/j.jcis.2021.10.162>.
- [215] J. Wang, X. Wang, S. Zhao, B. Sun, Z. Wang, J. Wang, Robust superhydrophobic mesh coated by PANI/TiO<sub>2</sub> nanoclusters for oil/water separation with high flux, self-cleaning, photodegradation and anti-corrosion, *Sep. Purif. Technol.* 235 (2020), 116166, <https://doi.org/10.1016/j.seppur.2019.116166>.
- [216] Q. Zhang, Y. Song, J. Guo, S. Wu, N. Chen, H. Fan, M. Gao, J. Yang, Z. Sheng, J. Lang, One-step hydrothermal synthesis of the modified carbon cloth membrane: Towards visible light driven and self-cleaning for efficient oil-water separation, *Surf. Coat. Technol.* 409 (2021), <https://doi.org/10.1016/j.surfcoat.2021.126879>.
- [217] X. Zhao, L. Cheng, N. Jia, R. Wang, L. Liu, C. Gao, Polyphenol-metal manipulated nanohybridization of CNT membranes with FeOOH nanorods for high-flux, antifouling and self-cleaning oil/water separation, *J. Memb. Sci.* 600 (2020), 117857, <https://doi.org/10.1016/j.memsci.2020.117857>.
- [218] A.J. Karabelas, K.V. Plakas, V.C. Sarasidis, How Far Are We From Large-Scale PMR Applications? Elsevier Inc., 2018 <https://doi.org/10.1016/B978-0-12-813549-5.00009-8>.
- [219] A.J. Karabelas, K.V. Plakas, V.C. Sarasidis, How Far Are We From Large-Scale PMR Applications?, in: *Curr. Trends Futur. Dev. Membr. Photocatalytic Membr. Photocatalytic Membr. React.* Elsevier Inc, 2018, pp. 233–295, <https://doi.org/10.1016/B978-0-12-813549-5.00009-8>.
- [220] G.K. Pearce, SWRO pre-treatment: cost and sustainability, *Filtr. Sep.* 36e38 (2010).
- [221] Steve Allgeier, Membrane Filtration Guidance Manual, US Environmental Protection Agency (EPA), 2005.
- [222] B. Judd, S. Jefferson, *Membranes for Industrial Wastewater Recovery and Reuse.*, Elsevier., 2003.
- [223] M. Pirnie, K.G. Linden, J.P.J. Malley, Ultraviolet disinfection guidance manual for the final long term 2 enhanced surface water treatment rule, *Environ. Prot.* 2 (2006) 1–436.
- [224] K.V. Plakas, V.C. Sarasidis, S.I. Patsios, D.A. Lambropoulou, A.J. Karabelas, Novel pilot scale continuous photocatalytic membrane reactor for removal of organic micropollutants from water, *Chem. Eng. J.* 304 (2016) 335–343, <https://doi.org/10.1016/j.cej.2016.06.075>.
- [225] M.H. Habibi, A. Hassanzadeh, S. Mahdavi, The effect of operational parameters on the photocatalytic degradation of three textile azo dyes in aqueous TiO<sub>2</sub> suspensions, *J. Photochem. Photobiol. A Chem.* 172 (2005) 89–96, <https://doi.org/10.1016/j.jphotochem.2004.11.009>.
- [226] N. Lior, Sustainability as the quantitative norm for water desalination impacts, *Desalination* 401 (2017) 99–111, <https://doi.org/10.1016/j.desal.2016.08.008>.